EUROPEAN LABORATORY FOR PARTICLE PHYSICS

Hadronization in Z^0 decay

I. G. Knowles† and G. D. Lafferty‡ ‖

† Department of Physics and Astronomy, The University of Edinburgh, Edinburgh, EH9 3JZ, UK.
‡ PPE Division, CERN, 1211 Genève 23, Switzerland.

Abstract. The confinement transition from the quark and gluon degrees of freedom appropriate in perturbation theory to the hadrons observed by real world experiments is poorly understood. In this strongly interacting transition regime we presently rely on models, which to varying degrees reflect possible scenarios for the QCD dynamics. Because of the absence of beam and target remnants, and the clean experimental conditions and high event rates, e^+e^- annihilation to hadrons at the Z^0 provides a unique laboratory, both experimentally and theoretically, for the study of parton hadronization. This review discusses current theoretical understanding of the hadronization of partons, with particular emphasis on models of the non-perturbative phase, as implemented in Monte Carlo simulation programs. Experimental results at LEP and SLC are summarised and considered in the light of the models. Suggestions are given for further measurements which could help to produce more progress in understanding hadronization.

Short title: Hadronization in Z^0 decay

May 6, 1997

‖ On leave from Department of Physics and Astronomy, The University of Manchester, Manchester, M13 9PL, UK.

1. Introduction

Hadronic systems produced in e^+e^- annihilation have their origin in a uniquely simple quark-antiquark state. While the standard model of particle physics provides a well tested description of the reaction $e^+e^- \rightarrow Z^0/\gamma^* \rightarrow q\bar{q}$, the subsequent production of observable hadrons is less well understood. A parton shower, described by perturbative quantum chromodynamics (pQCD), is normally invoked to describe the initial fragmentation phase. In the subsequent non-perturbative hadronization process, the partons become the hadrons which are experimentally observed. Multihadronic e^+e^- annihilation events, with no beam or target fragments to confuse their experimental or theoretical interpretation, provide the most powerful system available for the study of the transition from the partons of perturbative QCD to the hadrons of the laboratory.

Between 1989 and 1995, the Large Electron Positron collider (LEP) at CERN delivered an integrated luminosity of about 170 pb^{-1} per detector at and around the Z^0 peak, providing each of its four dedicated experiments, ALEPH, DELPHI, L3 and OPAL, with some 6 million e^+e^- annihilation events, 70% of which were multihadronic. These events have enabled the experiments to conduct detailed studies of many aspects of parton hadronization. Over the same period, the SLAC Linear Collider (SLC) delivered a more modest number of events, initially to the MARK II detector and then to the SLD detector, which has now accumulated about 200k Z^0 events. Although its luminosity is lower than that of LEP, the SLC is able to provide highly polarized electron beams. While LEP has now entered phase 2, running at higher energies, analysis of the Z^0 peak data will continue for some time. The SLC, with polarized beams, is scheduled to run at the Z^0 for several more years.

In this review, we look at the present understanding of the non-perturbative hadronization process in the context of the recent experimental results from LEP and SLC. A brief introduction to the electroweak theory of e^+e^- annihilation is followed by a heuristic picture of the transition from perturbative partons to final-state hadrons. After this, the role of perturbative QCD in determining the structures and particle content of events is discussed. Models of the non-perturbative hadronization phase are then covered — independent fragmentation, string fragmentation and cluster fragmentation are discussed in detail and a comparison is given of the main features of the different models. The LEP and SLC machines and their associated detectors are then described, with emphasis on the features relevant to measurements of individual hadrons from Z^0 decay. Next the experimental data on single inclusive identified particles are summarised, and the results interpreted in the light of the different models. Results on spin phenomena, such as baryon

polarization and vector meson spin alignment are then covered, and this is followed by discussion of results on correlations, including Bose Einstein effects, strange particle rapidity and angular correlations, and intermittency; where possible the results are interpreted within the context of theory and models. Differences between quark and gluon initiated jets are then dealt with, and the review ends with a look forward to what may still be learned from the available LEP and SLC data, and the forthcoming SLC data.

1.1. Electroweak aspects of e^+e^- annihilation

The (initial) numbers, directions, polarizations and flavours of the quarks produced in e^+e^- annihilation are determined by the electroweak couplings of the exchanged vector bosons. The full, tree-level expression for the differential cross section for $e^+e^- \rightarrow q\bar{q}$ in the centre of momentum (CoM) frame is given as a function of quark's polar angle, $\theta^\star$, measured relative to the electron beam direction, and total CoM energy squared, s, by:

$$\frac{\mathrm{d}\sigma}{\mathrm{d}\Omega}(s, \theta^\star) = \frac{3N_c\alpha_{\mathrm{em}}^2}{16s}\beta_{\mathrm{q}}\sum_{i,j}\chi_i(s)\chi_j^\star(s)(v_{\mathrm{e}}^i v_{\mathrm{e}}^j + a_{\mathrm{e}}^i a_{\mathrm{e}}^j)(v_{\mathrm{q}}^i v_{\mathrm{q}}^j + \beta^2 a_{\mathrm{q}}^i a_{\mathrm{q}}^j) \times$$

$$\left\{\left(\mathcal{P}_{\mathrm{e}}^{(1)} - \mathcal{P}_{\mathrm{e}}^{(2)} A_{\mathrm{e}}^{ij}\right)\left[\left(2 - \mathcal{P}_{\mathrm{q}}^{(1)}\right)B_{\mathrm{q}}^{ij}(1 - \beta_{\mathrm{q}}^2)\sin^2\theta^\star + \left(\mathcal{P}_{\mathrm{q}}^{(1)} + \mathcal{P}_{\mathrm{q}}^{(2)} A_{\mathrm{q}}^{ij}\right)(1 + \cos^2\theta^\star)\right]$$

$$+ \left(\mathcal{P}_{\mathrm{e}}^{(1)} A_{\mathrm{e}}^{ij} + \mathcal{P}_{\mathrm{e}}^{(2)}\right)\left(\mathcal{P}_{\mathrm{q}}^{(1)} A_{\mathrm{q}}^{ij} + \mathcal{P}_{\mathrm{q}}^{(2)}\right)2\cos\theta^\star\right\} \tag{1}$$

where,

$$\mathcal{P}_{\mathrm{f}}^{(1)} = 1 - \rho_{\mathrm{f}}\rho_{\bar{\mathrm{f}}} \qquad A_{\mathrm{f}}^{ij} = \frac{\beta_{\mathrm{f}}(v_{\mathrm{f}}^i a_{\mathrm{f}}^j + a_{\mathrm{f}}^i v_{\mathrm{f}}^j)}{v_{\mathrm{f}}^i v_{\mathrm{f}}^j + \beta_{\mathrm{f}}^2 a_{\mathrm{f}}^i a_{\mathrm{f}}^j} \qquad \chi_i(s) = \frac{s}{(s - M_i^2) + \mathrm{i}M_i\Gamma_i}$$

$$\mathcal{P}_{\mathrm{f}}^{(2)} = \rho_{\mathrm{f}} - \rho_{\bar{\mathrm{f}}} \qquad B_{\mathrm{f}}^{ij} = \frac{v_{\mathrm{f}}^i v_{\mathrm{f}}^j}{v_{\mathrm{f}}^i v_{\mathrm{f}}^j + \beta_{\mathrm{f}}^2 a_{\mathrm{f}}^i a_{\mathrm{f}}^j} \qquad \beta_{\mathrm{q}} = \sqrt{1 - \frac{4m_{\mathrm{q}}^2}{s}} \tag{2}$$

The summation is over all exchanged bosons, $i = \gamma^\star, Z^0, \ldots$, with mass and width M_i and Γ_i, and vector and axial couplings v_{f}^i and a_{f}^i. For example $v_{\mathrm{f}}^\gamma = Q_{\mathrm{f}}$, $a_{\mathrm{f}}^\gamma = 0$, $v_{\mathrm{f}}^Z = (T_{\mathrm{f}}^{3L} - 2Q_{\mathrm{f}}s_W^2)/2s_W c_W$ and $a_{\mathrm{f}}^Z = T_{\mathrm{f}}^{3L}/2s_W c_W$ etc, with Q_{f} the fermion's electric charge, normalized to that of the electron, T_{f}^{3L} the fermion's third component of weak, $\mathrm{SU(2)_L}$, isospin and $s_W(c_W)$ the sine(cosine) of the Weinberg angle. The number of colours is $N_c = 3$ and α_{em} is the electromagnetic fine structure constant. The dependence on the initial lepton and final quark longitudinal polarizations are via ρ_{f}, where $\rho_{\mathrm{f}} = +1$ for spin along the CoM direction of travel (helicity basis). In the absence of transverse beam polarization there is no azimuthal angular dependence.

At $\sqrt{s} = M_Z$ the Z^0 exchange term dominates and (1) simplifies

considerably. In this limit the partial width for $Z^0 \to q\bar{q}$ is given by:

$$\Gamma_{q\bar{q}} = \frac{N_c \alpha_{em} M_Z}{6} \beta_q \left[(3 - \beta_q^2) v_q^2 + 2\beta_q^2 a_q^2 \right] \qquad (3)$$

This implies relative hadronic branching ratios of $\approx 17\%$ to each up-type quark and $\approx 22\%$ to each down-type quark at the Z^0; the relative fraction of b quarks peaks on resonance. Figure 1 shows the relative fractions of light (u,d,s), charm and bottom quarks as a function of $\sqrt{s}$ obtained using the full expression (1). The total hadronic branching fraction is $\approx 70\%$. The beam polarization has
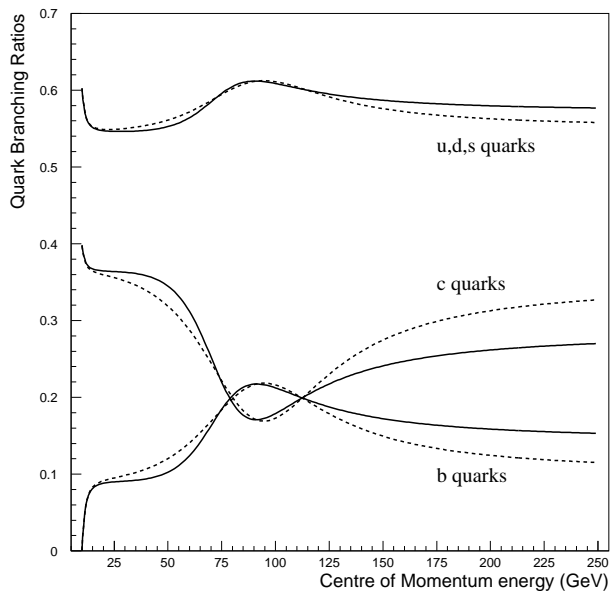
Figure 1. The relative branching fractions of light (u,d,s), charm and bottom quarks in e^+e^- annihilation as a function of $\sqrt{s}$ for an unpolarized (solid lines) and 100% right polarized (dashed lines) electron beam.

little influence on the relative rates of produced quarks, although the total rate is proportional to $(v_e^2 + a_e^2)\mathcal{P}_e^{(1)} - 2v_e a_e \mathcal{P}_e^{(2)}$. However only a single polarized beam can significantly alter the quark polar angle distribution, as can be seen from the forward-backward asymmetry (for pure Z^0 exchange and $\beta_q = 1$):

$$\frac{\frac{d\sigma}{d\Omega}(\cos\theta^\star) - \frac{d\sigma}{d\Omega}(-\cos\theta^\star)}{\frac{d\sigma}{d\Omega}(\cos\theta^\star) + \frac{d\sigma}{d\Omega}(-\cos\theta^\star)} = \frac{\mathcal{P}_e^{(1)} A_e - \mathcal{P}_e^{(2)}}{\mathcal{P}_e^{(1)} - \mathcal{P}_e^{(2)} A_e} \times A_q \frac{2\cos\theta^\star}{1 + \cos^2\theta^\star} \qquad (4)$$

Since A_e is only ≈ 0.16 ($A_d \approx 0.94$ and $A_u \approx 0.69$) then, given polarized beams, one has a powerful statistical way to identify separately quark and antiquark jets based on their direction. The quarks are naturally produced highly polarized:

$$\frac{\frac{d\sigma}{d\Omega}(\rho_f = +1) - \frac{d\sigma}{d\Omega}(\rho_f = -1)}{\frac{d\sigma}{d\Omega}(\rho_f = +1) + \frac{d\sigma}{d\Omega}(\rho_f = -1)} = A_q + \frac{A_e(1 - A_q^2)2\cos\theta^\star}{1 + \cos^2\theta^\star + A_e A_q 2\cos\theta^\star} \approx A_q \qquad (5)$$

This result is for unpolarized lepton beams, pure Z^0 exchange and $\beta_q = 1$; the full expression depends little on the lepton beam polarization.

For QCD studies at the Z^0 [1] the effect of initial-state electromagnetic radiation (ISR) is of rather minor significance, unlike in the case of electroweak studies [2, 3]. The primary effect of ISR is to lower the effective $\sqrt{s}$, leading to a distortion of the Breit-Wigner lineshape given by (1). However the basic quantities of relevance from a QCD perspective, quark flavour mix, polarization etc, are only rather weak functions of $\sqrt{s}$. Further, because of the Z^0 resonance the cross section falls rapidly when ISR occurs, mitigating against its effects (even so the peak cross section falls by $\approx 25\%$ compared to (1)), in contrast to the situation at LEP 2 and higher energies where ISR is very important [4]. The effects of *final-state* radiation, particularly of gluons but also of photons, form one theme of this review. The effect of final-state radiation on the total hadronic cross section can be summarized in the multiplicative factor [3, 5]:

$$1 + \frac{3}{4} \left(Q_q^2 \frac{\alpha_{\mathrm{em}}}{\pi} + C_F \frac{\alpha_s}{\pi} \right) + \cdots \tag{6}$$

where α_s is the strong coupling constant $(g_s^2/4\pi)$ and $C_F = 4/3$ is a measure of the quark-gluon coupling strength. Flavour (mass) dependent effects and electroweak radiative corrections are small — both occur at the 1% level, and need not concern us here [3].

1.2. A picture of the parton to hadron transition

The description of a multihadronic event commences by specifying a set of primary partons $(q/\bar{q}/g)$ distributed according to an exact Z^0 decay matrix element, such as (1). It is customary to identify three basic stages in the transition of these partons into detected hadrons [6]. First a parton (or, equivalently, dipole) cascade, formulated according to pQCD, evolves the primary partons from the hard scattering scale $Q \approx M_Z$ into secondary partons at a (fixed) cut-off scale $Q_0 \approx 1$ GeV. It is during the calculable stages, hard subprocess and shower, that the event's global features are determined: energy dependences, event shapes, multiplicity etc. In a second stage, carried out at the fixed, low virtuality scale Q_0, a model is employed to convert the secondary partons into hadrons. The second stage is essentially energy (Q) independent, up to power corrections, and assumed to be local in nature. Finally unstable primary particles are decayed into stable hadrons and leptons according to decay tables [7]. Schematically the fragmentation function is given by:

$$D_h^a(x, Q^2) = (\text{pQCD evolution: } Q^2 \to Q_0^2) \otimes (\text{model:} a \to \mathrm{H})\Big|_{Q_0^2} \tag{7}$$
$$\otimes (\text{tables:} \mathrm{H} \to \mathrm{h}, \mathrm{h}', ..)$$

Here, $D_h^a(x, Q^2)$ is the probability to find a hadron of type h carrying a fraction x of the parton's momentum, in a jet initiated by the parton a, whose maximum virtuality is Q. The H represent possible intermediate hadrons.
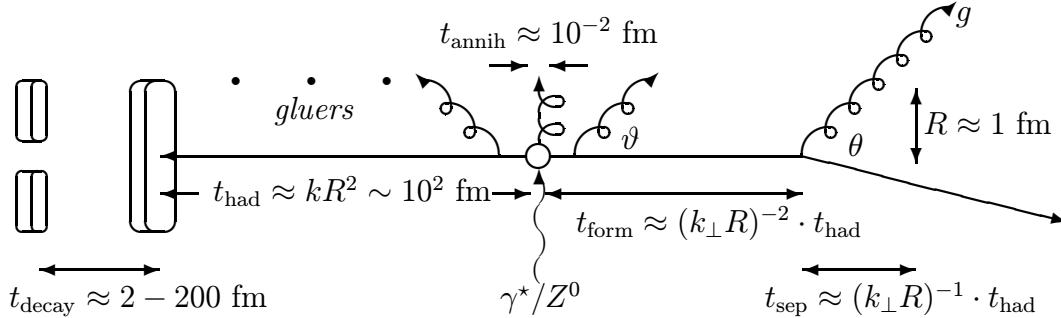
Figure 2. A schematic diagram of the spatial evolution of a hadronic Z^0 decay indicating the relevant time scales and distances associated with gluon bremsstrahlung and hadron formation.

We consider this process in terms of its space-time structure: the discussion is based on [8] and illustrated in figure 2. The hard subprocess, $e^+e^- \rightarrow q\bar{q}$, may be viewed as the production of a highly virtual photon, or a real Z^0, which impulsively kicks a $q\bar{q}$ pair out of the vacuum; the time scale is short, $t_{\text{annih}} \approx 1/\sqrt{Q^2} \sim 10^{-2}$ fm. In this non-adiabatic process the quarks shake off most of their cloud of virtual particles, so that any structure they have is on a scale below $1/\sqrt{Q^2}$. That is they behave as bare (more properly half-dressed) colour charges until the gluon field has had time to regenerate out to a typical hadron size $R \approx 1$ fm. Allowing for the boost, this takes a time $t_{\text{had}} \approx Q/m \times R \approx QR^2 \sim 10^2$ fm, where the second approximation is appropriate to light hadrons.

The fact that $t_{\text{had}} \gg t_{\text{annih}}$ raises the issue of how charges are conserved over the space-like separated distances involved. Of course the accelerated quarks will radiate gluons and here two new time scales are relevant. First, from the off-shellness of the quark prior to emission, the formation time of a real gluon of 3-momentum (=energy) k is $t_{\text{form}} \approx k/k_\perp^2$ (the uncertainty relation gives the proper lifetime of the virtual state as the reciprocal of its off-shellness, during which time it will travel a 4-distance q^μ/q^2 in the laboratory frame, where q^μ is the virtual state's 4-momentum). Second, for the gluon to reach a transverse separation of R and become independent of the quark takes a time $t_{\text{sep}} = (k_\perp R) \cdot t_{\text{form}}$, whilst the hadronization time may be written $t_{\text{had}}(\approx kR^2) = (k_\perp R)^2 \cdot t_{\text{form}}$.

For this quark-gluon picture to make sense we require $k_\perp > R^{-1}$ so that $t_{\text{form}} < t_{\text{sep}} < t_{\text{had}}$; this is natural as it implies that $\alpha_s(k_\perp^2) < 1$, making

perturbation theory applicable. If $k_\perp < R^{-1}$ then we can say nothing. On the borderline are quanta with $k_\perp = R^{-1}$; these feel the strong interaction and are responsible for holding hadrons together. We distinguish these from the essentially free perturbative gluons by the name *gluers*. The first *gluers* form after only 1 fm, having $k \approx k_\perp \approx R^{-1}$. Thus *gluers* immediately form in the wake of the primary partons blanching their colour field and leaving two fast separating charge neutral systems. Thus the slowest hadrons form first, close to the interaction point, in what may be called an 'inside-out' pattern [9].

On quite general grounds the distribution of *gluers* in QCD can be estimated using:

$$d\mathcal{N}_{\mathrm{gluers}} \sim C_F \left[\int_{k_\perp \sim R} \frac{\alpha_s(k_\perp^2)}{\pi} \mathcal{P}(k) \frac{\mathrm{d}k_\perp^2}{k_\perp^2} \right] \times \frac{\mathrm{d}k}{k} \propto \frac{\mathrm{d}k}{k} \qquad (8)$$

Here the logarithmic $k_\perp^2$ dependence reflects the fact that the coupling constant is dimensionless, the logarithmic k dependence follows from the gluon being massless and only the kernel function $\mathcal{P}$, which is of order unity, depends on details of the quark-gluon vertex. The distribution is thus governed by longitudinal phase space and leads to hadron production on rapidity plateaux along the directions of the initial partons.

Not all quanta are emitted at low $k_\perp$ and in a significant range, $R^{-1} \ll k_\perp < k \ll \sqrt{Q^2}$, a shower of perturbative gluons is possible. A hard gluon emitted at an angle θ becomes a separate colour source at $t_{\mathrm{sep}} = R/\theta (= (g_\perp R) \cdot t_{\mathrm{form}})$, again raising the issue of charge conservation. Fortunately a *gluer* emitted at the same angle θ would appear just in the right place and at the right time to blanch the tail of the separating gluon's colour field. This gluon then acts as a new source of *gluers*, restricted such that $k \gtrsim \theta^{-1} R^{-1}$. That is equivalent to a boosted ($\gamma = 1/\theta$) quark jet of a reduced scale $Q = k_\perp$ and with the substitution $C_F \mapsto C_A$ for the parton's charge in (8) [10]. It should be noted that *gluers* emitted at larger angles $\vartheta > \theta$ have $R/\vartheta < R/\theta = t_{\mathrm{sep}}$ and should therefore be associated with the parent q+g system. For example at time R the first *gluers* emitted actually see ensembles of partons equivalent to the original q$\bar{\mathrm{q}}$ pair. The coherence of soft emissions simply reflects colour charge conservation and is fundamental to a gauge theory such as QCD.

Finally, the time scales for the decay of the primary particles are set by the reciprocal of their widths: for the strong resonances typical values of $\Gamma \sim 1-100\,\mathrm{MeV}$ give $t_{\mathrm{decay}} \sim 200-2\,\mathrm{fm}$. Clearly these scales are commensurate with those for primary hadron production so that any distinction between hadronization and resonance decays may be only semantics. This is illustrated in figure 3 which shows a string-inspired space-time picture (see section 3.2) of two equivalent ways to form a $\pi^+\pi^-$ pair differing only in the time sequence of the string breaks. In the first figure the pions are directly produced whilst

in the second they appear to come from a ρ^0; however observationally they are indistinguishable. The time scale for the weak decays of s, c and b hadrons is of order $t_{\text{decay}} \sim (M_W/m_Q)^2 k/m_Q$ (where k/m_Q is the hadron's γ factor); this is $\approx 10^{12}$ fm for c and b and much longer for s, and so these decays may safely be treated as separate subprocesses.
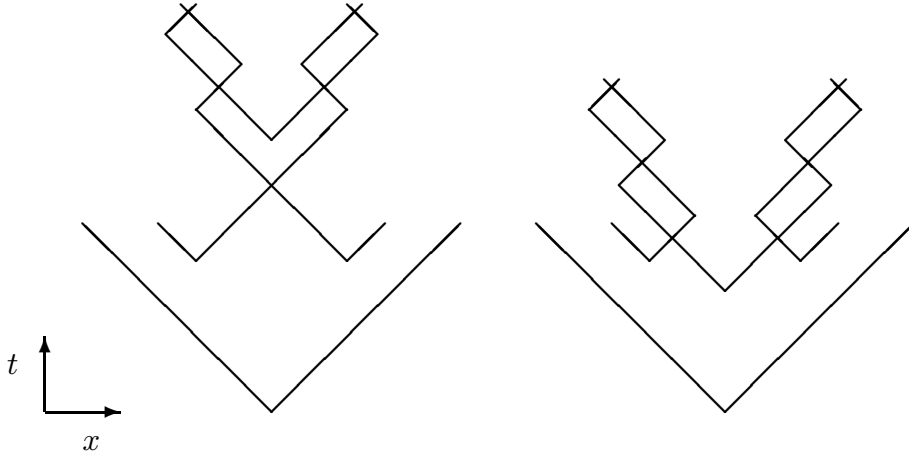
Figure 3. Two possible views from the string model perspective of $\pi^+\pi^-$ production via an intermediate ρ^0, illustrating the practical difficulty in separating strong resonance decays from the direct string fragmentation.

1.3. Monte Carlo event generators

A typical hadronic final state in Z^0 decay contains about 20 stable charged particles and 10 neutral hadrons, mainly π^0's. This is a complex, non-perturbative system beyond direct, first principles calculation at the present time. However Monte Carlo event generator programs [6, 11] have been developed which provide remarkably accurate, detailed descriptions of complete hadronic events. These are based on a combination of judicious approximations to pQCD, discussed in section 2, and per/in-spirational models for hadronization, to be discussed more fully in section 3. Here we list the main features of the major event generators used in Z^0 studies and refer the reader to later sections and to the literature for more complete descriptions.

ARIADNE [12] implements a pQCD shower based on the dipole cascade model [13], which is equivalent to a coherent parton shower. The evolving chain of dipoles corresponds naturally to a string and indeed the hadronization is performed using the JETSET implementation of the Lund string model [14].

COJETS [15] is based on a virtuality-ordered parton shower, that takes no account of colour coherence. The resulting jets are hadronized

using a refined version of the Field-Feynman independent fragmenation model [16].

HERWIG [17] is based on a highly developed parton shower algorithm [18, 19], that automatically takes into account colour coherence, and a relatively simple cluster hadronization scheme [20].

JETSET [21] uses a virtuality-ordered parton shower with an imposed angular ordering constraint to take into account colour coherence. A relatively sophisticated hadronization scheme based on the Lund string model is provided [14]. An option also exists which does not employ a parton shower but tries to use instead higher-order hard-subprocess matrix elements plus string hadronization.

2. The role of perturbation theory in e^+e^- annihilation to hadrons

As stated in section 1.2 the bulk properties of hadronic events in Z^0 decay are established early in the fragmentation when virtualities are large and QCD perturbation theory is valid. It is an important issue to establish to what extent pQCD dominates and what contributions are made by non-perturbative effects.

2.1. Matrix elements and showers

Two basic approaches are used to calculate hadronic event properties. The use of fixed-order perturbation theory is justified by the smallness of the running strong coupling constant [22] at M_Z, $\alpha_s(Q^2) = 4\pi/\beta_0 \ln(Q^2/\Lambda^2) \approx 0.12$. Known results include the total hadronic cross section to three loops, order-α_s^3 [5]. Complete one-loop, order-α_s^2 calculations are available [23] for planar (i.e. 3-jet dominated) event shapes, including contributions due to the orientation of the event plane with respect to the beam direction [24] and to quark mass effects [25]. Partial order-α_s^3 results are known for 4-jet distributions [26]. Tree-level calculations, up to order-α_s^3, of 5-jet distributions are also available [27]. However a complication arises in this approach because tree-level diagrams diverge whenever external partons become soft or collinear and related negative divergences arise in virtual (loop) diagrams (in addition to ultraviolet divergences). Fortunately, in sufficiently inclusive measurements such as the total hadronic cross section it is guaranteed that the two sets of divergences cancel [28]. Unfortunately in more exclusive quantities such as event shapes the cancellation is no longer complete and large logarithmic terms remain, generically of the form $L = \ln(Q^2/Q_0^2)$. Since $\alpha_s L$ is of order unity this can spoil the convergence of naive perturbation theory.

In the second approach the perturbation series is rearranged in terms of

powers of $\alpha_s L$: $\sum_n a_n(\alpha_s L)^n + \alpha_s(Q) \sum_n b_n(\alpha_s L)^n + \cdots$. The first infinite set of terms represent the leading logarithm approximation (LLA), then the α_s-suppressed next-to-LLA and so on. Many of these terms have been identified [29] and summed using renormalization group techniques. They are conveniently expressed via Q^2-dependent fragmentation functions whose evolution is controlled by Altarelli-Parisi type equations [30]:

$$Q^2 \frac{\partial D_h^a(x, Q^2)}{\partial Q^2} = \int_x^1 \frac{\mathrm{d}z}{z} \frac{\alpha_s}{2\pi} \sum_b P_{bb'}^a(z) D_h^b\left(\frac{x}{z}, Q^2\right) \tag{9}$$

Here, the so-called splitting functions, $P_{bb'}^a(z)$, may be thought of as giving the probability of finding parton b (and b') inside a and carrying a fraction z of its momentum. Monte Carlo event generators implement solutions to these equations as parton showers [6, 11, 31]. More recently the resummed results for a number of event shapes have been calculated [32] and combined with the fixed order approach [33]. The Durham jet clustering algorithm [34] for example was proposed to allow such a resummation for jet rates.

2.2. Global event properties

At very low $\sqrt{s}$ little structure is present in hadronic events, beyond that due to the presence of hadronic resonances, and these can be described essentially by isotropic phase space [35]. This is because the momentum scales involved in the hadronization, typically 200 MeV, are comparable with those of the proto-jets. At higher energy, due to the preferred collinear nature of gluon radiation, the hadrons clearly form collimated pairs of back-to-back jets with angular distributions compatible with those of the primary $q\bar{q}$ pairs [36]. Around $\sqrt{s} \approx 30$ GeV a significant fraction of events deviate from a simple linear configuration: this was interpreted as first evidence for gluons [37]. At the Z^0, hard, non-collinear, gluon radiation is manifested in multi-jet event structures [38].

Event shape variables have been developed to be sensitive to the amount of acollinearity and hence the presence of hard gluon radiation [1]. Since theoretical predictions are at parton level [39], hadronization corrections, derived from Monte Carlo models, must be applied before making comparisons to data. Away from phase space boundaries the corrections are modest, but not negligible (of order 10%), and order-α_s^2 calculations generally describe the data well [40], particularly so when resummed [41]. In the case of planar variables such as thrust, transverse momentum in the event plane, wide jet broadening etc, this allows α_s to be measured, and good consistency is seen with other measurements [42]. Only a leading-order description of aplanar, four-parton, event shapes such as the D-parameter, transverse momentum out of the event plane $p_\perp^{\mathrm{out}}$, the four-jet rate etc, are presently available, although partial results

are available [26] in higher order. Here agreement between data and Monte Carlo is less satisfactory, with 30% discrepancies occurring for $p_\perp^{\mathrm{out}}$ and the 4-jet rate [11, 43, 44]. Hopefully the situation will be improved by matching the showers to exact fixed-order results. This will prove important because of a reliance on Monte Carlo models in establishing variables to discriminate at higher energies between continuum QCD events and other physics signals, such as W^+W^- pairs. This is in addition to their importance in QCD and in increasingly demanding electroweak measurements such as those involving jet charge [45].

Establishing agreement between the predictions of event generator programs and data for event shape variables has proved very important for confirming our ability to model QCD as a whole and has led to a first generation tuning of the Monte Carlo models [46, 47]. A second generation of tunings, which also take into account data on identified particle production, are now becoming available [11, 43, 44]. This tuning is not a trivial exercise as it is often the case that a distribution depends in a complex way on a model's free parameters. However some specific sensitivities have been identified. The 3-jet rate is very sensitive to the QCD scale parameter Λ, indicating the dominance of the shower and pQCD. Event shapes and inclusive momentum spectra are sensitive to the shower cut-off Q_0, and also to parameters controlling the generation of transverse momentum in the hadronization. In programs that lack a shower stage it is necessary to retune the hadronization model at each $\sqrt{s}$ since this must describe the whole fragmentation process including the perturbative $\sqrt{s}$ dependence found in a shower.

2.3. Power corrections

As noted above, hadronization corrections, which at present are inherently model dependent, need to be applied to partonic predictions before comparison can be made to hadronic event properties. Empirically the differences between quantities measured at the hadron level and the partonic predictions are found to be power behaved: $\delta X \equiv X_{\mathrm{had}} - X_{\mathrm{par}} \sim 1/Q^n$. For example, in the case of massless quarks, $\delta R_{\mathrm{had}} \sim 1/Q^4$ [48], where R_{had} is the usual ratio of hadronic to μ pair cross sections; in fact this result follows from the operator product expansion (OPE) [49] and can be related to the value of the gluon condensate: $\delta R_{\mathrm{had}} \sim \langle \alpha_s G.G \rangle / Q^4$. In the case of average event shape variables, a $1/Q$ behaviour is found (the OPE does not apply in this case, due to the presence of multiple scales, and indeed no corresponding dimension-1 local operator exists). This behaviour may be established by going to the power-enhanced, low Q, region where a $1/Q^n$ variation is easily distinguished from the slow logarithmic variation of the perturbative expressions. Such a $1/Q$ behaviour is

significant because $\alpha_s^2(Q) \approx 1/Q|_{Q=M_{Z^0}}$; thus to be able to take advantage of a future $O(\alpha_s^3)$ prediction will require a better understanding of hadronization.

Three sources of power corrections are known: instantons, infrared (IR) renormalons and ultraviolet renormalons [48]. Only IR renormalons are believed to be relevant to the issue of hadronization corrections; instanton effects are too highly power-suppressed. The coefficients of pQCD series in α_s generically suffer from a factorial growth, $\sim \beta_0^n n!$, making the series formally divergent. A standard technique for dealing with this type of behaviour is to employ a Borel transformation [48]. A pole in the transform at $n.2\pi/\beta_0$ would correspond to an $\exp(-n.2\pi/\beta_0\alpha_s) = (\Lambda/Q)^n$ term in the Borel summed series: these poles are called renormalons. Unfortunately the 'residue' of the pole, equivalent to the coefficient of the $(\Lambda/Q)^n$ term, is not calculable by this purely mathematical technique.

Recently a relationship has been suggested between the positions of the renormalons and the power behaviour of perturbative series in the presence of an IR 'regulator' [50]. The basic idea is that the (resummed) perturbative calculation probes regions of phase space involving low-virtuality partons where non-perturbative confinement effects should also be important. If these regions are isolated by introducing a 'cut-off' into the perturbative calculation then requiring that any cut-off dependence is compensated by the non-perturbative hadronization correction allows the power behaviour to be determined. Using this idea, together with a gluon mass [51], a $1/Q$ correction was derived for the thrust T, C-parameter and longitudinal cross section σ_L with all the coefficients proportional to a common scale: $\delta\langle T \rangle \propto -4C_F/\pi$, $\delta\langle C \rangle \propto 6C_F$ and $\delta\langle \sigma_L \rangle \propto C_F$. Refinements of this calculation [52] have attempted to relate the common scale to a fixed $\overline{\alpha}_s$, representing an effective measure of long-range confinement forces at an inclusive level. A dispersive approach indicates that the numerator of the $1/Q$ term may involve several coefficients, for example proportional to $\ln(Q/\Lambda)$.

The subject of power corrections is an active theoretical area and still subject to dispute. However there exists the exciting prospect of a phenomenology of power corrections. This is particularly so if the corrections to various processes can be related and so shown to be universal [53] or could be developed for full distributions rather than average values. For example, according to the calculations above, $\langle T + (2/3\pi)C \rangle$ would have no leading $1/Q$ power correction, enabling a more accurate high-Q prediction [51].

It is interesting to compare these speculations with the results of a simple tube model [42, 54] calculation. The idea is that after hadronization a parton jet is equivalent to a tube of hadrons distributed uniformly in rapidity, y, along the jet axis with transverse mass μ/unit y and length Y. Thus the total energy and momentum of the jet are: $E = \mu \sinh Y$ and $P = \mu(\cosh Y - 1)$. In a two-

jet event the thrust is simply given by $T = P/E$, so that $\delta\langle T \rangle = -2\mu/Q$; likewise $\delta\langle C \rangle = 3\pi\mu/Q$ and $\delta\langle \sigma_L/\sigma_{\text{tot}} \rangle = (\pi/2)\mu/Q$. Fitting to data, all these estimates are consistent with $\mu = 0.5$ GeV.

2.4. Direct photons

Direct photons, which are unaffected by hadronization, offer an alternative way to probe the early perturbative event structure [55]. In these events, cross sections are not simply given in terms of the quark charges but reflect the competition in showers between q→qg and q→qγ branchings in a way that is sensitive to the choice of evolution variable [56]. Here agreement with experiment has been less satisfactory [57], particularly for rather soft or very isolated photons; for example n-jet+γ cross-section results [58] disfavour the virtuality ordering employed in JETSET's parton shower [21]. This has led to some development of the Monte Carlo shower algorithms [57]. A more critical test will be the rate of soft, wide-angle photons, but here one must be especially wary of non-prompt photons arising from decays of particles produced in the hadronization [59].

2.5. Colour coherence phenomena

Long-wavelength quanta see event structures on larger scales and so are sensitive to the presence of neighbouring charged partons [8]. This results in the effective radiating units being charge-anticharge dipoles [60] and leads to a suppression of soft gauge quanta due to the requirement of coherence. This is true of QED and QCD but in the latter, because gluons carry colour charge, one must also allow at leading order for changes in the colour antennae formed by the hard partons.

Effects due to colour coherence are expected in both the perturbative and non-perturbative stages of an event [61]. In the parton shower they can be simply incorporated by requiring angular ordering — that is successive branchings are nested [8, 62]; this is known as the modified leading logarithm approximation (MLLA). As noted earlier, in JESTET angular ordering is imposed on an initially incoherent shower [21], in HERWIG it is built into the choice of evolution variable [17], it is intrinsic to the colour dipole model used by ARIADNE [12] and it is not included in COJETS [15]. Hadronization models also respect an event's colour structure in accordance with Local Parton Hadron Duality (LPHD) [63], discussed below. Strings may be regarded as the natural limit of an evolving chain of colour dipoles whilst clusters may be thought of as the final, colour neutral, dipoles. In all Monte Carlo models the treatment of both stages is based on the large N_c approximation to the colour flow [64] which gives very good agreement with known full analytic results [65].

2.5.1. The string effect The classic direct test of inter-jet colour coherence is the 'string effect' — a comparison of the particle flows between the jets in qq̄g events [66]. As the historic name suggests, the relative depletion between the qq̄ and qg jets was expected to have a non-perturbative origin [67]; later, assuming LPHD, a perturbative explanation was found [60]. To describe the Z^0 data [43, 68, 69] it is necessary to employ a coherent shower with an approximately equal contribution coming from the non-perturbative hadronization model (but see [61]). A second classic measurement [70], proposed in [71], is the relative depletion between the qq̄ pair in qq̄g and qq̄γ events [69, 72, 73]. The azimuthal angular dependence of particle flow in qq̄g events has also been studied [74]. In order to avoid having to find jets, the energy-multiplicity-multiplicity correlation can be used to measure the inter-jet coherence [43], though in this case the pQCD calculation suffers large corrections [75]. (A related quantity, the asymmetry in the particle-particle correlation, has even been suggested [76] as a way to measure intra-jet coherence effects [43, 77].) Again all of the above studies at the Z^0 confirm that Monte Carlo models incorporating a coherent shower give the best descriptions of the data. Unfortunately a test for the 'negative qq̄ dipole', expected in qq̄g events when the large N_c approximation is not used, does not appear practical [60].

2.5.2. Fully inclusive momentum spectra The intra-jet effect of colour coherence is to limit the production of soft particles in the parton shower, leading to a 'hump-backed plateau' shape for the particle spectrum in the variable $\xi = \ln(1/x)$ [8, 78], where x is the ratio of the hadron momentum to the beam energy. By contrast, in the incoherent tube model, based on (8), there is no gluon suppression and no broad peak forms. The actual calculation is of the parton (essentially gluon) spectrum in a jet at the cut-off scale: $\sigma^{-1}d\sigma/d\xi = f(\xi; Q, Q_0, \Lambda)$, with $Q \gg Q_0 \gtrsim \Lambda_{QCD}$, which it is then argued also applies to the hadron spectrum. The result is a rather unwieldy expression so that often LPHD is invoked, in the rather technical sense of taking the limit $Q_0 \to \Lambda$ [63], to obtain the simpler, more fully evolved, limiting spectrum. Finally in the peak region a distorted (downward skewed, platykurtic) Gaussian function [79] is applicable. The Z^0 data [46, 80, 81, 82, 83, 84] are qualitatively well described; quantitatively the limiting spectrum is a little too narrow in the peak region, where the distorted Gaussian fits better, although not in the tails. The coherent Monte Carlo event generators [12, 17, 21] give the best fits (however see [85]).

A particularly interesting measurement on the ξ spectrum is that of the peak position, $\xi^\star$. This occurs at low momentum where the occurence of successive parton branchings should lessen any dependence on the primary

quark flavour. (Measurements of the width, skewness, etc are statistics limited and sensitive to primary quark flavour effects in the distribution's high momentum tail). In pQCD the Q dependence of $\xi^\star$ is predicted to be linear in $\ln(Q/Q_0)$ whie the width grows as $\ln^{3/2}(Q/Q_0)$ [78]. Specifically $\xi^\star = a + n\ln(Q/Q_0)$ (i.e. $x^\star = C(Q_0/Q)^n$) with $n = 1$ in the incoherent double logarithm approximation and $n = 1/2$ in the coherent MLLA, corresponding to a harder spectrum. The Z^0 data when combined with lower energy results (see [86]) clearly prefer $n = 1/2$ especially when higher-order corrections are included [79, 87]. Similar conclusions have been reached from Breit frame analyses of deep inelastic scattering ep events at HERA [88].

A closely related measurement is that of two-particle momentum correlations [89]. Qualitative agreement is seen with the expectations based on the pQCD distribution of gluon pairs in a shower [90]. However to obtain quantitative agreement large corrections to the prediction should be anticipated [91].

Finally, scaling violations are seen when comparing the fragmentation function, $\sigma^{-1}\mathrm{d}\sigma/\mathrm{d}x$, measured at the Z^0 to those from lower energies [83, 84], after making allowance for the varying primary quark favour mix (see figure 1). As in deep inelastic scattering these variations are controlled [30] by Altarelli-Parisi equations (9) which allows α_s to be determined [92].

2.5.3. Charged particle multiplicity The integral of the momentum distribution of all particles gives the event multiplicity. Soft particles make a significant contribution to this total so that again colour coherence is important. The $\sqrt{s}$ dependence of the first few moments of the distribution of event multiplicities is calculable in MLLA [93]. The effect of coherence is to slow the growth of the mean multiplicity with $\sqrt{s}$ [94] as compared to the LLA result [95]. The MLLA prediction for the mean works well when higher-order corrections are included [81, 87, 96, 97, 98, 99], as do several more phenomenological functions of $\sqrt{s}$ [100], including a simple statistical phase space model [101]. However this is not the case for the incoherent COJETS model. The width (or equivalently the second binomial moment) is larger than the data [97, 102] although further relatively large higher-order corrections might be anticipated from the ratio of leading to next-to-leading order predictions [93]. At high energy the ratios of these moments are expected to become $\sqrt{s}$ independent, a feature already present in the data. This would imply KNO scaling [103] which is indeed seen to work well. The ratios of moments as given by QCD behave approximately like those of the negative binomial distribution (NBD) [104] (with parameter $1/k \approx 0.4 - 0.9\sqrt{\alpha_s}$), though empirically the discretized log normal distribution (LND) [105] is a better fit to the multiplicity distribution.

Multiplicity distributions have also been studied in restricted rapidity

intervals [98, 106] where the influence of global conservation laws may be reduced. The shape of the distribution becomes narrower for small rapidity (y) windows, and some structure, possibly attributable to multi-jet events [107], arises at intermediate y ranges. These features are described well by JETSET, but less well by HERWIG or the simple NBD and LND.

In addition to studies of the natural flavour mix, light and heavy quark initiated events have been investigated separately [108, 109]. A large quark mass reduces phase space and shields the the collinear singularity associated with forward gluon emission, causing a relative suppression of forward hadrons [19]. In practice observation of the reduction in associated multiplicity due to this 'dead cone' [110] is hampered by the presence of the heavy hadron's decay tracks (5.5±0.1 per b-hadron [109]) which actually ensure a higher multiplicity than in u,d,s events. However the difference in multiplicity is predicted [111] and seen to be $\sqrt{s}$ independent [108, 109, 112]. (A variation of 0.4 tracks is expected from the change in the heavy quark fraction between 12 ($\Upsilon(4S)$) and 91 (Z^0) GeV [109]; this is below the level of the experimental errors).

2.6. Local parton-hadron duality

Implicit in the above calculations of event features, including those by Monte Carlo methods, is the assumption that pQCD provides the dominant contribution. This is especially true for infrared (soft gluon) sensitive quantities. In other words hadronization and resonance decays causes little disruption of the features already established by the cascade. In the absence of a well developed theory of hadronization this is in fact a minimum requirement for pQCD calculations to be worthwhile. In terms of the earlier space-time picture, described in subsection 1.2, this idea of 'soft confinement' appears very natural and it is indeed in many instances supported by data [113]. Since in this picture it is the relatively soft *gluers*, following in the wake of the hard quarks and gluons, which cause hadronization to occur, then except for a 'collective' action by the *gluers*, large momentum transfers during hadronization are precluded.

An important observation which allows this picture to be taken further is that after a coherent shower, hadronization should occur locally. This is seen by considering two separating perturbative partons, with opening angle θ, and two *gluers* each emitted at θ_ϵ to their parent partons [8]. At the time the two *gluers* simultaneously hadronize, their transverse and longitudinal separations are given by:

$$d_\perp \approx R.\frac{\theta}{\theta_\epsilon} \gg R \qquad\qquad d_\parallel \approx R\theta.\frac{\theta}{\theta_\epsilon} \gg R\theta \sim R \qquad\qquad (10)$$

Here the inequalities follow from the strong angular ordering condition $\theta_\epsilon \ll \theta$ [62]. This implies that the hadronizing *gluers* form only a rather low density system in configuration space. The large inter-*gluer* separations effectively limit the influence which one hadronizing parton system can have on a neighbour. This locality hypothesis also receives strong support from the pre-confinement property of pQCD [114] (see section 3.3).

In this scenario the local, and essentially independent, nature of each parton's hadronization leaves little scope for long-range effects. Therefore hadronization should not significantly alter an event's angular structure or its energy and multiplicity distributions or their correlations, but only provide a 'correction'. It is beyond this approach to predict actual production rates of specific hadrons; however it would support the notion that these rates are essentially constants, dependent on at most a few nearest neighbour partons. To a certain extent present models do respect this idea and it is the quantum numbers of a few nearby partons which determine the properties of a produced hadron. This in turn gives rise to an approximate local conservation of flavour, baryon number etc.

This idea has become known as local parton-hadron duality and represents perhaps the simplest working hypothesis for the effects of hadronization. Experimental results on 'hard event properties' clearly indicate that the concept contains a grain of truth but also that it is manifestly untenable at the level of 'one parton one hadron'. Its failure should be interpreted as a need for a less trivial, non-perturbative model of hadronization. A more specific, technical definition of LPHD in terms of the limiting momentum spectrum $(Q_0 \to \Lambda)$ [63] was encountered in section 2.5.2 and will be discussed further in section 5.4.

3. Models for hadronization

So far it has been argued that the parton to hadron transition should occur locally in space-time, only involving a few neighbouring partons, and that local parton-hadron duality provides a reasonable summary of its effects on perturbative event structures. However this does not mean that hadronization is simple in detail. In practice many factors influence the production of a specific hadron and a realistic description is presently feasible only within the context of stochastic, non-perturbative models.

3.1. Independent fragmentation

Independent fragmentation is perhaps the earliest framework for hadronization [115], later becoming synonymous with the work of Field and Feyn-

man [16]. As the name suggests, the hadronization of each individual parton is treated in isolation as a sequence of universal, iterative $q_1 \rightarrow q_2 + h$ branchings based on the excitation of (di)quark pairs. Unfortunately the scheme has no strong theoretical underpinning and is rather arbitrary in its details, leading to many variants. It is used by COJETS [15] (and ISAJET [116] for hadron-hadron collisions) and is a available as a set of non-default options in JETSET [21].

$$h = (q_1 \bar{q}_2) : xP_+, p_T, m_T^2/xP_+$$

$$q_1 : P_+$$

$$q_2 : (1-x)P_+, -p_T, p_T^2/(1-x)P_+$$
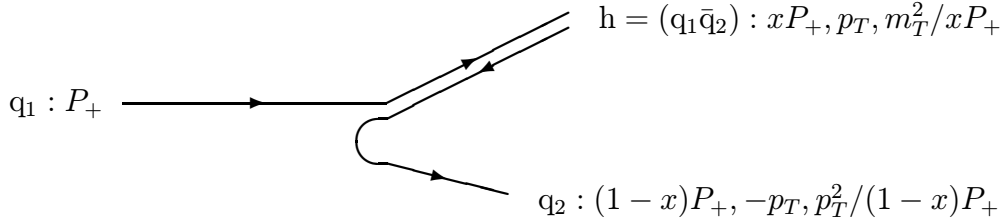
Figure 4. The 'unit cell' that is iterated in the independent fragmentation scheme, showing the light-cone momentum fractions: p_+, p_T, p_- where $p_\pm = (E \pm p_z)$. Note that the parent quark acquires a mass $(m_h^2 + p_T^2)/x + p_T^2/(1-x)$.

Figure 4 illustrates the 'unit cell' used in the iterative implementation of the scheme. The flavours of the (di)quarks generated are selected in fixed ratios. Empirically it is found necessary to suppress both strange quarks and diquarks, u:d:s $= 1:1:r_s$ with $r_s \approx 1/3$ and q:qq$' = 1:r_{qq}$ with $r_{qq} \approx 1/9$. Further rules are required to choose between the various (low lying) hadron states of a given flavour. The light-cone momentum fraction, $x = p_+^{had}/p_+^{q_1} = (E + p_z)_h/(E + p_z)_{q_1}$, of the produced hadron, h $= q_1 \bar{q}_2$, is given by a longitudinal fragmentation function, such as

$$f(x) = 1 - a + a(1 + b)(1 - x)^b \tag{11}$$

In COJETS a dependence on the mass of an emitted light hadron is also built in. Special forms are employed in the case of heavy quarks where harder momentum spectra are expected (see section 5.4.2). The transverse momentum is chosen from a Gaussian distribution $\exp(-p_T^2/\sigma^2)$ possibly with a width that narrows as $x \rightarrow 0$ and $x \rightarrow 1$, as expected from phase space considerations. The iteration continues until a backward moving hadron would be produced ($p_z < 0$) or, in the case of COJETS [15], the sum of jet masses violates an available energy bound [117]. Diquarks are treated just as quarks, whilst gluons are first split into a light q$\bar{q}$ pair (the momentum is shared equally in COJETS) and the above algorithm used but with retuned parameters.

Typically a large cut-off value, $Q_0 \approx 3$ GeV, is used, resulting in only a few final-state partons. Since these partons are treated in strict isolation,

essentially ad hoc remedies must be used to ensure global conservation of quantum numbers. Conserving four-momentum after the partons have acquired masses proves particularly troublesome because event shape variables, and hence α_s determinations, are sensitive to the nature of the chosen solution [118]. A fully Lorentz-invariant scheme has been proposed in [119] but it is hard to implement in general and only JETSET [21] contains a simplified version, as an option.

In addition to the independent hadronization of the final-state partons, independent fragmentation models also naturally employ incoherent parton showers, the combination of the two features offering, by today's standards, a mediocre description of the exacting Z^0 data. However when applied to the hadronization of a back-to-back $q\bar{q}$ pair there is little practical difference between independent and string-based models. (It is only after gluon jets occur that differences become apparent). One can therefore speculate that a possible way to improve the situation is, after the forced gluon splitting, to apply the model to each neighbouring, colour singlet $q\bar{q}'$ pair in its own CoM frame just as to a pair of back-to-back jets.
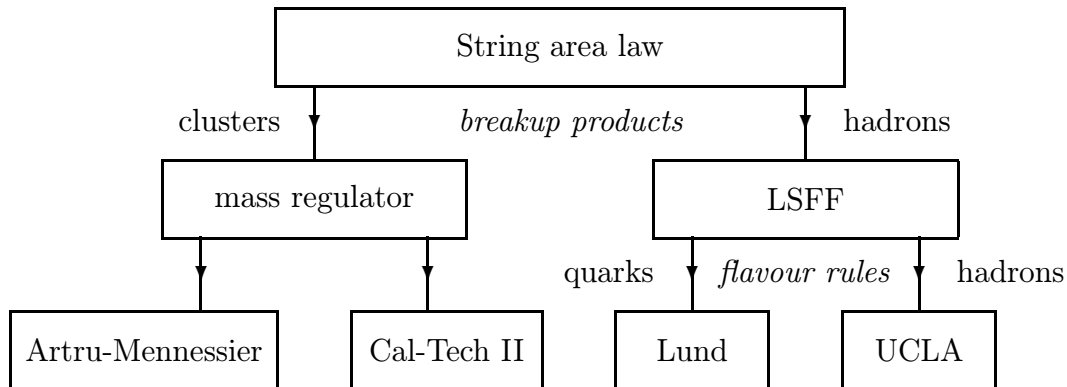
3.2. String models

When a pair of oppositely coloured quarks move apart it is thought that the self-interacting colour field between them collapses into a long, narrow flux tube/vortex line, called a string. Neglecting a short-range 'Coulomb' term the energy of this system appears to grow linearly with the separation. That is, the string has a uniform (rest) energy density or constant tension, estimated to be $\kappa \approx 1$ Gev/fm. This is equivalent to a linear confining potential as expected from Regge phenomenology ($\kappa = 1/2\pi\alpha'$) [120], bag model calculations [121], lattice studies [122] and quarkonium spectroscopy [123]. This picture of a collapsed field is analogous to a chain of magnets [124] and the behaviour of magnetic fields in (type I/II) superconductors [125].

The transverse size of a string, $\langle r^2 \rangle = \pi/(2\kappa)$, is small compared to a typical length. Therefore it is reasonable to try to model the string dynamics on those of a 'massless', relativistic string possessing no transverse excitations. The classical equations of motion, derived from a covariant area action, imply that in the CoM frame the two end quarks simply oscillate backwards and forwards along a line in what are known as yo-yo modes [126], seen as diamonds in figure 2. The equations of motion also admit solutions that include localized energy-momentum carrying 'kinks' which have successfully been identified with hard gluons [127]. At the end of a perturbative shower, string segments develop between neighbouring partons, the ends terminating on quarks. The full three-dimensional treatment of such a string system is rather complex,

being characterized by the appearance of new string segments as intermediate gluons lose all their momentum to the system. However, robust, covariant evolution algorithms are available [128, 129], and whilst ambiguities exist they are largely confined to the matching at gluon 'corners'. The classical equations of motion are also more complex, becoming non-linear when the end quarks are massive [130]. It is worth noting at this point that the quantized theory of the idealized string has spawned a rich and still growing subject of its own [131], which may still prove of relevance to the hadronization and confinement problems [132].

An alternative scenario for a string description of gluons arises when the possibility of an octet colour flux tube is admitted. For example, in a $q\bar{q}g$ event the quarks may be attached to triplet strings and the gluon to an octet string, all three of which join at a central node. A bag model calculation [121] suggests the ratio of octet to singlet string tensions is $r \equiv \kappa_8/\kappa_3 = \sqrt{C_A/C_F}$. If however $r > 2$ (as suggested by lattice calculations) then it becomes favourable for the octet string to split into two triplet strings and the above picture is recovered. The Montevay independent fragmentation model [119] requires choosing a frame in which the central junction is at rest.

The above describes the motion of an idealized classical string due to the exchange of energy between the end quarks and the string; in reality a second process is also believed to contribute. Quantum mechanical effects allow the the creation of $q\bar{q}$ or $qq'\bar{q}\bar{q}'$ pairs in the colour field of a stretched string, causing it to break in two *à la* the snapping of a magnet. This picture is the basis for the Lund group's familiar string hadronization model [14, 128, 133]. However the Lund version is only one of several possible [134, 135, 136], as illustrated in figure 5.

Figure 5. A family tree for string models.

The starting point for all string-inspired hadronization models is Wilson's exponential area decay law, $d\mathcal{P}/dA = P_0 \exp(-P_0 A)$ [122]. This describes the

probability of a string break occurring due to the creation of a $q\bar{q}$ or $qq'\bar{q}\bar{q}'$ pair in the colour field at a point containing the space-time area A within its backward light cone. As strings are believed to be uniform along their length, the probability of pair creation, P_0, is a constant per unit area. Now the momentum of a string fragment is proportional to its spatial extent ($E = \kappa\Delta x$ and $p_Z = \kappa\Delta t$) such that the string fragment mass is given by $m^2_{\text{string}} = 2\kappa^2 A$, so that the decay law can be reformulated as $\mathrm{d}\mathcal{P}/\mathrm{d}m^2 = b\exp(-bm^2)$ with $b = P_0/(2\kappa^2)$. Since $\langle A \rangle = P_0^{-1}$ this implies that on average the string break-up points, and hence the hadron formation points, lie scattered about a hyperbola: $\tau^2 = t^2 - x^2 = 4/P_0 \sim 2\langle m^2_{\text{string}}\rangle/\kappa^2$. This in turn implies that the slowest moving fragments form first near the centre of the string (this is true in any frame as the break-up points are space-like separated) — an inside-out pattern is assured [9].

Before constructing an actual model one must decide what the string fragments are to be identified with: either continuous mass fragments [134, 137] — clusters — which then decay into hadrons, or actual discrete-mass hadrons [138]. The first choice leads to the original Artru-Mennessier [134] or CalTech-II [135] schemes and the latter to the Lund [14] and UCLA [136] schemes.

3.2.1. The Artru-Mennessier/CalTech-II schemes Repeatedly applying the area decay law alone will result in an infinite sequence of ever smaller string fragments [134, 139]. One way to see this is to note that the area law is equivalent to a joint distribution in light-cone momentum fraction x and transverse mass $m^2_\perp$, which reduces to a divergent $m^2_\perp$ distribution:

$$\frac{\mathrm{d}^2\mathcal{P}}{\mathrm{d}x\mathrm{d}m^2_\perp} = \frac{b}{x}\exp\left(-b\frac{m^2_\perp}{x}\right) \implies \frac{\mathrm{d}\mathcal{P}}{\mathrm{d}m^2_\perp} = bE_1(bm^2_\perp) \overset{m^2_\perp \to 0}{\sim} \ln(bm^2_\perp) \qquad (12)$$

(E_1 is the first exponential integral function.) Since a physical interpretation of string fragments with very low mass is implausible, in practice a regulator is required.

In the more fully developed CalTech-II model [135] this regulator is supplied by introducing a probability to allow a given string fragment to undergo any further splitting:

$$\mathcal{P}(\text{further break}) = \Theta(m_{\text{string}} - m_0)\left[1 - \exp\left(-P_0\frac{(m_{\text{string}} - m_0)^2}{2\kappa^2}\right)\right] \qquad (13)$$

where P_0 and m_0 are free parameters, the latter related to the threshold mass for a string's decay to two hadrons. The function Θ is the Heaviside step function: $\Theta(x) = 0$ for $x < 0$ and $\Theta(x) = 1$ for $x \geq 1$. If allowed, a break-up point is selected according to the area law with the $q\bar{q}$ or $qq'\bar{q}\bar{q}'$ flavour chosen according to fixed probabilities from those kinematically allowed; at this point

no transverse momentum is introduced. Occasionally a final string fragment is below a second cut-off and this is replaced by a single hadron. Otherwise the fragments undergo a comparatively complex sequence of cluster decays in which phase space determines the produced flavours and momenta.

Whilst the CalTech-II model has attempted to combine the desirable features of both string and cluster models, its success in confronting data has been at best mixed. Consequently the Monte Carlo program has fallen out of favour and is no longer being actively developed.

3.2.2. The Lund scheme The alternative to a continuous mass spectrum for the string fragments is a discrete spectrum, the allowed values of which are identified with the masses of known hadrons. This approach is followed by the Lund [138] and UCLA [136] models. Requiring a string to fragment into hadrons of given (transverse) mass leaves only the choice of the hadrons' light-cone momentum fractions, x, free. These x values may be iteratively chosen according to several possible distributions [21] and still remain true to the area decay law. However a set of plausible assumptions greatly reduces the number of allowed fragmentation functions [140, 141]. The assumptions are: the equations of motion are those of a classical, relativistic, constant tension string with no transverse excitations; a statistical left-right symmetry; a central rapidity plateau; and negligible end effects. The resulting x-distributions are known as the Lund symmetric fragmentation functions (LSSF).

$$f(x) = \frac{N_{\alpha\beta}}{x} x^{a_\alpha} \left(\frac{1-x}{x}\right)^{a_\beta} \exp\left(-b\frac{m_\perp^2}{x}\right) \Bigg|_{a_\alpha = a} \equiv \frac{\mathrm{d}^2\mathcal{P}}{\mathrm{d}y\mathrm{d}A} = C_0 C_a A^a e^{-b\kappa^2 A} \ (14)$$

The coefficient a_α relates to the parent quark flavour and a_β to that of the quark or diquark produced in the colour field: in practice only diquarks are allowed a different value of a [21]. Taking every $a_\alpha = a$ the LSFF simplifies (compare to (12) where $a = 0$) and is equivalent [140] to a flat rapidity, $y = 1/2 \ln[(E + P_z)/(E - P_z)]$, distribution and the Wilson area law modified by a perimeter (Coulombic) term.

An important issue now is to prescribe how the actual hadrons are chosen, and here again the models diverge. The Lund approach [142] is based on an attempt to model, principally through flavour and spin selection rules, the supposed quark dynamics in the strong colour field that is a string. The idea is a development of the concept of fermion pair production in a strong electromagnetic field [143, 144]. To supply the energy for a $q\bar{q}$ pair, each of transverse mass $m_\perp^2 = m_q^2 + p_\perp^2$, it is necessary to consume a finite length of string $(2m_\perp/\kappa)$. The quarks have equal and opposite $p_\perp$ since no transverse string excitations are permitted in the model. If the $q\bar{q}$ pair are produced locally at a point then they must tunnel out to this classically

required separation. Using the WKB approximation for the matching of the quark wavefunctions at the classical turning points suggests a suppression factor [143, 144]:

$$\exp\left(-\frac{\pi}{\kappa}(m_{\mathrm{q}}^2 + p_\perp^2)\right) = \exp\left(-\frac{\pi}{\kappa}m_{\mathrm{q}}^2\right) \times \exp\left(-\frac{\pi}{\kappa}p_\perp^2\right) \tag{15}$$

This would be a crude approximation to the known full QED expression for the production of a single q$\bar{\mathrm{q}}$ pair, $\sum_n n^2 \exp(-n\pi m_\perp^2/\kappa)$. Unfortunately it is not known what to use for the quark masses in (15) (see reference [7] for some discussion of the range spanned by current and constituent quark masses) and so only qualitative conclusions can be drawn. Among these are:

- The transverse momentum suppression is the same for all quark flavours
- Charm and bottom quarks will not be produced from the string
- Since $m_{\mathrm{s}} > m_{\mathrm{u}} \approx m_{\mathrm{d}}$ (SU(3)$_{\mathrm{F}}$ is broken), strange quarks will be suppressed relative to up and down quarks:

$$\frac{\mathcal{P}(\mathrm{s})}{\mathcal{P}(\mathrm{u})} \equiv \gamma_{\mathrm{s}} < 1 \tag{16}$$

- Production of diquarks will be suppressed:

$$\frac{\mathcal{P}(\mathrm{uu})}{\mathcal{P}(\mathrm{u})} < 1 \qquad \frac{\mathcal{P}(\mathrm{us})}{\mathcal{P}(\mathrm{uu})} \lesssim \gamma_{\mathrm{s}} \qquad \frac{\mathcal{P}(\mathrm{ss})}{\mathcal{P}(\mathrm{uu})} \approx \gamma_{\mathrm{s}}^4 \tag{17}$$

  the power 4 arising in the last term because of the quadratic dependence of the tunnelling probability on the diquark mass.

Also the Gaussian $p_\perp$-distribution in (15) is best regarded as a first approximation, leaving open the possibility of long tails originating from unresolved gluon emission [21, 145]. This may account for the fact that the prediction for the width of the hadron $p_\perp$-distribution, $\sqrt{\kappa/\pi} = 0.25$ GeV, proves too narrow compared with measurements of ≈ 0.40 GeV [43, 44].

As yet the model does not supply as much guidance on how to account for any possible spin dynamics. Two factors influence the relative production ratios of same flavour mesons [14, 146]. First are the $(2J + 1)$ spin counting factors. Second is the need for the quark produced in the string to match onto the wavefunction of the produced meson. At the classical boundary to the tunnelling region the meson wavefunction is expected to behave as $1/\sqrt{m_\perp}$ [14]. The result for the vector to pseudoscalar meson production ratio is therefore:

$$\frac{V}{P} = 3 \times \left(\frac{m_\perp(V)}{m_\perp(P)}\right)^{\alpha \approx 1} \tag{18}$$

As $(m_V - m_P)/(m_V + m_P)$ is 0.69 for π/ρ and 0.004 for B/B*, the primary ρ/π ratio is taken to be 1 whilst the B*/B ratio is fixed at 3. Radially and orbitally excited mesons are expected to be suppressed [21], although $L = 1$ mesons may be included at the expense of a new parameter for each of the four additional families of states.

The fact that the transverse mass is involved in the suppression factor proves unimportant except for pions, since $\langle p_\perp^2 \rangle \approx (0.3 \text{ GeV})^2 \gtrsim m_\pi^2$. Hence it is anticipated that (directly produced) pions will be enhanced at low $p_\perp$ and have a tighter $p_\perp$ distribution than, say, ρ mesons or kaons. Also, because of their small mass, neighbouring-pion correlations are anticipated [147].

To summarize, the Lund prescription for an iterative string fragmentation scheme is: first choose a quark flavour; then choose a produced hadron species; select a quark transverse momentum; and finally select an x value. The normalization, N, of the LSFF in (14) for this case is thus:

$$N^{-1} = \int dx \frac{(1-x)^a}{x} \exp\left(-b\frac{m_\perp^2}{x}\right) \equiv F(m_\perp^2) \qquad (19)$$

The resulting model requires the specification of a relatively large number of free parameters [21]. Much of this can be traced back to the unknown properties and dynamics of (di)quarks. The UCLA model [136] attempts to finesse these problems by formulating an iterative scheme only in terms of known hadron properties, thereby trying to avoid the issue of quark production in a string

3.2.3. The UCLA scheme At the heart of the difference between the Lund and UCLA models is a reinterpretation of the LSFF [148]. In the UCLA model [136] the LSFF is used to choose both x and the species of produced hadron. This means that N (19) becomes an *absolute* normalization:

$$N^{-1} = \sum_h (\text{CG})^2 \int dp_\perp^2 F(m_h^2 + p_\perp^2) \qquad (20)$$

The sum runs over all hadrons containing the parent quark, with CG the appropriate Clebsch-Gordon coefficients for the hadron wavefunction. Since N is now a common constant the hadron mass dependence appearing in the exponential term in (14) immediately implies a suppression of heavy hadrons and a stiffening of their fragmentation function [148].

An instructive way to view the difference between the Lund and UCLA approaches is to consider the complete weight for the production of a set of N hadrons $\{h_i\}$ in a string of mass s stretched between two quarks q_0 and $\bar{q}_N$, as illustrated in figure 6.

The 'master' equation for this process's weight is given by:

$$dW_{\{h_i\}}^{q_0 \bar{q}_N}(s) = \delta^{(4)}(P_0 - \sum_{i=1}^{N} p_{h_i}) \exp\{-bA\} \times \prod_{i=1}^{N-1} S_{q_i} \exp\{-\kappa(p_\perp^2)_{q_i}\}$$

$$\times \prod_{i=1}^{N} N_{h_i} [\text{CG}(q_{i-1}, \bar{q}_i; h_i)]^2 \exp\{-\kappa'(p_\perp^2)_{h_i}\} d^4 p_{h_i} \delta(p_{h_i}^2 - m_{h_i}^2) \qquad (21)$$

The first two terms impose overall four-momentum conservation and the area decay law. The second set of terms is associated with the production of
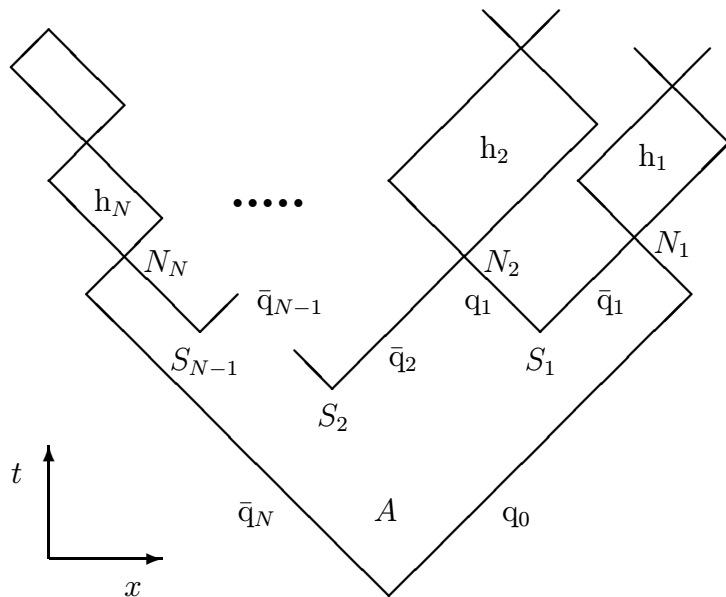
Figure 6. A schematic diagram of a fragmenting string: the S_i control the production of quark flavours; the "knitting" factors N_i control which hadrons form from the quarks.

the $N-1$ intervening $q\bar{q}$ pairs: S_{q_i} is a possible quark flavour suppression factor and κ controls the quark's Gaussian $p_\perp$-distribution. The third set of terms is associated with the N hadrons $\{h_i\}$ formed out of the quark-antiquark pairs $\{(q_{i-1}\bar{q}_i)\}$: CG is the Clebsch-Gordon coefficient for the hadron's SU(6) wavefunction, N_{h_i} is an additional "Knitting factor" and κ' controls the hadron's assumed Gaussian $p_\perp$-distribution. The approaches to these various terms in the UCLA and Lund models are summarized in table 1.

Table 1. The two sets of factors appearing in (21) and figure 6 in the UCLA and Lund string models indicating the typical values assigned.

Factor	UCLA [136]	Lund [21]	Controls
S_q	1	γ_s, $(ud)_1/(ud)_0, \ldots$	quark flavour suppression
κ	0	"π/κ"	quark $p_\perp^2$ suppression
κ'	$(n-2)b/(n+1)$	0	hadron $p_\perp^2$ suppression
N_h	N (const.)	$F(m_\perp^2)^{-1}\{V/P,\ldots\}$	hadron "knitting" factor

A number of points in the iterative implementation of the UCLA scheme are noteworthy. First, the original model was designed to look ahead to the next iterate. For example, if the first hadron leaves behind a u or an s quark then the next hadron is most likely to be a pion or a kaon, and the latter choice

is (doubly) suppressed because of the higher masses of strange hadrons. This was an attempt to mimic the quantum mechanical projection of the string onto a set of hadrons {h}. In fact, using (21) and the UCLA ansatz for an event's overall weight it is possible to derive an iterative scheme that automatically generates chains of hadrons according to this overall distribution. That is, the projection from partons to hadrons is automatically taken into account. The required fragmentation function is remarkably similar to the original LSFF:

$$\frac{(1-x)^a}{x}\left(1-\frac{m_\perp^2}{xS}\right)^a \exp\left(-b\frac{(m_\perp^2+p_\perp^2/(n-1))}{x}\right) \tag{22}$$

Compared to (14) a finite mass correction term appears together with a term, $p_\perp^2/(n-1)$, coming from local transverse momentum compensation, ($n \approx 2$). In the case of hadrons containing a heavy quark, x is replaced by $x_{\text{eff}} > x$ which softens the momentum spectrum and favours heavier states [136]. Second, 'multiple' so-called popcorn (discussed below) baryon production $B\overline{B}$, $BM\overline{B}$, $BMM\overline{B}$... is included (here B represents a baryon and M a meson), but due to its slow 'convergence' an ad hoc suppression needs to be introduced: $\exp(-\eta \sum m_M)$ with η free (≈ 10 GeV^{-1}). Third, the mechanism for the local conservation of hadron transverse momentum proves awkward due to an ambiguity between the quark and hadron levels. Finally, but perhaps most significantly, the model only contains four (+two) free parameters: a, b, n and η (+Λ and Q_0).

3.2.4. Consequences of the string's space-time structure   A further interesting aspect of string models is that inferences can be drawn from their associated space-time picture. These include predictions on spin correlations and effects due to quantum statistics.

If a $q\bar{q}$ pair are produced with some (equal and opposite) transverse momentum, $p_\perp$, with respect to the string, then because they are separated by a distance $2m_\perp/\kappa$ a non-zero angular momentum $L = 2m_\perp p_\perp/\kappa$ is necessarily introduced. Since total angular momentum $J = L \otimes S_q \otimes S_{\bar{q}}$ must be conserved and $\langle L \rangle \approx 1\hbar$ the $q\bar{q}$ pair typically form in a $^3P_0$ state, particularly so at higher $p_\perp$. This is expected to lead to $p_\perp$−transverse-spin correlations, and spin correlations between neighbouring hadrons [149]. Transverse polarizations are only possible because the string introduces a preferred axis. (Such an axis is implicit in the chain-like structure found in cluster models, though it is not presently utilized in them). Conservation of angular momentum is also expected to lead to a suppression of orbitally excited hadrons.

If two identical hadrons are produced from a string there exists an ambiguity in the possible rank ordering of the particles, unless they have exactly equal momentum. These two string drawings, illustrated in figure 7,
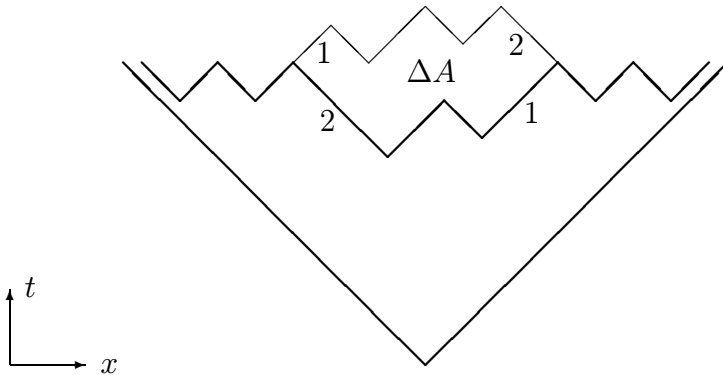
Figure 7. The two sequences of string breakings possible when two identical particles are present; all other particles are the same. This results in a difference ΔA between the enclosed total string areas.

enclose different areas. Now if, as is believed, the string area law derives from the modulus squared of a matrix element $\mathcal{M} = \exp[iA(\kappa + iP_0/2)]$ then quantum mechanical interference will occur [150]. Dependent on the Bose-Einstein or Fermi-Dirac nature of the particles the expected joint production probability becomes

$$(P_{12} + P_{21})\left[1 \pm \frac{\cos(\kappa \Delta A)}{\cosh(P_0 \Delta A/2)}\right] \tag{23}$$

which is clearly modified from the naive sum of the weights. (A quark transverse momentum correction, $(\pi/2\kappa)\Delta p_\perp^2$, is not shown in (23).) As the momentum difference squared between the identical hadrons vanishes, $\Delta A \to 0$ and any enhancement or cancellation becomes maximal. The area difference, ΔA, is related to the size of the emitting volume, likened to the Hanbury-Brown Twiss effect in optical astronomy [151], but not related directly to the total string size. This approach therefore has close parallels to a more geometric picture based on the Fourier transform of the source distribution [152]. Only identical neutral pions can be produced side by side from a string — identical charged pions must have at least one intervening hadron. Therefore ΔA will be larger for charged pions, leading to smaller correlations than for neutral pions [145]. The effects of correlations on short lived resonance decays can also be included [153, 154].

Two basic algorithms are currently available for including a Bose-Einstein event 'weight' [155]. The standard scheme available in JETSET [21, 156] involves rearranging identical boson momenta so that they are distributed according to the pairwise correlation function. Full multiboson correlations

may be included, but at the cost of additional computing time. The effect of including Bose-Einstein correlations may be likened to adding an attractive inter-boson force, leading to 'lumpier' distributions. The experimental situation is discussed in section 7.1.

3.2.5. Baryons and the popcorn mechanism In the Lund string model, baryon production poses particular problems of principle. The basic difficulty appears to stem from incomplete knowledge of the internal structure of a baryon [157]. Is it a quark-diquark system or a three quark system? This ignorance poses less of a problem for HERWIG and to some extent the UCLA string model because these essentially only need to know a baryon's mass and spin. However the Lund string works directly with the (di)quarks themselves and so in the absence of a guiding principle it therefore allows for two options, the diquark [158] and popcorn [133] baryon production mechanisms.

Figure 8. A schematic of baryon production in the diquark model (left) and 'popcorn' model (right) leading to $MB\overline{B}$ and $BM\overline{B}$ configurations respectively.

The diquark mechanism is a straightforward generalization of the quark meson production model and was the first to be fully developed [158]. However a stepwise quark model for the production of baryons was the first to be proposed [144] and implemented [159]. Whilst this only evolved later [133] (and is continuing to evolve [160]) into the popcorn mechanism it would be a misconception to regard it as especially contrived or unnatural. When a $qq'\overline{q}\overline{q}'$ (or $q\overline{q}$) pair is produced in a string's colour field with the same colour as the end quarks they precipitate a string break: the diquark mechanism [158]. When a (virtual) $q\overline{q}$ pair is produced the possibility that they have a different colour to that of the end quarks allows a non-zero colour field to exist between them in which further real $q\overline{q}$ pairs could form, leading to the sequence $B\overline{B}, BM\overline{B}$ etc: popcorn production [133]. Perhaps not unsurprisingly the popcorn mechanism requires a (modest) number of new free parameters.

The main practical consequence, so far, of introducing popcorn production appears to be a lessening of the phase space correlations between baryon-antibaryon pairs (see section 7.3). The fragmentation function for baryons is also expected to be softened [161] (compared to a meson with the same transverse mass) due to popcorn production: in particular $BM\overline{B}$ sequences cause a suppression of leading baryons [160]. (This would suggest using
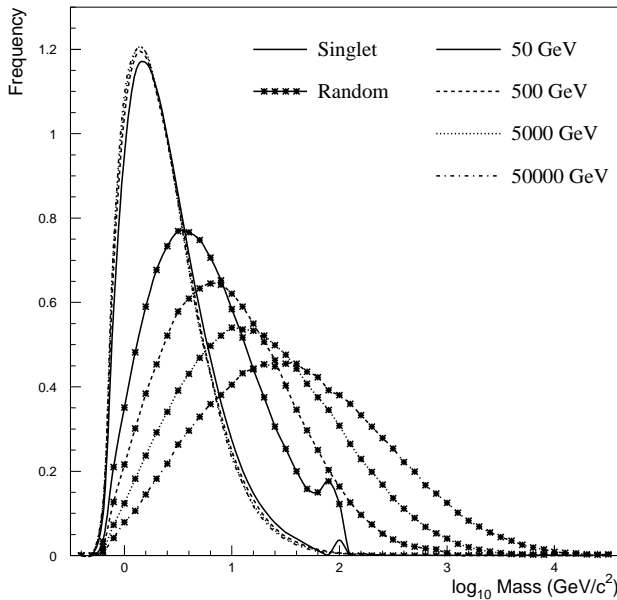
Figure 9. The mass spectrum for colour singlet and random $q_1\bar{q}_2$ clusters in a u-quark jet of four initial energies. In the random sample $q\bar{q}$ pairs from gluon splittings are excluded.

$a_{qq} > a_q$ in the LSFF (14).) The actual level of popcorn production required to describe data is still the subject of debate but it may be related to the a parameter of the LSFF [161]. Interestingly a search for the expected chain like structures, such as correlated $\Lambda K^+\bar{p}$ systems, has failed to see any positive evidence [162]. Allowing three body decays of clusters is expected to have similar effects to introducing popcorn production in string models.

3.3. Cluster models

Whilst clusters initially appeared as intermediate states in the string model of Artru and Mennessier [134] the first fully fledged cluster hadronization models originated at CalTech [137, 163]. (Cluster-like structures also naturally arose in the earlier statistical bootstrap model [164] and multiperipheral models [165].) Today the scheme is best known through the HERWIG implementation of Webber [17, 20]. This is based on the pre-confinement property proved for pQCD [114]: at the end of the perturbative shower the mass and spatial distributions of colour singlet clusters of partons spanned by quark-antiquark pairs have a universal distribution. In practice gluons remaining at the cut-off scale Q_0 are forcibly split into light $q\bar{q}$ pairs, the Wolfram ansatz [166], so that in the planar approximation [64] neighbouring quark-antiquark pairs form colour singlets. Figure 9 illustrates the resulting cluster mass distributions for u-quark initiated jets at four energies, showing clearly

the universality of the colour singlet cluster mass distribution, in contrast to the distributions for random clusters.

The mean cluster mass is of order Q_0, a few GeV, and for a colour-coherent parton shower has a spectrum falling faster than any power [167]. The distribution is independent of the initial parton type (q or g) and virtuality: this is in contrast to random quark-antiquark pairs. This universality is suggestive of the formation of intermediate 'super-resonances' which independently decay into the familiar resonances. Figure 10 illustrates the stages in the fragmentation of a parton into hadrons via cluster hadronization.
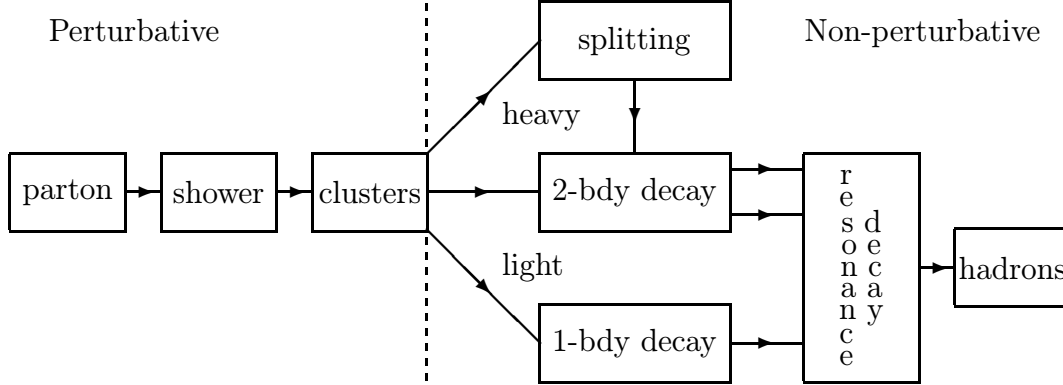
Figure 10. A schematic diagram for fragmentation via cluster hadronization.

Three masses of cluster need to be treated:

Average Most clusters have masses, m_{cl}, close to Q_0 and undergo two-body decays [20]. A quark or light diquark pair (here the diquarks serve only as a mnemonic device for quantum number conservation), $\bar{q}_3 q_3 / q_3 q_4 \bar{q}_3 \bar{q}_4$, is selected at random, and for a cluster of flavours $q_1 \bar{q}_2$ the putative hadrons $h_1 = q_1 \bar{q}_3 / q_1 q_3 q_4$ and $h_2 = \bar{q}_2 q_3 / \bar{q}_2 \bar{q}_3 \bar{q}_4$ are formed. The selection is accepted or rejected according to its phase space weight: $(2J_{h_1} + 1)(2J_{h_2} + 1)\hat{p}(m_{cl}, m_{h_1}, m_{h_2})\Theta(m_{cl} - m_{h_1} + m_{h_2})$ where J and m are the hadron spins and masses, and $\hat{p}$ is the CoM momentum of the kinematically allowed two-body decays. If accepted, the decay momenta are selected isotropically in the cluster rest frame. This prescription is in accord with the OZI rule [168].

Heavy A number of clusters in the tail of the distribution are too massive for an isotropic decay to be plausible. The criterion used is: $m_{cl} \equiv m_{q_1 \bar{q}_2} \geq m_f$ where $m_f^n = m_{max}^n + (m_{q_1} + m_{\bar{q}_2})^n$ and constituent quark masses are used. Here the label f denotes the flavour type of the cluster and m_{max} and n are variable parameters of the model. By the (repeated) device of introducing a light quark pair, heavy clusters are forcibly split into

two daughter clusters whose masses are chosen according to a power law spectrum and whose directions are aligned with the $q_1 - \bar{q}_2$ axis in the cluster rest frame [17]. This appearance of a preferred, colour field, axis is reminiscent of a string splitting.

Light Occasionally it is kinematically impossible for a cluster to decay into two hadrons. Such a cluster is decayed into the lightest hadron $h_0 = q_1 \bar{q}_2$ and four-momentum transferred to a neighbouring cluster to satisfy the mass-shell constraint [17].

In the absence of a theory of cluster decay the simplest viable approach, pure phase space, is adopted (Okham's razor) [20, 137] resulting in very few free parameters [17, 135]. Here two-body dominance of the decays is one such simplification [137]. However non-trivial matrix elements are not precluded and parameters controlling the relative production rates of (di)quark pairs in the cluster decays and also weights for the hadron representations (knitting factors) are made available to users [17, 137]. The details of heavy cluster splitting prove important: $m_{\max}$ (related to the available kinetic energy) influences the light baryon yield, n the heavy hadron yield and both influence the momentum spectra [44]. The one-body cluster decay mechanism is important for the production of rare, heavy states such as the Υ or B_c, and also for describing leading particles, to which end a number of extra parameters have been added [17].

Despite the fact that its initial purity has been somewhat corrupted by the need to handle exceptional mass clusters, the model remains a simple, compact and predictive scheme. Since clusters are typically light, limited transverse momentum is automatic, hadrons with non-zero strangeness and baryon number are suppressed because they are heavier, and the spin ratios of iso-flavour hadrons follow partly from the $(2J + 1)$ factor and partly from the larger masses of higher spin states. The model represents a well founded attempt to go as far as possible with as little as possible.

3.4. A comparison of the main hadronization models

All the major hadronization models, cluster, independent and string, are local, universal, stochastic models. They are based on a small number of recursively applied branchings, where at each iterative step probabilistic rules are applied to select flavours, spins and momenta. The main features the models are summarized in table 2.

Lorentz invariance and quantum number conservation are not troublesome for strings or clusters but are an issue for independent hadronization models requiring post facto adjustments. These essentially ad hoc remedies are

Table 2. A comparison of the main hadronization model approaches.

Feature	Hadronization Model			
	Cluster	Independent	String	
			Lund	UCLA
Principle	very simple	simple	complex	less complex
Lorentz invariant	yes	no	yes	
Flavour, charge etc, conservation	automatic	ad hoc	automatic	
Mass dep. via	hadrons	quarks	quarks	hadrons
Strangeness supp.	predicted	free param.	restricted params.	predicted
Baryon supp.	predicted	free param.	restricted params.	predicted
J^P ratios	predicted	free params.	restricted params.	predicted
Limited P_T	natural	built in	built in	natural
Frag. fn.	N/A	free	restricted by L–R symm.	
Cut-off (Q_0) dep.	significant	very strong	modest	
Stability	infrared prob.	collinear prob.	stable	
Limitations	massive clusters treated like 'strings'	requires large Q_0	light strings treated like clusters	

not always implemented (particularly in application to dirtier hadronic collisions [116]), and, worse, physical observables are known to be sensitive to details of the chosen solution [118].

Only the cluster and UCLA models, with their emphasis on hadron properties, provide succinct basic algorithms for flavour, spin and momentum selection. In their initial formulations the lack of free parameters gives these models a laudable predictive power, which is in marked contrast to the Lund string and independent hadronization models. Of course, poor fits to data could mandate elaborations of the models which in turn may then dilute their predictive power. The Lund model ought to have an advantage because it is based on a semi-quantitative picture of an underlying dynamics but this is undermined by the indirect measurability of the basic (di)quark parameters. Thus whilst the model's parameters possess a large degree of internal coherence, their must be disappointment at their large number and seemingly Byzantine complexity. To emphasize this point, 13 inputs are needed in the basic Lund model [21] to describe the 13 (assuming u↔d isospin) $L = 0$ light (u,d,s) hadrons (the number of hadrons increases to 27 if u and d are distinguished). Thus the flavour and spin aspects of the Lund model show little practical difference to the rather similar, but assumed, rules found in an empirical

independent hadronization model. However a significant difference is the way in which a string's causal structure restricts the longitudinal fragmentation function to a unique family of left-right symmetric functions [140]. No such restriction applies to independent models.

The issue of stability with respect to collinear and soft gluons arises in cluster and independent hadronization models. Specifically, the spectrum of clusters is sensitive to the emission of isolated, soft gluons. This infrared instability may be regarded either as a serious problem or, perhaps, as a warning that it is important to treat the theory correctly. Perturbative QCD does not like isolated colour charges, which are strongly Sudakov suppressed; this is responsible for the fast falling tail of the cluster mass spectrum [167]. (Recall also that many other observables, such as the mean multiplicity, are known to be infrared sensitive.) In independent fragmentation a similar problem arises when one final-state parton is replaced by two parallel partons of equal net energy, giving a different multiplicity. This collinear instability occurs essentially because the two partons are oblivious to each other's presence.

To recap, the motivation for the rules used in these models varies from the QCD-inspired, complex dynamics of strings through the minimalism of clusters to the simple expediency of independent fragmentation. In the subsequent sections we shall see how well these hadronization models compare to the various Z^0 data. However since independent hadronization makes no claim to be based on QCD, a fact reflected in the extreme arbitrariness of its parameters, we drop it from further discussion. While it is not considered a viable scheme for describing Z^0 physics it does however survive in the ISAJET [116] Monte Carlo program for hadron hadron collisions.

3.5. Colour rearrangement

Recently interest has arisen in the possibility that soft, long wavelength, gluons may cause non-perturbative rearrangements in the colour structures of events developed during the showering stage, particularly in relation to W^+W^- pair production [11, 169]. Several phenomenological models are available based on the three main e^+e^- event generators, and are summarized in table 3.

The rearrangement criterion in the ARIADNE-based models is a decrease in the λ-measure [173] which quantifies the momentum-space size of a string system. Only the second model [171] should be considered as realistic for typical events. In HERWIG at the end of the perturbative shower pairs of $q\bar{q}'$ singlet clusters may be rearranged, with fixed probability ($\approx 1/9$), if this results in a reduction in the quadratic sum of their space-time sizes. In JETSET the rearrangement criterion is based on the space-time evolution of the strings. In model I the spatial overlap of 'wide' flux tubes is used to assign probabilities for

Table 3. The main features of colour rearrangement models.

Feature	Colour Rearrangement Model				
Basic MC	ARIADNE		HERWIG	JETSET	
Author(s)	J. Häkkinen	L. Lönnblad	B.R. Webber	T. Sjöstrand	Š. Todorova
	G Gustafson			V A Khoze	
Reference(s)	[170]	[171]	[17]	[21, 172]	[11]
rearrangement:			decrease cluster	I space-time overlap	
- criterion	decrease λ measure		spatial size	II string crossing	
- in shower	no	yes	no	no	yes
- in hadron.	yes	yes	yes	yes	yes
- mult. re-arr.	yes	yes	yes	no	yes
- inter-singlet	yes	yes	yes	yes	yes
- intra-singlet	no	yes	yes	no	yes

rearrangement, whilst in model II rearrangement occurs at the first crossing of the 'narrow' vortex lines. Todorova's model [11] is an elaboration of the original model [172], allowing for multiple reconnections, including within a single colour singlet system, and self-interactions; this leads to string loops — glueballs.

As yet these models have not been thoroughly investigated, nor their consequences for Z^0 decays found. Note that when including colour rearrangement the Monte Carlos must first be retuned: for example reducing the λ-measure also lowers the average multiplicity, which must be compensated. Since the physics of colour rearrangement is universal in nature, effects should also be anticipated in all other types of hadronic interactions, including for example B-hadron decays (B$\rightarrow J/\psi X_s$) and rapidity gap events [174], where important constraints may be found.

4. The colliders and experiments

4.1. The colliders

4.1.1. LEP The LEP machine, a 27 km circumference storage ring, was conceived and constructed primarily as a Z^0 factory. In the LEP 1 mode, running at and near the Z^0 peak, a luminosity of 2.2×10^{31} cm^{-2}s^{-1} could be obtained, with beam lifetimes of up to 20 hours. Until 1992, four bunches of electrons and positrons crossed every 22 μs at the experiments. During 1993 and 1994 LEP ran in a mode allowing eight bunches, with a crossing time reduced to 11 μs. In 1995, so-called bunch trains were introduced, with four trains, each of three bunches of particles, providing a further increase in luminosity. The beam spot in 1995, the last year of extensive running at the

Z^0, was 250 μm in the vertical and 5 μm in the horizontal directions. In the years 1990, 1992 and 1994, LEP ran on the Z^0 peak to produce the largest possible number of events. In 1991, 1993 and 1995, the centre-of-mass energy was scanned across the Z^0 peak to allow studies of the Z^0 line shape and other tests of the electroweak theory.

4.1.2. SLC Unlike LEP, the SLC is a single pass collider, with the electron and positron bunches lost after each pass. The bunch crossing frequency, 120 Hz, is therefore very much lower than at LEP. The SLC is however capable of providing electron beams with large polarization. In order to increase the luminosity, the beams are tightly squeezed before the collisions to reduce their cross sectional area. This technically difficult procedure results in a beam spot of diameter 0.5 μm in the vertical plane and 2.3μm horizontally. The experiment, SLD, is able to exploit this by placing precision microvertex detectors only 3 cm from the interaction point. Since 1989 the SLC luminosity has steadily improved to around 6×10^{29} cm^{2}s^{-1}, and electron beam polarization values of 80% are now routinely achieved.

4.1.3. Experimental conditions Both LEP 1 and SLC could provide their host experiments with clean, low background, experimental conditions. In addition, the relatively low beam crossing rates allowed the experiments to implement bias-free triggers and to collect data with essentially no dead time. For studies of multihadron production at the Z^0 peak, initial-state radiation is negligible. Multihadronic Z^0 decay events could be triggered with efficiencies greater than 99% and selected offline with backgrounds (mainly due to τ lepton pair production) of less than 1%.

4.2. The detectors

The four LEP detectors, ALEPH, DELPHI, L3 and OPAL, and the SLD detector at the SLC are typical large, multipurpose, particle physics detectors designed to allow measurement of events over a large part of the solid angle. For studies of hadronization, certain features of the detectors are particularly relevant. A large, active tracking volume within a strong magnetic field allows reconstruction of jets of charged particles and of secondary vertices from strange particle decays; good track momentum and direction measurement give accurate reconstruction of systems of two or more particles; charged particle identification permits the study of inclusive identified hadrons; electromagnetic calorimetry allows measurement of inclusive π^0 and η mesons; and precision secondary vertex reconstruction and inclusive electron and muon identification may be used to identify charm and beauty particles.

The coordinate systems used by the experiments define z to be along the beam direction, so that the xy plane is perpendicular to the beams. Then r and ϕ are the usual cylindrical polar coordinates, and the xy plane is also called the $r\phi$ plane. The angle θ is normally the polar angle to the z (beam) axis.

4.2.1. ALEPH The ALEPH detector [175] was designed to provide high three-dimensional granularity with large solid angle coverage for charged particle tracking and for calorimetry. Its silicon vertex detector, drift chamber and large time projection chamber (TPC), in a 1.5 T magnetic field, give a resolution on momentum transverse to the beam directions of $\sigma(1/p_T) = 0.6 \times 10^{-3}$ $(\text{GeV/c})^{-1}$ for 45 GeV/c tracks. At low momentum, the resolution is dominated by multiple scattering which contributes 0.5% to $\sigma(p_T)/p_T$. The silicon vertex detector permits the measurement of track impact parameters with an accuracy of 25 μm+95 μm/p (with p in GeV/c) in both the $r\phi$ and rz planes, allowing excellent reconstruction of charm and beauty particles. The TPC also measures ionization energy loss, dE/dx, giving good electron identification to high momenta, π/K separation at two standard deviations (2σ) in the relativistic rise region above 2 GeV/c, and K/p separation at 1σ for momenta over 5 GeV/c. The efficiency to measure K_s^0 and Λ particles is about 50% at maximum, which occurs at about 8 GeV/c momentum. The lead/wire-chamber electromagnetic calorimeter has an energy resolution of $\sigma(E)/E = 0.18/\sqrt{E}+0.009$ and an angular resolution of $(2.5/\sqrt{E}+0.25)$ mrad (E in GeV). Along with the dE/dx information, the calorimeter gives an average electron identification efficiency of 65% in hadronic jets. The efficiency for reconstruction of π^0 mesons peaks at about 50% at 10 GeV, falling to 20% at 2 GeV and 10% at 30 GeV. The π^0 energy resolution is around 7%, independent of energy. Muons are identified using the hadron calorimeter and muon chambers; only muons above 3 GeV/c momentum penetrate the system, and these are detected with an average efficiency of 86%.

4.2.2. DELPHI A pivotal feature of the DELPHI [176] detector is the particle identification capability of its ring imaging Cherenkov detectors (RICH). These cover both the barrel and end cap regions, and have both liquid and gas radiators. When combined with ionization energy loss information from the tracking detectors, the system gives clear identification of charged particles over the whole momentum range at LEP 1. The tracking detectors of DELPHI operate in a magnetic field of 1.23 T and consist of a silicon vertex detector, an inner drift chamber, a TPC and an outer detector of drift tubes. In addition there are two forward chambers, containing planes of drift tubes, to improve reconstruction at low polar angles. The system gives a momentum

resolution $\sigma(p)/p$ of 0.7% to 1.4% in the barrel region, varying with track momentum. Measurement of K_s^0 and Λ in multihadron events has an efficiency of 30–40% over a wide momentum range. The silicon vertex detector allows track impact parameters to be measured with an accuracy which depends on momentum and polar angle, and which varies between 30 and 130 μm in $r\phi$ and between 40 and 200 μm in z. DELPHI's electromagnetic calorimeters consist of high-density projection chambers in the barrel region and lead glass blocks in the endcap regions. They are preceded by $0.8/\sin\theta$ radiation lengths of material in the barrel region, and more in the endcap regions, so that resolution is somewhat degraded. When combined with dE/dx information, the system allows electron identification with efficiency and purity values both around 50% over a wide momentum range. Photons are identified both in the calorimeters and by measuring conversion e^+e^- pairs in the TPC, allowing reconstruction of π^0 mesons. Muons above 3 GeV/c are detected using a hadron calorimeter and muon chambers with an efficiency between 75 and 85%.

4.2.3. L3 The L3 detector [177] was designed with the primary aim of reconstructing electrons, muons and photons. It is therefore more limited than the other detectors in its capabilities for studying hadronization. L3 has a low magnetic field of 0.5 T in a large cylindrical volume of diameter 12 m. The central time expansion chamber measures tracks out to a radius of 31.7 cm with a high spatial resolution in the $r\phi$ plane. It is supplemented by a z-chamber to measure the polar angle of tracks. The L3 arrangement gives optimized momentum resolution for penetrating muons, with $\sigma(p)/p \approx 2.5\%$ for 45 GeV/c muons. Its bismuth germanium oxide (BGO) electromagnetic calorimeter is preceded by less than 10% of a radiation length in the barrel region, and has a spatial resolution better 2 mm above 2 GeV. The energy resolution is about 5% at 100 MeV and 1.4% at 45 GeV. The calorimeter permits electron identification, with only 0.1% probability of misidentifying a hadron. It is also well suited for measurements of inclusive π^0, η and η' production.

4.2.4. OPAL The OPAL [178] detector has a warm solenoid providing a magnetic field of 0.435 T. The main central tracking jet chamber lies outside of a silicon microvertex detector and a precision vertex drift chamber; a set of z-chambers around the jet chamber give precise measurement of track polar angles. The combination of the tracking chambers gives a momentum resolution of $\sigma(p_T)/p_T \approx \sqrt{0.02^2 + (0.0015 p_T)^2}$ with p_T in GeV/c. Efficiency for reconstruction of K_s^0 and Λ particles varies with momentum, having a maximum value of 30% at about 5 GeV/c. The silicon detector, orginally an $r\phi$ device but improved in 1993 to also measure z, gives an impact parameter

resolution of 15 μm in $r\phi$ for high momentum tracks. The jet chamber measures ionization energy loss, dE/dx, of tracks in multihadronic events with a resolution of 3.8%, allowing excellent identification efficiency and high purity for electrons, pions, kaons and protons over almost the whole momentum range at LEP 1. OPAL's lead glass electromagnetic calorimeter, which is preceded by some two radiation lengths of material, has an energy resolution varying with energy from 1 to 5%. The muon chambers, together with the instrumented flux return of the hadron calorimeter, are highly efficient for identification of muons with momentum greater than 3 GeV/c.

4.2.5. SLD The SLD [179] experiment, like DELPHI, makes use of Cherenkov ring imaging to identify charged particles, with a detector which uses both liquid and gas radiators to allow coverage of a wide momentum range. Tracking is done by a central drift chamber within a 0.6 T magnetic field which gives a momentum resolution, $\sigma(p_T)/p_T^2 = \sqrt{0.005^2 + (0.01/p_T)^2}$, with p_T in GeV/c. For electromagnetic calorimetry, the SLD uses a liquid argon device, inside the magnet coil, which gives a resolution of around $15\%/\sqrt{E}$ (with E in GeV). The SLD has silicon charge-coupled-device pixel detectors for microvertex measurements. The pixels are 22 micron square, and the setup covers radii from 3 to 4 cm from the interaction vertex. Resolution on track impact parameter in $r\phi$ is in the range 11 to 20 μm, depending on track momentum and polar angle. Muons are identified by layers of streamer tubes between the slabs of iron which make up SLD's warm iron calorimeter.

5. Measurements of inclusive single identified particles

Inclusive single identified particles are usually studied in terms of their fractional energy (x_E) or momentum (x_p) relative to that of the beams, with the fragmentation functions being reported as $(1/\sigma_h)d\sigma/dx$. Here σ_h is the total cross section for $e^+e^- \to Z^0/\gamma^* \to$ hadrons. Its inclusion is experimentally advantageous since it obviates the need to measure absolute cross sections, so reducing systematic errors: $d\sigma/\sigma_h$ is simply calculated as the number of particles, ΔN, in bin dx relative to the total number, N_{tot}, of Z^0 hadronic decays. In a real measurement the bin width is finite, Δx, and the differential cross section is taken as $1/N_{tot} \times \Delta N/\Delta x$. Because fragmentation functions vary rapidly with x, care has to be taken for large values of Δx in interpreting a measurement as a differential cross section at some particular value of x [180].

Total inclusive particle yields, or average multiplicities per hadronic Z^0 decay, are obtained by integrating the measured fragmentation functions and extrapolating into any unmeasured regions of x with the aid of one or more models or interpolation functions. Systematic errors are included to account

for uncertainties in this procedure.

Fragmentation functions and total inclusive yields have been measured for an impressively large number of particle species at LEP. The string and cluster models, as implemented in JETSET and HERWIG, are usually confronted with the data. A comprehensive compilation of inclusive particle production data in e^+e^- annihilation at all available CoM energies above the Υ mass, as of mid-1995, may be found in [86] where measured fragmentation functions are plotted along with curves obtained from JETSET version 7.4. A more recent review [181] contains a good summary of measurements published after [86].

5.1. Overall inclusive rates

Tables 4 and 5 list of all the measured inclusive yields of mesons and baryons published to date. Where an experiment has reported more than one measurement, only the most recent is taken. For each measurement of a particular particle, statistical and systematic errors have been combined in quadrature; then the weighted mean of the available measurements has been calculated to give the results shown in the tables (no attempt has been made to take into account systematic errors correlated between experiments). Yields reported over a restricted x range are given separately.

In general there is very good agreement among the measurements of the different experiments. In only two cases, where the measurements are listed separately in the tables, is there evidence of disagreement: the DELPHI and OPAL measurements of the $\Delta(1232)^{\pm\pm}$ are possibly inconsistent, and the $\Xi(1530)^0$ yield reported by DELPHI does not agree well with the numbers given by ALEPH and OPAL.

5.2. Conclusions for Monte Carlo models

In tables 4 and 5 the measured rates are compared with the outcome of the three major Monte Carlo models which attempt a full simulation of particle production. The numbers in bold font show results which are more than three standard deviations from the experimental measurements. In each case, the default versions of the programs have been used, although for JETSET version 7.4 various sets of alternative parameters have been suggested which improve the agreement with the overall rates. The most recent HERWIG version 5.9 does not fit as well as version 5.8, but a new default set of parameters will no doubt follow careful comparisons with data.

It is clear from the various JETSET tunings suggested by the four LEP experiments in [11] that there are strong correlations among the program's parameters, possibly such that there is no unique best set. To this extent JETSET may be underconstrained despite the large number of experimental

Table 4. Average measured charged particle and identified meson multiplicities in Z^0 decay together with the rates from Monte Carlo models. The letters ADLMO indicate the contributing experiments. Where appropriate, the rates always include both particle and antiparticle.

Particle	Multiplicity	HERWIG59	JETSET74	UCLA74	Comments
Charged	20.96 ± 0.18	20.40	20.95	20.88	ADLMO [97, 98, 81, 82, 99]
π^+	17.05 ± 0.43	16.62	16.95	17.04	O [182]
π^0	9.39 ± 0.44	10.15	9.59	9.61	ADL [183, 184, 185]
η	0.282 ± 0.022	0.246	0.286	0.232	A [43] $x_E > 0.1$
	0.93 ± 0.09	0.92	1.00	0.78	L [186]
$\rho(770)^0$	1.29 ± 0.12	1.12	1.50	1.17	AD [187, 188]
$\omega(782)$	1.11 ± 0.11	1.05	1.35	1.01	AL [187, 189]
$\eta'(958)$	0.064 ± 0.014	0.071	**0.127**	0.061	A [43] $x_E > 0.1$
	0.25 ± 0.04	0.143	0.297	**0.121**	L [189]
$f_0(980)$	0.098 ± 0.016	0.068	—	—	D [188] $x_E > 0.06$
$\phi(1020)$	0.108 ± 0.005	**0.181**	**0.194**	**0.132**	ADO [187, 190, 191]
$f_2(1270)$	0.170 ± 0.043	0.137	—	—	D [188] $x_E > 0.05$
$f'_2(1525)$	0.020 ± 0.008	0.021	—	—	D [192]
K^+	2.37 ± 0.11	2.08	2.30	2.24	DO [193, 182]
K^0	2.010 ± 0.029	**1.87**	2.07	2.06	ADLO [194, 188, 185, 195]
$K^*(892)^+$	0.714 ± 0.044	**0.524**	**1.10**	0.779	ADO [43, 188, 196]
$K^*(892)^0$	0.759 ± 0.032	**0.530**	**1.10**	0.760	ADO [187, 190, 191]
$K_2^*(1430)^0$	0.079 ± 0.040	0.067	—	—	D [190]
	0.19 ± 0.07	**0.054**	—	—	O [191] $x_E < 0.3$
D^+	0.187 ± 0.014	0.190	0.174	0.196	ADO [197, 198, 199]
D^0	0.462 ± 0.026	0.406	0.490	0.497	ADO [197, 198, 199]
$D^*(2010)^+$	0.181 ± 0.010	0.151	**0.242**	**0.227**	ADO [197, 198, 199]
D_s^0	0.131 ± 0.020	0.087	0.129	0.130	O [199]
B^*	0.28 ± 0.03	**0.182**	0.260	0.254	D [200]
$B_{u,d}^{**}$	0.118 ± 0.024	**0.032**	—	—	D [201]
J/ψ	0.0054 ± 0.0004	**0.0018**	0.0050	0.0050	ADLO [202, 203, 204, 205]
$\psi(3685)$	0.0023 ± 0.0005	0.00097	0.0019	0.0019	DO [203, 205]
χ_{c1}	0.0086 ± 0.0027	0.00088	—	—	DL [203, 204]
Υ	$1.4 \pm 0.7 \times 10^{-4}$	$< \mathbf{1.0 \times 10^{-7}}$	$\mathbf{2.2 \times 10^{-6}}$	$\mathbf{1.8 \times 10^{-6}}$	O [206] Σ(3 lightest Υ)

Table 5. Measured baryon multiplicities in Z^0 decay together with the rates from Monte Carlo models. The letters ADLO indicate the contributing LEP experiments. Where appropriate, the rates always include both particle and antiparticle.

Particle	Multiplicity		HERWIG59	JETSET74	UCLA74	Comments
p	0.98	$\pm$ 0.09	**1.41**	1.19	1.09	DO [193, 182]
$\Delta(1232)^{++}$	0.079	$\pm$ 0.015	**0.278**	**0.189**	**0.139**	D [207]
	0.22	$\pm$ 0.06	0.278	0.189	0.139	O [208]
Λ	0.373	$\pm$ 0.007	**0.605**	0.385	**0.332**	ADLO [194, 209, 185, 210]
$\Lambda(1520)$	0.0213	$\pm$ 0.0028	—	—	—	O [210]
Σ^+	0.092	$\pm$ 0.017	0.123	0.073	0.061	O [211]
Σ^-	0.084	$\pm$ 0.017	0.102	0.068	0.056	O [211]
$\Sigma^+ + \Sigma^-$	0.174	$\pm$ 0.021	0.225	0.140	0.118	DO [212, 211]
Σ^0	0.074	$\pm$ 0.009	0.093	0.073	0.074	ADO [43, 213, 211]
$\Sigma^{\star +} + \Sigma^{\star -}$	0.0474	$\pm$ 0.0024	**0.202**	**0.074**	**0.074**	ADO [43, 212, 210]
Ξ^-	0.0265	$\pm$ 0.0009	**0.0746**	0.0271	**0.0220**	ADO [43, 212, 210]
$\Xi(1530)^0$	0.0072	$\pm$ 0.0007	**0.0352**	0.0053	0.0081	A [43]
	0.0041	$\pm$ 0.0006	**0.0352**	0.0053	**0.0081**	D [212]
	0.0068	$\pm$ 0.0007	**0.0352**	0.0053	0.0081	O [210]
Ω^-	0.0012	$\pm$ 0.0002	**0.0093**	0.00072	0.0011	ADO [43, 213, 210]
Λ_c^+	0.078	$\pm$ 0.017	0.0129	0.059	**0.026**	O [199]

measurements. DELPHI have published [44] comprehensive sets of tuned parameters for various Monte Carlo models (including ARIADNE and JETSET with matrix elements as well as with parton showers) in which they take account of event shape variables as well as inclusive identified particle rates. This exercise is useful but probably premature. Some of the recent measurements differ significantly from those used in the tuning, and many have much reduced errors. For example the Ω^- baryon is now known to be produced at a much lower rate than previously measured, and it turns out the DELPHI tuned rate fits better with this new rate than with the one used as input; the same is true of the $\phi(1020)$ meson rate. All of the models considered in [44] describe the inclusive rates reasonably well, with the exception of the performance of HERWIG in the baryon sector.

5.2.1. Production of L=1 mesons Although the available meson measurements are predominantly of the $L = 0$ pseudoscalar and vector states, the presence of the $L = 1$ mesons shows clearly their importance in the hadronization; this is confirmed also in the baryon sector with the observation by OPAL

of the $\Lambda(1520)$. Other scalar, axial vector and tensor mesons, together with orbitally excited baryons, must presumably also be produced, although large widths and small branching ratios will make them difficult to measure. Many of the lighter particles are therefore decay products of other hadrons, and care has to be taken in any interpretation of the data using only relative light particle rates. So far only HERWIG 5.9 includes by default the P and some D wave meson states, and as the tables show their inclusion does not mar the agreement with data in the u,d sector. However HERWIG does poorly with mesons containing s quarks as well as with baryons.

The production of the light tensor mesons is discussed by DELPHI in [188] where a comparison is made of relative rates of tensor to corresponding vector mesons. While the production ratio f_2/ρ^0 is similar to that for f_2'/ϕ, at about 20%, there is evidence for a lower K_2^*/K^* ratio, in agreement with results from hadroproduction experiments. This suggests an extra suppression of strange tensor mesons. However OPAL [191] measures a larger rate for K_2^* and so the picture is not yet clear. Some evidence has also been reported [188] for a rise in the ratio f_2/ρ^0 with meson momentum; in other words the fragmentation function of the tensor meson may be harder than that of the vector meson, as generally expected of heavier hadrons [214]. However, these are difficult resonances to measure; they have large widths, large combinatorial backgrounds and uncertainties in the resonance line shapes. As usual, more results would help.

Only one measurement of a scalar meson, the $f_0(980)$, has been reported [188], with a ratio f_0/ρ^0 of 0.14 ± 0.03. Thus if the f_0 is indeed a conventional 0^{++} meson (see [7] for a mini-review of the scalars) then the scalar and tensor mesons are produced with similar rates. But again the measurements are difficult, and other studies [187] of the inclusive $\pi^+\pi^-$ mass spectrum with higher statistics have failed to report a measurement of the $f_0(980)$ because of systematic uncertainties. One should therefore be wary of too much interpretation of one measurement.

The $f_0(980)$ and $a_0(980)$ have aroused interest [215] as potential probes of the Gribov confinement scenario [216]. In this theory the QCD vacuum is likened to the intense QED fields expected around super charged ions, $Z > 180$ (or > 137 for point-like charges) [217]. This results in the production of spatially compact 'novel vacuum scalars', identified with the $f_0(980)$, which are expected to be produced in relative isolation. Particular signatures include enhanced production at central rapidities (with respect to the thrust axis) and in low multiplicity events [215].

From a semiclassical point of view, the orbital angular momentum l of a $q\bar{q}$ pair from string fragmentation is given by $< p_T > \times d$ where $< p_T >$ is the mean quark momentum transverse to the string and d is the size of the resulting

hadron [14]. Typical values give $l \approx 0.05\hbar$ so that the rate for mesons with non-zero orbital angular momentum is expected to be less than about 10% of the rate for the corresonding L=0 mesons. The large average quark-antiquark separation in radially excited states also works to prevent production of these mesons in string fragmentation. Although the $L = 1$ mesons can be simulated in JETSET at the correct rates by the adjustment of appropriate parameters, the large experimental rates are nevertheless a problem for the basic model assumptions about production of hadrons from strings.

5.2.2. Strangeness suppression Strangeness suppression is immediately apparent from both the meson and baryon measurements given in the tables. There is a large number of ways to determine, from the data, values for γ_s, the quark-level strangeness suppression assumed in the string model. Results are tabulated for example in [11] where all measurements agree on a value of 0.3, a result which accords with reasonable values for the strange quark mass [7] and the string energy density κ. Since the various methods in [11] use both light and heavy quark states, this consistency suggests that the suppression occurs at the quark level, in agreement with the string-model assumption. On the other hand the UCLA model also reproduces reasonably well the strange particle rates, and previous versions of HERWIG have been tuned to do so. And hadronization studies in ep collisions at HERA [218] give a lower value of $\gamma_s \approx 0.2$, in apparent disagreement with the Z^0 decay measurements. Therefore it is fair to say that the data are not yet conclusive. A direct method to measure the strangeness suppression in $e^+e^- \rightarrow Z^0/\gamma^* \rightarrow$ hadrons has been proposed [219] which makes use of the electroweak forward-backward asymmetry and which could possibly distinguish between quark-level and hadron-level suppression. Recently SLD [220] have applied this method to their data on inclusive K^{*0} and $\overline{K^{*0}}$ production using 150k events, with the result $\gamma_s = 0.26 \pm 0.12$.

5.2.3. Relative rates of vector and pseudoscalar mesons In the absence of mass effects, the ratio of direct pseudoscalar to vector meson production may depend simply on spin statistics, in which case the value P/(P+V) would be expected to be 3/4. However feed-down from decays is also important and may obscure the interpretation of the experimental results. One approach to determine the underlying P/(P+V) value is to tune the appropriate parameter in the JETSET model, but this can only be done within the limited knowledge available on production of the higher states. Alternatively, one can use the measurements in the b and c sectors where vector to pseudoscalar mass differences are much smaller and there are some hopes to measure the orbitally excited states. The average ratio for primary $B^*/(B+B^*)$ is found to be 0.75 ± 0.04 [200, 221, 222], in excellent agreement with simple spin counting.

However the picture is not so clear when charm is considered: here the ratio $D^*/(D+D^*)$ is measured [197] to be 0.51 ± 0.04. The difficulty here arises from incomplete knowledge of the production rate and decay modes of the orbitally excited D^{**} states which are likely to feed down into the D and D^* production. The question then arises as to why B^{**} production does not similarly muddy the waters in the b sector; it may be that production and decay rates of the four different J^P states of B^{**} conspire to leave the value of $P/(P+V)$ at 3/4. More measurements are needed before definite conclusions can be reached.

5.2.4.   Baryon production   In the string model, baryon yields are determined by many parameters. The overall baryon rates relative to mesons depend on the relative probability to produce a diquark pair from the sea. Spin-1 diquarks may be suppressed relative to spin-0 diquarks. The strangeness suppression enters in a similar way as for meson production, but there is in addition the possibility of extra suppression of strangeness in a diquark. And the popcorn mechanism may introduce one or more mesons locally in phase space between a baryon and an antibaryon.

Although JETSET does rather well, there are some discrepancies with measured rates. Attempts by OPAL [210] to tune the parameters which control baryon production have shown that it is not possible to reproduce simultaneously all of the measured rates. The suggestion then is that the mechanisms for baryon production in the string model, and particularly for the strangeness suppression, are deficient. However, as has been said, there is now clear experimental evidence also for orbitally excited states in baryon production. The rate for the $J^P = \frac{3}{2}^- \Lambda(1520)$, at 0.02 per hadronic Z^0 decay, is around 5% of that for the $J^P = \frac{1}{2}^+ \Lambda$. And there are many similar baryon states which cannot be measured experimentally but which, it is fair to assume, must be produced in the hadronization. So since JETSET, like all of the other models, does not include production of orbitally excited baryons, no clear conclusions can yet be reached.

Neither HERWIG nor UCLA, both of which rely only on phase space, mass and spin, are successful in the strange baryon sector, with the former consistently overestimating the rates, and the latter underestimating them. As presently implemented, baryon production in HERWIG does not take account of the appropriate SU(6) Clebsch-Gordon coefficients and this will lead to an overestimation of baryon production rates. As with JETSET, neither of these models includes the production of baryons other than the lowest lying $L = 0$ states. In principle their inclusion would lower the predicted rates for primary low lying baryons, since some higher states would be produced in their stead. However there would be a compensatory increase in the rates due to feed down from decays. Since HERWIG consistently overproduces and UCLA

underproduces the baryons, it seems reasonable to deduce that at least one of them is incapable of being fixed up by this mechanism.

The conclusion then from the baryon yields is that the string model of JETSET, while certainly not perfect, is in reasonable accord with the measurements. Recent work on the baryon production within the popcorn model has further improved the agreement [160]. Whether or not this is to be taken as a strong endorsement of the model is however an arguable point, given the large amount of freedom available to tune parameters in order to reproduce the observations. Both the HERWIG cluster model and the UCLA string model are clearly in difficulty, and it remains to be seen whether they can be rescued.

5.2.5. Comparison to models of total yields A number of models have been proposed to treat only the overall yields of identified particles. Such models are necessarily of limited physical content, although they turn out to be reasonably successful in describing the inclusive rates. Why they do so is not at all clear.

In the thermodynamic model [223] the source of particles is assumed to be a hadron gas in thermal and chemical equilibrium. The model has three parameters, a temperature, a volume and a parameter to allow for incomplete strange chemical equilibrium (similar to the strangeness suppression of the Lund string model). The model gives a good fit to the LEP data, as well as to lower energy e^+e^- annihilation data, with a temperature of around 170 MeV, close to Λ_{QCD} and the temperature found in the earlier statistical model of Hagedorn [164]. The author of the model speculates that the thermal equilibrium could be a feature of the quark-hadron transition, brought about by strong interactions. This argument was also invoked by Fermi [101] to justify his phase space model for hadron production. However it is difficult to reconcile this picture with the conventional view of hadronization in e^+e^- annihilation as occuring locally in the wake of rapidly separating colour sources.

A "striking regularity" [224] has been noted in the particle yields, and a simple formula proposed which reproduces well the observations (apart from the pions and possibly the Ω^- baryon): $N = (2J+1)/(I_m+1) \times a \exp\left(-bM^2\right)$. Here, N is the yield for a particle of spin J and mass M, and I_m is the isospin for baryons and a "modified" isospin for K and K* mesons and isosinglet pseudoscalar mesons. The introduction of the "modified" isospin appears rather ad hoc, although there are plausible arguments to justify it. The model makes no attempt to explain the yield differences between members of the same isomultiplet which, for example, are significant for kaons. The parameters a and b are fitted to the data, and the slope parameter b, at about 3.9 GeV^{-2}, is found to be the same for LEP as for lower energy measurements, implying that the regularity may be universal. It is unclear as to the physical origin of the

expression, and it will be interesting to see how the formula copes with future measurements. This observed regularity has a less successful predecessor of the form $N = (2J+1) \times a \exp(-bM)$ [225], which was applied to lower energy data.

Another model [226] of the total yields is based on string fragmentation, and proposes a simple formula with only three parameters: a strangeness suppression, an effective temperature and a relative normalization factor between mesons and baryons. Following the string model, the rate N of light meson and baryon production is taken as $N = (C/C_B) \times (2J+1) \times (\gamma_s)^{N_s} \times \exp(-E_{\mathrm{bind}}/T)$. The normalization C depends on the centre-of-mass energy, C_B is a relative suppression of baryons, J is the particle spin, $\gamma_s^{N_s}$ gives the suppression for a hadron containing N_s strange quarks, E_{bind} is the hadron binding energy and T is the effective temperature. The model gives a good simultaneous fit to LEP and lower energy data, with a temperature of 298 ± 15 MeV and a strangeness suppression γ_s of 0.29 ± 0.02. The model also gives a good description of heavy flavour production. Its predictions for production rates of excited charm states have recently been shown to agree with OPAL measurements [227].

5.3. Rates for heavy quarkonia

Due to their narrow widths and the availability of clean leptonic decay channels the principle heavy quarkonium states measured are the J/ψ and $\Upsilon(1S, 2S, 3S)$, based upon which further excitations can be reconstructed [202, 203, 204, 205, 206, 228]. The production of these heavy $Q\overline{Q}$ bound states is thought to be rather atypical of hadron production in general, especially for the Υ, due to the significant part played by perturbative physics.

In the case of charmonium the dominant production mechanism is expected to be weak b hadron decays: b→c+($\bar{c}$s) plus subsequent colour rearrangement. In the case of $B_{u,d}$ mesons the J/ψ branching ratios ($\approx 1.15\%$) have been previously measured at the $\Upsilon(4S)$ [229], so allowing reliable predictions for charmonium rates at the Z^0. (The presence of B_s and b baryons at the Z^0 makes little difference to the inclusive b hadron branching ratio [203]). Perturbative fragmentation contributes only at the few percent level to charmonium production [230, 231], as is indeed observed [232], but 100% to bottomonium production. Three basic pQCD production mechanisms, illustrated in figure 11, are considered [233]:
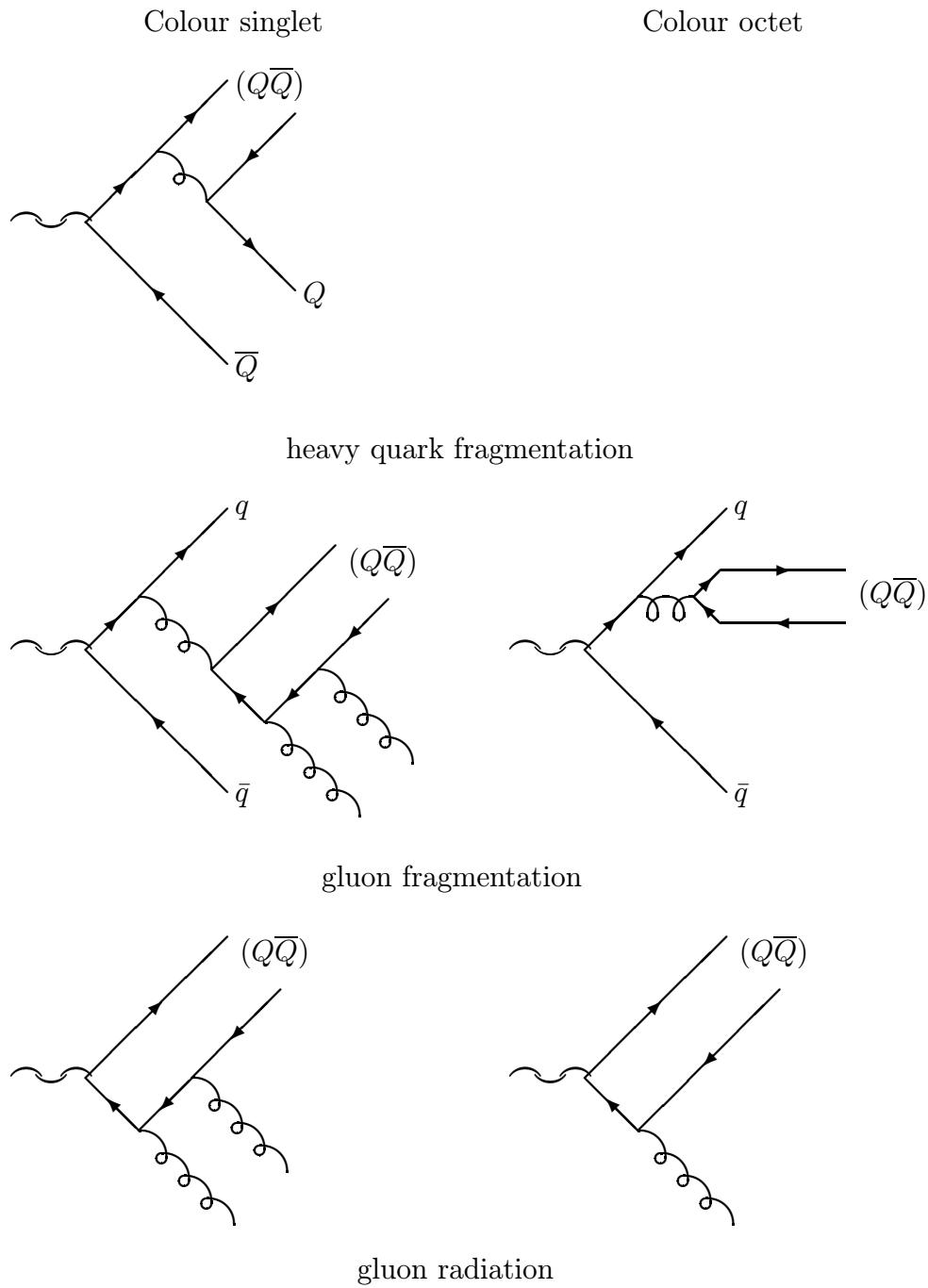
- Heavy quark fragmentation [230], $Z^0 \rightarrow (\Upsilon)b\bar{b}$. Here the production of a primary b$\bar{b}$ pair is followed by the radiation of a gluon which splits into a second b$\bar{b}$; a b and $\bar{b}$ from these two pairs then bind in a colour singlet system. It is noteworthy that in addition to the quarkonium two other

heavy hadrons occur in this process.

- Gluon fragmentation [231], $Z^0 \to q\bar{q}g^\star$, $g^\star \to (b\bar{b})gg$. The need to remove the colour from the $b\bar{b}$ pair, whilst forming a positive C parity Υ (or J/ψ in the case of $c\bar{c}$), requires the emission of two perturbative gluons. Thus this is an order-α_s^4 process and typically the quarkonium state has a relatively large transverse momentum.

- Gluon radiation [234], $Z^0 \to (b\bar{b})gg$. Here two gluons are emitted from a primary heavy (anti)quark allowing it to recoil and form a colour singlet with the other (anti)quark. This results in a very hard, isolated, quarkonium state.

All of the above prompt production mechanisms give comparatively isolated quarkonia originating from the interaction point, in contrast to charmonium from b decays. Here the $b\bar{b}$ system is produced in a colour singlet state by the emission of perturbative gluons. The dominant process is quark fragmentation [233]. However the theoretical predictions are significantly low compared to the Z^0 data. Also no evidence for displaced vertices, associated with additional heavy quarks, is observed in quarkonium events. A similar situation has occurred at the TEVATRON where colour singlet fragmentation mechanisms fail to account for the number of observed high-p_T quarkonium states [235, 236].

Fortunately recent theoretical developments suggest that colour octet quarkonium production may play an important role [237]. Here the $Q\overline{Q}$ forms a colour octet system from which the colour is leached away (by exchange of soft gluons) in an, as yet unspecified, non-perturbative mechanism. Two new contributions, also shown in figure 11, arise: gluon fragmentation $Z^0 \to q\bar{q}g^\star$, $g^\star \to (b\bar{b})$; and gluon radiation $Z^0 \to b\bar{b}g$. These new diagrams are lower order in α_s but suppressed by larger powers of v, the relative velocity of the b and $\bar{b}$. To calculate these processes requires knowledge of the octet matrix elements; until recently these have been taken from fits to the CDF data [236] though now a potential model based calculation is available [238]. (*Ab initio* lattice calculations have so far only been performed for octet decay matrix elements [239] and not the technically demanding production matrix elements). In the the octet case the dominant fragmentation contribution to Υ production becomes gluon fragmentation [233]. Taking into account all contributions, agreement with the Z^0 data is possible. Although the data are insufficient to be able to isolate components due to the individual processes, the lack of an observed hard Υ spectrum does rule out a large contribution from octet gluon radiation [232]. It is also noteworthy that the octet mechanism predicts a large transverse polarization for the vector quarkonium states [238, 240] particularly so at high momentum.

Colour singlet

Colour octet

$(Q\overline{Q})$

Q

$\overline{Q}$

heavy quark fragmentation

q

$(Q\overline{Q})$

$\overline{q}$

q

$(Q\overline{Q})$

$\overline{q}$

gluon fragmentation

$(Q\overline{Q})$

$(Q\overline{Q})$

gluon radiation

Figure 11. The leading production mechanisms for heavy quarkonia assuming the colour singlet and octet mechanisms.

Looking at the J/ψ data in table 4, one can conclude that since b hadron decays dominate charmonium production, HERWIG is deficient in this aspect of its b decay description. Possible remedies include adding more explicit decay channels to the decay tables or refining the partonic b decay model, particularly in its treatment of light clusters. Next, because none of the models considered include the dominant octet production mechanism the large underestimates of Υ [206, 228] production are not too surprising. Only ARIADNE, version 4.09 onwards, been extended to include an approximation to the perturbative colour octet production mechanism [241]. This program is therefore the only one containing the necessary physics to attempt to describe the Υ data.

5.4. Semi-inclusive momentum spectra

Having discussed the total production rates of identified particles, we now turn to their momentum distributions: $\sigma^{-1}\mathrm{d}\sigma/\mathrm{d}x$. All particle spectra vanish as $x \to 1$ and are expected to vanish as $x \to 0$, though measurements are rarely available at sufficiently low momentum to see indications of this behaviour. However changing to the commonly used variable $\xi = -\ln x$, a clear 'hump-backed plateau' shape (see section 2.5) is seen.

5.4.1. *Light hadrons* A compilation of many of the measurements of the x and ξ spectra of identified hadrons at the Z^0 can be found in [86] and [181]. References to the more recent measurements are listed in table 6. In addition, a recent measurement of the charged particle momentum spectrum is available in [84].

Table 6. A summary of momentum spectrum measurements that have appeared since [86]. The letters ADL indicate the contributing experiments.

Particle		Reference	Particle		Reference
Mesons					
π^0	A	[183]	$f_2'(1520)$	D	[192]
η	A	[43]	K^0	A	[43]
$\omega(782)$	L	[189]	$K^\star(892)^\pm$	A	[43]
$\eta'(958)$	AL	[43, 189]	$K^\star(892)^0$	D	[190]
$\phi(1020)$	D	[190]	$K_2^\star(1430)^0$	D	[190]
Baryons					
Λ	A	[43]	Ξ^-	A	[43]
$\Sigma(1385)^\pm$	A	[43]	$\Xi(1530)^0$	A	[43]

In section 2.5.2 the calculation of the charged particle momentum spectrum

was discussed; these results can also be applied to identified hadron spectra [8]. Especially in the case of identified hadrons a dependence on the primary quark flavour is anticipated: Monte Carlo studies and recent SLD results [220] suggest that the main effects are at high momentum but that residual effects could also occur at low momentum. Consequently investigations have again concentrated on the peak position, $\xi^\star$, which occurs at low momentum and for which the complete prediction is of the form [242, 243]:

$$\xi^\star = F\left[\ln\left(\frac{Q_0}{\Lambda}\right)\right] + \frac{1}{2}\ln\left(\frac{Q}{\Lambda}\right) + \cdots \tag{24}$$

Observe that the cut-off, Q_0, dependence only occurs through the first term which has the property that $F(0) = 0$ whilst the scale, Q, dependence only arises in the second term: the constant Λ is the usual (effective) QCD scale. In order to create a particle of a given mass it is reasonable to expect that the final-state partons will require virtualities of the same magnitude, so that Q_0 is a simple function of the hadron mass $m_{\rm h}$ [244]. Invoking the LPHD concept one can hope that these parton level calculations are then sufficient to predict an identified hadron's energy spectrum.

Application of (24) has caused some confusion. First, there are small differences between experiments in the practical definition of $\xi^\star$. Second, it is common to set $Q_0 = \Lambda$ so that the first term vanishes, the limiting spectrum case, but then somewhat inconsistently to introduce a new variable $Q_0' = \Lambda$ in the second term. That is (24) is replaced by:

$$\xi^\star = \frac{1}{2}\ln\left(\frac{Q}{Q'}\right) \tag{25}$$

Given the availability of low energy data it is possible to investigate the $\ln Q$ dependence of $\xi^\star$ for the π^+, π^0, K^+, K_s^0, p and Λ hadrons separately [245, 243]. The data for each hadron species appear to lie on straight lines each of slope $\approx 1/2$ but with differing offsets, indicating that F in (24) decreases with increasing hadron mass. ALEPH also finds that the linearity of these fits can be improved by using JETSET to remove the effects of secondary hadron decays [245]. For example kaons produced in the weak decays of hard B mesons stiffen the kaon spectrum causing a decrease in their $\xi^\star$. However this correction procedure is somewhat at odds with the original idea of LPHD which was thought to account for such decays. At the Z^0 it is also possible to study the hadron mass dependence of $\xi^\star$ with $Q = M_{\rm Z}$ fixed [182, 193, 243], which probes the relationship between $Q_0^{(\prime)}$ and $m_{\rm h}$. Adopting (25) OPAL [182] claim two linear relationships between $\xi^\star$ and $m_{\rm h}$ (an exponential dependence of Q' on $m_{\rm h}$) one describing the mesons, except pions, and the other the baryons. This pattern is well reproduced by JETSET allowing a correction to remove secondary decays to be applied after which all the points, including pions, now

fall on a single curve. However DELPHI [193] report that mesons and baryons lie on two curves corresponding to a negative logarithmic dependence of $\xi^\star$ on m_h (linear relationship between Q' and m_h) which again reduce to a single curve after correcting back to primary hadrons using JETSET.

Whilst the full shape of the momentum spectrum can be calculated within pQCD [8, 63, 78, 79] comparison is more commonly made to Monte Carlo predictions, particularly so in the case of identified particle momentum spectra, reflecting the expected interplay between perturbative and non-perturbative contributions. From a practical point of view the primary concern is with a correct description of the pion momentum spectra [86, 182, 183, 185, 245] which dominate the total event multiplicity. These fall by five orders of magnitude over the measured momentum range. Here, and in general, the predictions of ARIADNE and JETSET are rather similar and typically agree with the data a little better than HERWIG, though all suffer problems at very low and very high x. Meson spectra are described reasonably well on the whole, though the $K^\pm$ spectrum is notably too soft [86, 182, 193, 245] which might be attributable to an inadequate description of heavy hadron decays. However the description for baryons is less satisfactory. In particular the number of fast, predominantly primary, protons is consistently overestimated [182, 193, 245]. In the case of ARIADNE and JETSET this may be remedied [43, 44] by invoking a suppression of leading uds-baryons [21], which may have an underlying physics motivation [160].

An intriguing possibility is that of an inequality in the fragmentation function of strange quarks into protons and antiprotons, $D_p^s(x, Q^2) \neq D_{\bar{p}}^s(x, Q^2)$ [246]. This prediction follows from a possible asymmetry, of non-perturbative origin, in the sea quark structure functions of protons [247] and application of the 'reciprocity rule' [248]. A test of this idea may be possible by SLD using a strangeness tag [249] and exploiting their polarization asymmetry to distinguish the quark from the antiquark jet.

5.4.2. Heavy quark hadrons Hadrons containing heavy (c,b) quarks are special since the heavy quark is expected to be principally (if not exclusively) of perturbative origin. In practice non-perturbative physics also plays a role and the delineation of the two contributions is not clear cut. If the fragmentation function can be written as a convolution of perturbative (PT) and non-perturbative (NP) parts, $D(x) = d_{PT} \otimes d_{NP}$, then it immediately follows that $\langle x \rangle = \langle x \rangle_{PT} \cdot \langle x \rangle_{NP}$. In leading order pQCD predicts [250] $\langle x \rangle_{PT} = (\alpha_s(E_{\text{jet}})/\alpha_s(m_Q))^{8/(9\pi\beta_0)}$; the NLO calculation of $d_{PT}(x)$ [251] is sharply forward-peaked, vanishing at $x = 1$. The perturbative result alone is too hard ($\langle x_b \rangle_{PT}|_{E=M_Z/2} \approx 0.8$) and a non-perturbative component is required, especially in those rare cases (of order 1%) where no gluon radiation occurs at

all.

A simple argument [214] shows that the non-perturbative hadronization should also be very hard for heavy quarks due to their inertia, $\langle x \rangle_{NP} \approx 1 - R^{-1}/m_Q$, where R is a typical hadron size, with the remaining energy uniformly distributed in rapidity between $\pm \ln(\sqrt{s}/2m_Q)$. A full expression for $d_{NP}(x)$ depends on the details of the hadronization mechanism assumed, and several are available.

The most commonly adopted standard is due to Peterson et al [252]. In an independent fragmentation approach, the amplitude for the transition $Q \rightarrow (Q\bar{q}') + q'$ in perturbation theory is proportional to the inverse of the energy transfer, assuming a constant matrix element. The fragmentation function is then given by the amplitude squared and the appropriate flux factor as:

$$D_h^Q(x) = \frac{N}{x}\left(1 - \frac{1}{x} - \frac{\epsilon_Q}{1-x}\right)^{-2} \xrightarrow{x\to 1} N\frac{(1-x)^2}{\epsilon_Q^2} \qquad N \approx \frac{4\sqrt{\epsilon_Q}}{\pi} \qquad (26)$$

Theoretically one predicts $\epsilon_Q = R^{-2}/m_Q^2$; experimental fits yield small ϵ values with $\epsilon_c/\epsilon_b \sim 10$, consistent with $(m_b/m_c)^2$ [253, 254, 255, 256, 257, 258]. On average, $\langle x \rangle = 1 - \sqrt{\epsilon_Q} \approx 1 - R^{-1}/m_Q$ as anticipated above.

A perceived problem with the Peterson form is its $\sim (1-x)^2$ behaviour (it is sometimes argued that including gluon radiation is equivalent to an additional $(1-x)$ factor) as $x \to 1$ which is in conflict with the 'reciprocity' rule [248]. This posits that the $x \to 1$ behaviour of the $Q \rightarrow h$ fragmentation function should equal the $x \to 1$ behaviour of the $h \rightarrow Q$ structure function $F_h^Q(x, Q^2)$. Furthermore it is expected from dimensional counting arguments [259] that as $x \to 1$, $F_h^q(x, Q^2) \sim (1-x)^{2n_s-1}$ where n_s is the number of spectators in the hadron H. In a meson $n_s = 1$ and therefore the $x \to 1$ behaviour of the fragmentation function should be $(1-x)$. Two alternatives are available. By adopting an explicit meson wavefunction [260] and thereby introducing a non-trivial matrix element, a 'refined' Peterson form may be derived:

$$D_h^Q(x) = N(1+x^2)\left(\frac{1-x}{x} + \frac{\epsilon(2-x)}{1-x}\right)\left(1 - \frac{1}{x} - \frac{\epsilon}{1-x}\right)^{-2} \xrightarrow{x\to 1} N\frac{2(1-x)}{\epsilon}(27)$$

An earlier approach [261], based directly on the structure function analogy, leads to:

$$D_h^Q(x) = (\alpha+1)(\alpha+2)x^\alpha(1-x) \xrightarrow{x\to 1} (\alpha+1)(\alpha+2)(1-x)(28)$$

Here $\alpha \sim m_Q$ so that $\langle x \rangle = 1 - 2/(\alpha+3)$ in accord with expectation.

In string models two approaches have been elaborated according to whether the momentum or space-time aspects are emphasized. In the presence of massless quarks, which move along linear light-cone trajectories, these pictures are simply related, $\Delta p = \kappa\Delta t$, $\Delta E = \Delta p_z$; however massive quarks move along displaced hyperbolae. In the Lund momentum-space approach the

relevant string area is given, as for light quarks, by $m_\perp^2/(x\kappa^2)$ and the same reasoning then leads to the LSFF (14). However this gives $\langle x \rangle \approx 1 - (1 + a)/bm_\perp^2$ which is too hard compared to both theoretical expectation and experiment [253, 254, 255, 256, 257, 258]. Adopting a space-time based approach [139], *à la* Artru Mennessier, the string fragments randomly into clusters and the relevant string area becomes:

$$\frac{m_Q^2}{2\kappa^2} \left[\frac{m_{\mathrm{str}}^2}{m_Q^2} \frac{1}{x} - 1 - \ln\left(\frac{m_{\mathrm{str}}^2}{m_Q^2} \frac{1}{x} \right) \right] \tag{29}$$

where m_{str} is the mass of the string segment containing the heavy quark. In the $Q/M_Q \to \infty$ limit this results in a generalization of the LSFF but with no a-term present. Elaborating this scheme [262] to multiple string breaks along a finite size string leads to the following effective fragmentation function:

$$D_{\mathrm{h}}^Q(x)\frac{1}{x^{1+bm_{\mathrm{H}}^2}}x^{a_\alpha}\left(\frac{1-x}{x}\right)^{a_\beta}\exp\left(\frac{-bm_{\mathrm{H}}^2}{x}\right) \xrightarrow{x\to 1} (1-x)^{a_\beta} \tag{30}$$

Now $m_{\mathrm{str}} \approx m_{\mathrm{H}}$ should be identified with the mass of the lightest Q hadron, where in fact the cluster mass spectrum peaks. This has a softer spectrum, $\langle x \rangle \approx 1 - R^{-1}/m_Q$, and is very similar to the Peterson form in practice.

It should be noted that the non-perturbative fragmentation functions can be expected to describe effects due to the perturbative emission of soft gluons, as found in a parton shower. However effects due to the emission of hard gluons cannot be accounted for. In particular when defining x as a light-cone momentum fraction this may lead to a difference between the reconstructed value x_{rec}, measured along a jet axis, and the primary value x_{pri}, generated with respect to the 'string' axis: the Lund model indicates [263] that $\langle x_{\mathrm{rec}} - x_{\mathrm{pri}} \rangle_{\mathrm{b}} \approx 0.08$.

The experimental measurement of the b fragmentation function is difficult; to date it has been based on reconstructed B$\to$D$^{(\star)}\ell\nu_\ell(X)$ decays or the rapidity method [264]. Also, the interpretation of the results is delicate, and ambiguous conclusions have been drawn. Two sources of confusion are the delineation of the perturbative and non-perturbative contributions and whether a distinction is made between primary and secondary b hadrons cascading down from excited states. At the Z^0 there is substantial production of B* [200, 221, 222] and the four B** [201, 221, 265] mesons: the primary rate is approximately 1:3:2 for B:B*:B**. OPAL [257] finds reasonable agreement with the Peterson *et al* (26), Collins and Spiller (27), Kartvelishvili *et al* (28) and Lund-Bowler (30) fragmentation functions. On the other hand, the ALEPH data [254] would rule out the Collins and Spiller form whilst favouring the Kartvelishvili *et al* form; the data also disfavour an untuned version of HERWIG, which is too soft. Preliminary studies from DELPHI [255] indicate that JETSET with parton showers (PS) and the Peterson form, (26), gives the best description of the

data but with a peak that is appreciably too wide. Using JETSET PS with Lund-Bowler functions, (30), gives a very poor fit as does using JETSET with matrix elements and the Peterson function. This last combination gives too narrow a peak, indicating the need for a contribution from gluon radiation. HERWIG gives a reasonable description of the data but must be tuned to avoid too many heavy b clusters. DELPHI [255] also give measurements of the primary $B^{\star}$ and $B^{\star\star}$ fragmenation functions. L3 [256] find agreement within errors with the Peterson *et al* fragmentation function.

6. Spin phenomena

As discussed in 1.1, the primary quarks produced via $e^+e^- \to Z^0/\gamma^* \to q\bar{q}$ are highly polarized. Whether, and in what circumstances, this polarization survives the hadronization or whether spin-spin forces wash out any memory of the initial polarization is an open question. The primary quarks may become constituents of unstable baryons or of vector or tensor mesons, the angular distribution of whose decay products may be used to extract information about spin states.

In the particular case of leading (large x) spin-1/2 Λ-type baryons, considerable polarization is expected [266], though also see [267]. In the constituent quark model, the spin of such baryons is carried by the heavy quark, with the light diquark system in a spin zero, isospin zero state (though see the discussion in section 3.2.5). Thus fast Λ_b particles could carry a substantial fraction of the polarization of the initial b quark, with the light diquark system carried along as a spectator. Similarly, high-x Λ_c, and Λ baryons formed in fragmentation of s quarks, are expected to be polarized. Since Λ particles can also arise from hadronization of initial u and d quarks, the polarization in this case is considerably reduced.

6.1. Λ_b polarization

ALEPH have measured the polarization of Λ_b baryons [268] using semileptonic decays, $\Lambda_b \to l^-\bar{\nu}_l$+charmed hadrons. The method [269] is based on measurement of the ratio of the average lepton to average neutrino energy. The measured longitudinal polarization, $P_{\Lambda_b} = -0.23^{+0.25}_{-0.21}$, is well below the theoretical expectation of -0.69 ± 0.06 although the error is large. This is a surprising result and, if confirmed, would indicate the likely existence of depolarizing mechanisms in the b quark hadronization.

6.2. Λ polarization

Because of the parity-violating nature of the decay, $\Lambda \to p\pi^-$, the distribution of the polar angle, θ^*, of the proton direction in the Λ rest frame, relative to the Λ direction in the laboratory, is proportional to $1 + \alpha P_L \cos\theta^*$, where P_L is the degree of longitudinal polarization. The value of the weak decay parameter α is well measured [7]. ALEPH [270] have exploited this distribution to measure a value $P_L = -0.32 \pm 0.07$ for leading ($x_p > 0.3$) Λ baryons. When all sources of Λ baryons are taken into account, a result of -0.39 ± 0.08 is expected if Λ's containing a primary s quark carry all of its initial polarization. Thus the ALEPH measurement is in agreement with standard electroweak theory together with the assumption that the initial strange quark polarization survives hadronization to become a leading Λ baryon.

This result is clearly at odds with the conclusion from the Λ_b study which indicated significant depolarization in the hadronization. Indeed, the polarization of the heavier b quark may be expected to survive more easily than that of the s quark.

6.3. Vector meson spin alignment

Study of spin alignment of vector mesons, particularly at large x, where the meson may be expected to contain one of the primary quarks, may provide information on the nature of the quark to meson transition. Such analyses are normally done in terms of the vector meson helicity density matrix, $\rho_{\lambda\lambda'}$, some of whose elements can be determined by measuring the distribution of the vector meson decay products [271]. The element ρ_{00} is the fraction of mesons which are in the helicity zero state. In strong vector meson decays it is not possible to infer separately the values of elements ρ_{11} and ρ_{-1-1}, since the decay angular distributions are the same for helicity $+1$ and helicity -1 vector mesons.

In statistical models [272], the fragmentation is assumed to produce extra quarks with both helicities equally likely. Parallel alignment of primary and secondary quark spins will produce a vector meson with helicity $\lambda = \pm 1$. If the spins are initially antiparallel, the value of ρ_{00} will depend on the relative probability to produce a vector or a pseudoscalar meson; in this case $\rho_{00} = (1 - P/V)/2$, with a maximum value of $1/2$ when $P/V = 0$ and a value of $1/3$ if there is no suppression of vector mesons. In the model of [273] vector mesons are produced via vector currents q→qV which conserve the quark helicity. The vector meson then has helicity zero. Another model [274], for production of leading mesons, assumes multiple emission of soft gluons by the fragmenting quark, a process which conserves the quark helicity. The leading vector meson may be formed when the leading quark combines with

a soft antiquark in a process which results in meson helicity ± 1. The basic string and cluster models have little to say about vector meson spin alignment, although [14] does point out that no alignment may be expected in the simplest string picture.

ALEPH [221], DELPHI [200] and OPAL [275] have measured the alignment of B* mesons using the angular distribution of γ rays from the decay B$^* \to$Bγ. The measurements agree, and produce a weighted average of $\rho_{00}= 0.33 \pm 0.04$ (although they all express the result in terms of a relative contribution of longitudinal polarization states). These results, which imply no spin alignment, are consistent with simple spin counting and with heavy quark effective theory (HQET). They are also in accord with the measurements of the ratio B* to B meson production [200, 221, 222] which imply no suppression of the vector state (see 5.2.3).

Results from OPAL [276] on lighter vector mesons show deviations from $\rho_{00}= 1/3$. For D$^{*\pm}$ mesons, a value $\rho_{00} = 0.40 \pm 0.02$ has been measured, consistent with lower energy results [277]. And for primary $\phi(1020)$ mesons at $x > 0.7$, OPAL report an even larger value, $\rho_{00}= 0.54 \pm 0.08$. These mesons therefore appear to be preferentially in the helicity zero state. Measurements of some off-diagonal elements of the helicity density matrix show small deviations from zero for both mesons. Such non-zero off-diagonal elements are a natural consequence of coherence in the hadronization, and are a firm prediction [278] of any general model other than independent fragmentation. There is clearly more to be learned about hadronization from such measurements.

7.   Correlation phenomena

Correlations in hadronic systems may be defined as departures from phase space in distributions for groups of two or more particles. Such correlations may be associated with

- quantum mechanics — Bose-Einstein and Fermi-Dirac effects
- hadron dynamics — resonances, reflections and final-state interactions
- local baryon number conservation — baryon-antibaryon phase space correlations
- local strangeness conservation — strange particle rapidity correlations
- soft gluon coherence in QCD showers — two-particle momentum correlations and possibly intermittency
- fragmentation dynamics — transverse-momentum limitation of phase space

In so far as one wishes to understand the underlying dynamics of the hadronization phase, it is important to take into account all of these effects.

7.1. Bose-Einstein correlations

Bose-Einstein correlations (BECs) have been extensively studied in hadronic systems from Z^0 decay. A review may be found in [279]. The correlations are interesting in their own right as a quantum mechanical phenomenon whose experimental details can give information on the space-time structure of the source of hadrons. The correlations arise from the necessity to symmetrize the wavefunction for systems of two or more identical bosons. In most experimental analyses, a simple model is assumed where the source of particles is spherical with a Gaussian density. Then the two-particle phase space is enhanced by a factor $C(Q) = 1 + \lambda \exp(-Q^2 R^2)$ relative to its density in the absence of the correlations. Here Q, the square of the 4-momentum difference between two bosons, is the measure of the separation in phase space, λ measures the degree of coherence in the particle emission ($\lambda = 0$ corresponds to full coherence) and R is the radius of the Gaussian source.

Table 7. Measurements of Bose-Einstein correlations in Z^0 decay.

Particle System	R (fm)	λ	References	Comments
$\pi^\pm \pi^\pm$	0.65 ± 0.16	0.51 ± 0.12	A [280]	
	0.49 ± 0.05	1.06 ± 0.17	D [281]	Direct π
	0.93 ± 0.15	0.87 ± 0.14	O [282]	
$\pi^\pm \pi^\pm \pi^\pm$	0.62 ± 0.05	0.28 ± 0.09	D [283]	
$K^\pm K^\pm$	0.48 ± 0.08	0.82 ± 0.27	D [284]	
$K_S^0 K_S^0$	0.71 ± 0.07	$1.4 \ \pm 0.3$	A [194]	not corrected for f_0
	0.55 ± 0.14	0.61 ± 0.23	D [284]	
	0.76 ± 0.15	1.14 ± 0.39	O [195]	

BECs have been studied at LEP for systems of $\pi^\pm \pi^\pm$, $\pi^\pm \pi^\pm \pi^\pm$, $\pi^+ \pi^- \pi^\pm$, $K^\pm K^\pm$ and $K_S^0 K_S^0$. A summary of measured values of λ and R is given in table 7. It is not straightforward to compare the various results, nor to interpret the findings. For example, in order to measure the enhancement $C(Q)$ due to BECs it is necessary to know the phase space density in their absence, and there are several ways to tackle this. In addition particles which arise from resonance or weak decays may be removed (if the detector has the capability). The BEC effect will be diluted in data samples containing mixtures of different particle types, and the purity of pion or kaon samples may be increased, depending again on the capabilities of the detector. In the LEP analyses, various different approaches to these problems have been used.

Nevertheless, in all cases it is clear that the model based on a spherical source with Gaussian density gives a reasonable fit to the observations, although there is no real evidence that other models would not fit equally

well. The coherence parameter λ varies from close to zero to greater than one; the latter is unphysical and possibly indicates deviations from the model. The source has a typical size of 1 fm, which at first sight seems inconsistent with a picture of hadrons arising from a rapidly expanding linear colour string. However the length scale measured by the BECs is not the longitudinal size of the string, but the distance in production points for which particles are close together in momentum space [150]. Recently BEC studies at LEP have been extended to three-particle systems [283], and the multiplicity dependence of the correlations has been investigated [285].

Even if all of the measurements had been made in a consistent way, the interpretation of the results would not be straightforward: the correlations depend in a poorly understood way on final-state interactions, resonance production and rescattering of resonance decay products. According to [153] the situation may be "impossibly complicated". And [279] says "it seems very difficult to make progress in studying the Bose-Einstein effect in the context of e^+e^- physics, and it is not clear to what extent it can be considered a useful and interesting activity."

It is nevertheless important to understand at least the phenomenology of the Bose Einstein correlations since they impact on studies of other features of hadronic systems. For example, although the effect primarily influences systems of identical bosons, in the relatively high-multiplicity, jet-like environment of Z^0 decay, "residual" correlations [286] arise between pairs of unlike particles. The BECs produce a general collimation of the jets and a tendency to reduce the mean transverse momentum; this brings all particles closer together in momentum space. The effect is to produce a distortion of $\pi^+\pi^-$ mass spectra, especially at low momentum where the multiplicity is highest. This means for example that the use of opposite charge particle pairs to determine the phase space in the absence of BECs can result in biased values of λ and R. An important practical result of the residual correlations is the considerable difficulty in inclusive measurements of $\pi^+\pi^-$ resonances [187, 188, 287] such as the $\rho(770)^0$ and the $f_0(982)$ whose line shapes are distorted by the correlations and possibly also by other mechanisms [286].

In the process $e^+e^- \to W^+W^- \to$ hadrons at LEP 2, correlations may arise between the hadrons from one W and those from the other, an effect recently investigated by DELPHI [288]. Such an effect could result in a shift of the reconstructed W mass in multihadronic W decays [156]. A good understanding of the role of BECs in hadronization at the Z^0 may help to reduce uncertainties introduced by this effect.

7.2. Fermi-Dirac anticorrelations

While BECs between identical bosons are firmly established experimentally, anticorrelations between identical fermions are more difficult to observe. In Z^0 decay, baryons are produced at much lower rates than mesons, and local conservation of baryon number suppresses production of identical baryons close together in phase space. The only evidence for anticorrelations comes from a study by OPAL [289] of $\Lambda\Lambda$, $\overline{\Lambda}\,\overline{\Lambda}$ and $\Lambda\overline{\Lambda}$ pair production. Close to threshold it is found the the spin states of the di-hyperon systems agree with expectations of a simple statistical mixture, with no indication of any resonance in the $\Lambda\overline{\Lambda}$ threshold enhancement. In the case of the identical baryon pairs, there is a tentative indication of suppression close to threshold, as would be expected by the Pauli exclusion principle. However, further measurements are needed to confirm this result.

7.3. Baryon-antibaryon phase space correlations

Since baryons, and strange hadrons, are both heavier and less frequently of secondary origin than ordinary hadrons investigating their production and pairwise correlations appears to offer a more direct probe of the momentum and quantum number flow during hadronization. However, allowance must always be made for secondary hadrons coming from decays, such as $\Sigma^0 \to \Lambda \to p$ (here further data [162, 290] on $\Lambda^{(}\bar{p}^{)}$ correlations would be welcome). Baryon number conservation implies that a baryon is always accompanied by an antibaryon; flavour conservation, via diquark pairs, suggests that the baryons may be preferentially particle-antiparticle pairs; and LPHD argues that these baryons occur close by in phase space. So far, studies have concentrated on measuring the proximity in phase space of $p^{(}\bar{p}^{)}$ [43, 291], $\Lambda^{(}\overline{\Lambda}^{)}$ [194, 209, 292] and $\Lambda^{(}\bar{p}^{)}$ [162] baryon pairs. By introducing an event axis, typically the thrust or sphericity axis, correlations can be studied in rapidity, azimuthal angle or polar angle with respect to the axis.

Several models of baryon production are available [293]. Section 3 discusses the independent fragmentation [16, 115], the diquark [158] and popcorn [133, 160] (triplet) string options and the cluster [20] models. In addition a possible contibution from direct, $\gamma^\star \to (qq')(\bar{q}\bar{q}')$, diquark production has been proposed [157, 294]. Also there is the recombination model of hadron production [295]. In this approach a spectrum of partons occuring after a shower at the fixed scale Q_0^2 is convoluted with an explicit wavefunction for a particular hadron. In the case of a baryon [296] this gives (c.f. (7)):

$$D_{\mathrm{B}}^a(x, Q^2) = \sum_{a_1, a_2, a_3} \int \mathrm{d}x_1 \mathrm{d}x_2 \mathrm{d}x_3 D_{a_1, a_2, a_3}^a(x_1, x_2, x_3, Q^2; Q_0^2)$$
$$\times\ R_{a_1, a_2, a_3}^{\mathrm{B}}(x_1, x_2, x_3, x; Q_0^2) \quad (31)$$

Here a typical wavefunction is $R \propto (x_1 x_2 x_3)^2 \delta(x - x_1 - x_2 - x_3)$, consistent with reciprocity [248] and quark counting rules [259], and on the assumption of uncorrelated partons $D_{a_1, a_2, a_3}^a(x_1, x_2, x_3, Q^2; Q_0^2) = \prod_i D_{a_i}^a(x_i, Q^2; Q_0^2)$. It may be mentioned in passing that the recombination model makes interesting predictions for baryon polarizations [297].

7.3.1. *Rapidity correlations* At the Z^0 strong, short-range correlations in rapidity are seen between baryon-antibaryon $B\overline{B}$ pairs.   (Unlike-baryon distributions have the like-baryon (BB) distributions subtracted to remove secondary correlations due to more than one $B\overline{B}$ pair in an event.)   For example, the distribution of baryon rapidity (y) in such events, $\mathrm{d}n/\mathrm{d}y(y_{\mathrm{B}}|y_{\overline{\mathrm{B}}})$, is measured to be compact and centred on $y_{\overline{\mathrm{B}}}$ [43, 162, 194, 292]. In a $B\overline{B}$ pair, given the rapidity of the $\bar{\mathrm{p}}$ $(\overline{\Lambda})$ there is $\approx$ 70 (50)% probability that the p (Λ) will be found within $|y_{\mathrm{B}} - y_{\overline{B}}| \le 1(0.6)$ and vice versa [43, 292]; a marginally weaker short-range $\Lambda \bar{\mathrm{p}}$ correlation is found [162]. A much weaker long-range anticorrelation is also seen for far forward/backward $B\overline{B}$ pairs, as anticipated from a leading particle effect. In contrast, when BB pairs occur in an event, the $\mathrm{d}n/\mathrm{d}y(y_{\mathrm{B}_1}|y_{\mathrm{B}_2})$ distribution is nearly flat with just a weak short-range anticorrelation, particularly so away from the central region [292] where phase space constraints become important. Similar, though statistically limited, results have been seen at lower energy [298, 290].

Qualitatively these features are reproduced by both the HERWIG and JETSET models, though quantitatively the strength of the correlations is overestimated by HERWIG and by JETSET without popcorn [43, 292]. The recombination model predicts rapidity correlations which are much too weak whilst direct diquark production predicts long-range correlations that are too strong; both are disfavoured by the data [209].

7.3.2. *Azimuthal angle correlations* Somewhat weaker correlations are seen between the azimuthal angles in baryon pairs at the Z^0 [43, 194]. $B\overline{B}$ pairs show a tendency towards $\Delta\phi = 0$, though in those pairs which lie out of the event plane there is a tendency towards $\Delta\phi = \pi$. BB pairs show a weaker tendency towards $\Delta\phi = \pi$. Two competing mechanisms might be envisaged to explain the azimuthal angle correlations. First is a local compensation of transverse momentum which leads to an enhancement for $\Delta\phi = \pi$. Second is a tendency for any off-axis boost to be shared by neighbouring baryons, leading

to an enhancement at $\Delta\phi = 0$. The latter effect might be expected to become more important at higher energies where three-jet effects come into play (these by definition involve higher transverse momentum scales than hadronization), more so for baryons lying in the event plane. At low CoM energy (10 GeV) the first, back-to-back, effect appears to dominate [299] but this is seen to weaken at higher energy (30 GeV) [298, 300, 301] and at the Z^0 the second, side-by-side, effect is more important.

7.3.3. Polar angle correlations Historically a very powerful way to discriminate between hadronization models is the orientation of the $B\overline{B}$ pair with respect to the event axis [301]. If $\theta^\star$ is the angle between the axis of the $B\overline{B}$ pair and the event axis as seen in the $B\overline{B}$ pair rest frame then $\cos\theta^\star$ is measured to be highly forward-backward peaked [43, 209]. By utilizing the lepton beam polarization information (see section 1.1) SLD are capable of determining the primary quark direction and have recently been able to demonstrate that the baryon preferentially follows the quark direction [291].

In string models the colour field typically aligns along the event axis, so that provided that the transverse momenta acquired by the baryons are small compared to the longitudinal momenta transferred from the string, the baryons will retain a strong memory of the string/event axis direction. In contrast, because clusters are deemed to be structureless, they have no means of retaining any information about an original event axis (they are unpolarized) and so decay isotropically in their rest frame. Not surprisingly then the highly peaked $\cos\theta^\star$ strongly disfavours the essentially flat prediction from HERWIG whilst JETSET offers a good description of the data. In HERWIG version 5.7 an option was introduced to allow non-isotropic decays of clusters containing primary quarks; this was implemented to stiffen the momentum spectrum of c and b hadrons and has little influence on $B\overline{B}$ pair polar angle distributions.

7.4. Strangeness correlations

In the previous section, 7.3, phase space correlations were discussed for baryons; we now turn to similar measurements made on strange hadrons. The conservation of strangeness in strong interactions implies that strange hadrons are pair-produced during hadronization. The probability that hadron h_1 is accompanied by h_2 is defined as $P(h_1, h_2) = 2 \times \langle n_{h_1,h_2}\rangle/\langle n_{h_1} + n_{h_2}\rangle$ where the 2 is included because of double counting. Measurements give $P(\Lambda, \overline{\Lambda}) = 49\pm6\%$ whilst $P(\Lambda, \Lambda) = 13\pm1\%$ [194, 209, 292], $P(\Lambda, K_s^0) = 17\pm2\%$ and $P(K_s^0, K_s^0) = 29 \pm 4\%$ [194], $P(\Xi^-\overline{\Lambda}) = 40 \pm 7\%$ [212, 292] and $P(\Xi^-\overline{\Xi}^+) = 4 \pm 6\%$ [292].

Two sources of strange hadrons can be anticipated: leading hadrons associated with initial $s\bar{s}$ quarks and those pair-produced locally in the event's

colour field. To help distinguish these possibilities requires information on the phase-space correlations between pairs of strange hadrons. A short-range rapidity correlation occurs between $K_s^0 K_s^0$ pairs and a slightly weaker one between $K_s^0 \Lambda$ pairs [194] indicating a local mechanism for strangeness compensation. Also visible are: weaker long-range correlations, as expected from leading quarks; and evidence of phase-space suppression, particularly when both hadrons are leading. Weak correlations are also seen at $\Delta\phi = 0, \pi$ for centrally produced $K_s^0 K_s^0$ and $K_s^0 \Lambda$ pairs.

The possible influence of introducing the popcorn baryon production mechanism, see section 3.2.5, is of particular interest for string models. The presence of an intermediate meson, $BM\overline{B}$ tends to soften all correlations. At present, taking account of systematic errors, measurements of baryon and strangeness correlations are insufficient to place any significant constraint on the level of popcorn production required. The $B\overline{B}$ pair rapidity difference is mainly sensitive to the amount of popcorn production, with data favouring a substantial component [209, 292]. The substantial rate of $\Xi^- \overline{\Lambda}$ pair production also favours a high level of popcorn production in order to supply an intermediate kaon [190, 292]. Interestingly the number of $B^{(\overline{B})}$ pairs decreases linearly with the amount of popcorn introduced so that their measured multiplicity can be (rather simplistically) used to constrain the amount of popcorn to around 50% [194].

A more direct test of the popcorn mechanism is to look at rapidity ordered $BM\overline{B}$ triples [162]. Using nearby baryon pairs, $|y_B - y_{\overline{B}}| < 1$, a probability of 7% (25%) is obtained for finding an intervening kaon (pion) in a $p^{(\overline{p})} \Lambda^{(\overline{\Lambda})}$ or $\Lambda\overline{p}$ pair. In addition to there being no enhancement of popcorn-favoured $\Lambda K^+ \overline{p}$ triples, unfavoured $\Lambda K^- \overline{p}$ triples are found equally likely. However, in events containing a kaon and a close Λp pair, the kaon is found very close in rapidity to the baryon pair.

7.5. *Intermittency*

Intermittency [302], the non-random clustering of particles in phase space, is a somewhat obscure phenomenon of uncertain dynamical origin. In essence, intermittency corresponds with large, non-statistical, fluctuations in the numbers of particles in particular events which are found in narrow rapidity bins. It is normally studied by measuring factorial moments of multiplicity distributions in rapidity bins. Intermittent behaviour has been observed in hadronic systems from Z^0 decay at both LEP [303] and SLC [304] as well as in lower energy $e^+ e^-$ collisions.

The intermittency observed in hadronic Z^0 decays is in fact reproduced by the Lund parton shower Monte Carlo model with string fragmentation. It is

a possibility that the self-similarity inherent in the QCD parton shower, with its successive q→qg and g→gg branchings, is the source of the intermittency seen in the distribution of the final-state hadrons. Certainly the JETSET model contains no feature explicitly introduced to simulate the dynamics of intermittency.

The appearance of intermittency in the Z^0 decay data would seem to be an ideal opportunity to gain a good understanding of the mechanisms which lie behind it. Previously its interpretation in hadroproduction experiments has been obscured by the complicated nature of the final states and the effects of beam and target fragments.

8. Quark-gluon jet differences

The determining property of quark and gluon jets is the colour charge of the initiator partons, $C_F = (N_c^2 - 1)/(2N_c)$ and $C_A = N_c$ respectively. Due to the gluon's larger charge it should radiate more subsequent gluons in a parton shower. This leads to the anticipation that gluon jets, as compared to quark jets, will have: a higher multiplicity, softer momentum spectrum and wider angular distribution [305, 306]. These global features are largely borne out by experimental results [307, 72, 308, 309, 310, 311]. However whilst clear differences are now established between gluon and light-quark jets, b-jets appear to be rather like gluon jets at Z^0 energies [308, 309]; the ratios of measured properties typically fall short of the naive asymptotic predictions. For example the multiplicity ratio is, in leading order, predicted to be $C_A/C_F = 9/4$ [305]; at NNLO this becomes ≈ 2 [93, 312] and after imposing energy (but not momentum) conservation on the shower this drops to $\approx 1.6 - 1.8$ [313] (the exact predictions depend on jet energy and the scale used for α_s). The measured ratio, which is seen to be sensitive to the precise jet definition, is typically in the range $1.1 - 1.3$, though OPAL has obtained 1.55 in an event hemisphere-based analysis [310]. It should be borne in mind that the these basic predictions are made for back-to-back pairs of quark or gluon jets whilst growing evidence suggests that the relative topology of a jet is important in determining the appropriate scale [311].

The above discussion relates to the perturbative properties of quark and gluon jets. Current cluster and string models of hadronization make no distinction between whether a set of final-state partons arose from a fragmenting primary quark or gluon; they are treated the same. This does allow the possibility of a 'leading particle' effect (for example one should expect more leading kaons in an s-quark jet than a gluon jet) but no other 'anomalous' effects [249]. An interesting possibility is that some isoscalar states, η, η', ϕ, $\omega, \ldots$, may contain a significant gg component and hence

might appear more frequently as leading particles in gluon jets. These particles are very often primary hadrons coming directly from a cluster or string. At present the possibility of hadrons containing gluons is not allowed for and only quark constituents are considered. Indeed in the cluster framework gluons are split into light $q\bar{q}$ pairs whilst in the string approach they represent energy-momentum 'kinks' on a string. However modifying the models to accommodate gluonium would not, *a priori*, appear to pose significant problems of principle or practice.

A more radical scenario is offered by the independent fragmentation model of Peterson and Walsh [314]. This is based on the suggestion that a gluon is attached to an octet colour flux tube and quarks to triplet flux tubes (see section 3.2). A gluon now fragments into a sequence of isoscalar gg or $gq\bar{q}g$ clusters leading to a prediction of greatly enhanced η, η' etc production and harder momentum spectra as compared to quark jets.

A third alternative scenario for gluon jet hadronization is provided within the recombination model [295] discussed in section 7.3. Calculations predict: a softer pion spectrum [315], an enhanced multiplicity ratio $\langle n_{\eta'}\rangle/\langle n_{\pi^0}\rangle$ [316] and enhanced baryon production [296] in gluon jets compared to quark jets.

The L3 Collaboration have reported tentative indications that η production is enhanced in gluon jets [186]. Studying the lowest energy — gluon — jet in three-jet events they see a a harder η momentum spectrum than predicted by both the HERWIG and JETSET Monte Carlos with an enhancement in the ratio $\langle n_{\eta}\rangle/\langle n_{\pi^0}\rangle$. The use of a ratio takes into account the established increase in multiplicity found in gluon compared to quark jets and is designed to make the measurement sensitive to any additional enhancement or suppression. The Monte Carlos provide a satisfactory description of the spectrum and $\langle n_{\eta}\rangle/\langle n_{\pi^0}\rangle$ ratio in quark jets. DELPHI have studied the production rates of kaons, Λ^0 and $\Xi^\pm$ in multi-jet events [212]. They find that the relative yields of strange hadrons in multi-jet, normalized to two-jet, events is constant in events with widely separated jets but favours increased production in multi-jet events at small resolutions, particularly so for kaons. In a more direct study DELPHI have looked at identified particle production rates in actual quark (natural flavour mix) and gluon jets, normalized to the charged multiplicity in the jet: the double ratios $(\langle n_{\rm H}\rangle/\langle n_{\rm ch}\rangle)_g/(\langle n_{\rm H}\rangle/\langle n_{\rm ch}\rangle)_q$ [317]. The evidence suggests values for the double ratios of approximately 1.1 for the K^0, 0.9 for K^+, 1.2 for p and 1.4 for Λ. In general these results are in qualitative agreement with the Monte Carlos but quantitatively the deviations from unity are larger than typically predicted, apart for the K^0 result where a small suppression was expected. However the errors are relatively large. OPAL have also reported preliminary studies of the double ratios [318]. For $K_{\rm s}^0$ and ϕ mesons they report a slight, $\leq 10\%$, increase in the relative production rates in gluon jets, whilst for

p and Λ baryons they measure a significant 30–40% increase. These enhanced production rates are presumably at the expense of pion production. At present more measurements are required before hard conclusions can be drawn.

The possibility of enhanced identified hadron production in gluon as compared to quark jets has received previous attention. The results for mesons, in particular hard η relative to π^0, production are not conclusive. At $\sqrt{s} = 10$ GeV ARGUS [319] saw no evidence for enhanced η or ϕ production in the continuum, $\gamma^\star \rightarrow q\bar{q}$. Also comparison has been made between continuum and $\Upsilon(1, 2S) \rightarrow$ ggg events; here Crystal Ball [320] see no enhancement whilst DASP-II, CLEO and ARGUS [321] see a slight enhancement for a number of mesons. At $\sqrt{s} = 30$ GeV JADE [322] reported very weak (statistically insignificant) evidence for a small enhancement in the $\langle n_\eta \rangle / \langle n_{\pi^0} \rangle$ ratio in acollinear, gluon rich, events. The situation is clearer for baryons. The production rate of baryons in $\Upsilon(1, 2S)$ decay (gluon dominated) to continuum (quark dominated) events shows an excess of 200–300% [321].

In the context of conventional Monte Carlos a number of partial explanations have been offered. A study using JETSET indicates that the relative production rates of mesons in quark and gluon jets is energy independent and just less than one, whilst for baryons it is 20–25% larger and shows a slight increase with jet energy [318]. This latter effect may be attributed to an edge effect associated with the suppression of leading baryons. In cluster models it has been argued that in gluon rich environments, the topology, rather than any intrinsic properties of the jets, leads to heavier clusters and hence larger baryon production rates [323]. At the Υ it has also been emphasized [324] that secondary decays are important, and that 40% of the events are in the continuum to b and c quarks (see figure 1) which, being heavy, 'eat up' the available phase space for baryon production.

9. Outlook

That Monte Carlo event generators, solidly based on sound physics, are essential in modern high energy experiments, from detector conception to data analysis, ought not to be forgotten. It therefore almost goes without saying that the reliability of Monte Carlo predictions should be a prime concern if only for mere practical reasons. To this end the large event rates and pristine conditions available in hadronic Z^0 decays at e^+e^- colliders play a particularly important role. Here, as nowhere else, the physics assumption built into the Monte Carlo models can be confronted with ever more exacting tests. The relatively complex conditions associated with initial-state hadrons have largely precluded this activity using ep and $p\bar{p}$ data, thereby making physicists reliant on the quality of the Z^0 data. Two caveats to the wider application of the

models are the questions of the reliability of the factorization theorem in perturbative QCD and the presumption of universality in the hadronization process.

Focusing on the models for the hadronization processes one may ask what is left that should be done with the Z^0 data and what might be learned from it. We list a number of topics, perhaps not all of which can be done with available data (but one can always hope for more Z^0 data):

- A study of the transverse momentum distributions of identified particles, especially pions where low mass effects and correlations may occur [147] — In string models the fact that the predicted width of the Gaussian $p_\perp$-distribution, $\sqrt{\kappa/\pi}$, proves too narrow has raised questions about the adequacy of a tunnelling mechanism explanation: is unresolved (non-perturbative) gluon emission [145] the real explanation?
- An attempt to establish properties of the relatively rare, directly produced pions — Pions are special particles by virtue of their nature as Goldstone bosons (of the chiral symmetry); this mandates them to have small masses which in a string model implies a very small size, in fact uniquely less than a string's width.
- Further measurements of orbitally excited mesons and baryons — Are the production rates for these states too high to be compatible with the string model?
- A search for D-wave states, such as the $K_3^\star(1780)$ — These could help elucidate the role of the wavefunction in determining a hadron's production rate.
- A study of $f_0(980)$ production as a function of rapidity and of total event multiplicity — This would test the Gribov confinement scenario [215].
- A search for deuterium production — This has been reported previously in studies at the Υ [325] and is expected, on the basis of a string model calculation [326], at the level of 5×10^{-5} per hadronic Z^0 event.
- Further measurements of strangeness suppression (γ_s) which ideally can be directly compared to those available in ep collisions, particularly those associated with the current region of the Breit frame [88] — If it turns out that $\gamma_s^{e^+e^-} \neq \gamma_s^{ep}$ then effort should go to establishing any other differences.
- A measurement of the s-quark to p and $\bar{p}$ fragmentation functions — Is there a measurable difference as suggested [246] by the possible asymmetry in sea quark structure functions?
- Measurements of identified particle production rates in quark and gluon jets — Are there measurable differences and, if so, what is the mechanism?
- A search for glueball candidates, particularly in the gluon-rich environment provided by gluon jets.

- Further measurements of leading baryon polarization — Is there a depolarizing mechanism for the b baryons which does not apply to those arising from s quark fragmentation?

- Measurements of the helicity density matrix for the light and heavy vector mesons — Does hadronization produce spin-aligned vector mesons, and does any alignment depend on x? Are some off-diagonal elements non-zero as predicted by coherent hadronization? Spin physics has a long history of producing surprises.

- More detailed studies of intermittency — Can it be firmly established that the phenomenon is due to the self-similar evolution of the initial q$\bar{\text{q}}$ state via a QCD parton shower?

- A search for direct evidence of popcorn-type baryon production via, for example, further study of ΛK$^+$$\bar{\text{p}}$ type correlations — Three-body cluster decays would also induce such correlations but perhaps with different intensity.

- A search for $\Omega^-\bar{\text{p}}$ type correlations — These are possible in a generalized popcorn mechanism although they will be hard to find experimentally because of low rates.

- An attempt to establish directly the existence of the 'dead cone' [110] in non-leading particles, by removing the leading particles using fully reconstructed b-hadron decays.

- Direct measurement of the rates and momentum spectra of hadrons produced in b-quark events to ensure adequate descriptions of the weak decays in the Monte Carlos — b hadrons contribute a tenth of all particles in hadronic Z^0 decays, and significantly more at large x.

- A tuning of the Monte Carlo models to Z^0 data, incorporating colour rearrangement — This is important in order to determine the effects of colour rearrangement and to provide constraints which may prove significant for later W mass measurements.

- A simultaneous tuning of the Monte Carlo programs to the Z^0 data and lower energy data, particularly from PEP and PETRA — At lower energies the relative contribution to event properties made by hadronization is more important, whilst the influence of the perturbative shower can be tested using the CoM energy dependence of observables.

- An 'ultimate' tuning of the Monte Carlo models to the final Z^0 data — This will be an invaluable service to experimentalists and theorists allowing the experience gained from LEP1/SLC to be applied at future machines.

- A continuation of the search for tests which discriminate between the competing models of the non-perturbative physics underlying the hadronization, and continuing development of these models.

In summary, the $e^+e^- \to Z^0/\gamma^* \to$ hadrons data have already provided a wealth of information on the phenomena of parton hadronization. Of the available models of the non-perturbative physics involved, the Lund string model, as implemented in JETSET, has met with most success, particularly in the baryon sector, and most notably in its prediction of the angular distribution of correlated baryon-antibaryon pairs in their rest frame. However, the model has many free parameters and consequently has little predictive power. But the parameters are not arbitrary — most are based on incomplete knowledge of physics. Therefore it could be argued that their values, when fully tuned to reproduce observations, provide important information about hadronic physics. On the other hand, while the weight of evidence tends to favour the string picture, the other models, particularly the cluster model of HERWIG, are not dead, and more analyses of the existing and future data are essential to provide further discrimination between the models and to help elucidate the physics of hadronization.

Acknowledgements

References

[1] Kunszt Z, Nason P, Marchesini G and Webber B R 1989 *Z Physics at LEP 1* vol 1 yellow report CERN 89-08 p 373

[2] Altarelli G *et al* 1989 *Z Physics at LEP 1* vol 1 yellow report CERN 89-08

[3] Bardin D *et al* 1995 *Reports of the Working Groups on Precision Calculations for the Z Resonance* yellow report CERN 95-03

[4] Altarelli G *et al* 1996 *Physics at LEP 2* vol 1 yellow report CERN 96-01

[5] Gorishny S G, Kataev A L and Larin S A 1991 *Phys. Lett.* **B259** 114
Surguladze L R and Samuel M A 1991 *Phys. Rev. Lett.* **66** 560 and *erratum* 2416
Chetyrkin K G, Kühn J H and Kwiatkowski A 1996 *Phys. Rep.* **277** 189

[6] Sjöstrand T *et al* 1989 *Z Physics at LEP 1* vol 3 yellow report CERN 89-08 p 143

[7] Particle Data Group, Barnett R M *et al* 1996 *Phys. Rev.* **D54** 1

[8] Dokshitser Yu L, Khoze V A and Troyan S I 1989 *Perturbative QCD* ed A H Mueller (World Scientific: Singapore) p 241
Dokshitser Yu L, Khoze V A, Mueller A H and Troyan S I 1991 *Basics of Perturbative QCD* (Gif-sur-Yvette: Editions Frontières)

[9] Bjorken J D 1973 *Proc. SLAC Summer Inst. on part. Phys.* vol 1 report SLAC-167 p 1

[10] Bjorken J D 1992 *Phys. Rev.* **D45** 4077

[11] Knowles I G *et al* 1996 *Physics at LEP 2* vol 2 yellow report CERN 96-01 p 103

[12] Lönnblad L 1992 *Comp. Phys. Comm.* **71** 15
URL: http://surya11.cern.ch/users/lonnblad/ariadne/

[13] Gustafson G 1986 *Phys. Lett.* **B175** 453
Gustafson G and Pettersson U 1988 *Nucl. Phys.* **B306** 746
Andersson B, Gustafson G and Lönnblad L 1990 *Nucl. Phys.* **B339** 393

[14] Andersson B, Gustafson G, Ingelman G and Sjöstrand T 1983 *Phys. Rep.* **97** 31

[15] Odorico R 1992 *Comp. Phys. Comm.* **72** 238
URL: http://www.bo.infn.it/preprint/odorico.html

[16] Field R D and Feynman R P 1978 *Nucl. Phys.* **B136** 1

[17] Marchesini G *et al* 1992 *Comp. Phys. Comm.* **67** 451
URL: http://surya11.cern.ch/users/seymour/herwig/

[18] Marchesini G and Webber B R 1984 *Nucl. Phys.* **B238** 1
Knowles I G 1988 *Nucl. Phys.* **B310** 571 and 1990 *Comp. Phys. Comm.* **58** 271
Catini S, Webber B R and Marchesini G 1991 *Nucl. Phys.* **B349** 635
Seymour M H 1995 *Comp. Phys. Comm.* **90** 95

[19] Marchesini G and Webber B R 1990 *Nucl. Phys.* **B330** 261

[20] Webber B R 1984 *Nucl. Phys.* **B238** 492

[21] Sjöstrand T 1994 *Comp. Phys. Comm.* **82** 74 and Lund University report LU TP 95-20
URL: http://thep.lu.se/tf2/staff/torbjorn/

[22] Gross D J and Wilczek F 1973 *Phys. Rev. Lett.* **30** 1343 and 1973 *Phys. Rev.* **D8** 3633
Politzer H D 1973 *Phys. Rev. Lett.* **30** 1346
Tarasov O V, Vladimirov A A and Zharkov A Yu 1980 *Phys. Lett.* **B93** 429
van Ritbergen T, Vermaseren J A M and Larin S A 1997 preprint archive hep-ph/9701390

[23] Ellis R K, Ross D A and Terrano A E 1981 *Nucl. Phys.* **B178** 421
Fabricus K, Kramer G, Schierholtz G and Schmitt I 1981 *Z. Phys.* **C11** 315

[24] Körner J G, Schüler G A and Barreiro 1980 *Phys. Rev.* **D1** 1416
Kramer G and Lampe B 1985 *Comm. Math. Phys.* **97** 257
Zijlstra E B and van Neerven W L 1992 *Nucl. Phys.* **B383** 525

[25] Rodrigo G V 1997 preprint archive hep-ph/9703359
Bernreuther W, Brandenberg A and Uwer P 1997 preprint archive hep-ph/9703305

[26] Signer A and Dixon L 1997 *Phys. Rev. Lett.* **78** 811
Glover E W N and Miller D J 1997 *Phys. Lett.* **B396** 257
Bern Z, Dixon L, Kosower D A and Weinzierl S 1997 *Nucl. Phys.* **B489** 3

[27] Ali A *et al* 1979 *Phys. Lett.* **B82** 285 and 1980 *Nucl. Phys.* **B167** 454
Berends F A, Giele W T and Kuijf H 1988 *Nucl. Phys.* **B321** 39
Falck N K, Graudenz D and Kramer G 1989 *Phys. Lett.* **B220** 299

[28] Lee T D and Nauenberg M 1964 *Phys. Rev.* **133** 1549
Kinoshita T 1965 *J. Math. Phys.* **3** 56
Sterman G 1978 *Phys. Rev.* **D17** 2789 and 2773

[29] Gribov V N and Lipatov L N 1972 *Sov. J. Nucl. Phys.* **15** 438
Dokshitzer Yu L 1977 *Sov. Phys. JETP* **46** 641

[30] Altarelli G and Parisi G 1977 *Nucl. Phys.* **B126** 298
Owens J F 1978 *Phys. Lett.* **B76** 85
Uematsu T 1978 *Phys. Lett.* **B79** 97

[31] Konishi K, Ukawa A and Veneziano G 1979 *Nucl. Phys.* **B157** 45
Bassetto A, Ciafaloni M and Marchesini G 1983 *Phys. Rep.* **100** 201
Webber B R, *Ann. Rev Nucl. Part. Sci* 1986 **36** 253

[32] Catani S, Turnock G and Webber B R 1991 *Phys. Lett.* **B272** 368 and 1992 *Phys. Lett.*
      B295 368
      Catani S, Trentadue L, Turnock G and Webber B R 1991 *Phys. Lett.* **B263** 491 and
      1993 *Nucl. Phys.* **B407** 3
      Dissertori G and Schmelling M 1995 *Phys. Lett.* **B361** 167

[33] Catani S *et al* 1991 *Phys. Lett.* **B269** 432

[34] Stirling W J 1991 *J. Phys. G: Nucl. Part. Phys.* **17** 1537
      Bethke S, Kunszt Z, Soper D E and Stirling W J 1992 *Nucl. Phys.* **B370** 310
      Brown N and Stirling WJ 1992 *Z. Phys.* **C53** 629

[35] Ceradini F *et al* 1972 *Phys. Lett.* **B42** 501

[36] SLAC-LBL Collaboration, Hanson G *et al* 1975 *Phys. Rev. Lett.* **35** 1609
      TASSO Collaboration, Althoff M *et al* 1984 *Z. Phys.* **C22** 307

[37] Söding P and Wolf G 1981 *Ann. Rev. Nucl. Part. Sci.* **31** 231
      Duinker P 1982 *Rev. Mod. Phys.* **54** 325
      Wu S L 1984 *Phys. Rep* **107** 59
      MARK-J Collaboration, Adeva B *et al* 1984 *Phys. Rep.* **109** 131
      Narosoka B 1987 *Phys. Rep.* **148** 67

[38] DELPHI Collaboration, Abreu P *et al* 1990 *Phys. Lett.* **B247** 167
      L3 Collaboration, Adeva B *et al* 1990 *Phys. Lett.* **B248** 464
      OPAL Collaboration, Akrawy M Z *et al* 1991 *Z. Phys.* **C49** 375 and Akers R *et al*
      1994 *Z. Phys.* **C63** 197
      SLD Collaboration, Abe K *et al* 1993 *Phys. Rev. Lett.* **71** 2528

[39] Kunszt Z and Nason P in [1]
      Giele W T and Glover E W N 1992 *Phys. Rev.* **D46** 1980
      Frixione S, Kunszt, Z and Signer A 1996 *Nucl. Phys.* **B467** 399
      Catani S and Seymour M H 1996 *Phys. Lett.* **B278** 287

[40] ALEPH Collaboration, Decamp D *et al* 1991 *Phys. Lett.* **B255** 623 and 1991 *Phys.*
      Lett. **B257** 479
      DELPHI Collaboration, Abreu P *et al* 1992 *Z. Phys.* **C54** 55
      L3 Collaboration, Adriani O *et al* 1992 *Phys. Lett.* **B284** 471
      OPAL Collaboration, Acton P D *et al* 1992 *Z. Phys.* **C55** 1
      SLD Collaboration, Abe K *et al* 1994 *Phys. Rev.* **D50** 5580 and 1995 *Phys. Rev.*
      D52 4240

[41] ALEPH Collaboration, Decamp D *et al* 1992 *Phys. Lett.* **B284** 163
      DELPHI Collaboration, Abreu P *et al* 1993 *Z. Phys.* **C59** 21
      OPAL Collaboration, Acton P D *et al* 1993 *Z. Phys.* **C59** 1
      SLD Collaboration, Abe F *et al* 1995 *Phys. Rev.* **D51** 962

[42] Webber B R 1995 *Proc. Int. Conf. on H.E.P. (Glasgow 1994)* vol 1 eds P J Bussey
      and I G Knowles (Bristol: Inst. of Physics) p 213

[43] ALEPH Collaboration, Barate R *et al* 1996 preprint CERN-PPE/96-186, submitted
      to *Phys. Rep.*

[44] DELPHI Collaboration, Abreu P *et al* 1996 *Z. Phys.* **C73** 11

[45] ALEPH Collaboration, Buskulic D *et al* 1996 *Z. Phys.* **C71** 357

[46] ALEPH Collaboration, Decamp D *et al* 1992 *Z. Phys.* **C55** 209

[47] OPAL Collaboration, Akrawy M Z *et al* 1990 *Z. Phys.* **C47** 505
      L3 Collaboration, Adeva B *et al* 1992 **C55** 39

[48] Mueller A H 1993 *QCD 20 years later* vol 1 ed P M Zerwas and H A Kastrup (Singapore: World Scientific) p 162

[49] Wilson K 1969 *Phys. Rev.* **179** 1499
Wilson K and Kogut J 1974 *Phys. Rep.* **12** 75

[50] Bigi I I, Shifman M A, Uraltsev N G and Vainshtein A I 1994 *Phys. Rev.* **D50** 2234

[51] Webber B R 1994 *Phys. Lett.* **B339** 148: see also
Manohar A V and Wise M B 1995 *Phys. Lett.* **B344** 407

[52] Dokshitzer Yu L and Webber B R 1995 *Phys. Lett.* **B352** 451
Dokshitzer Yu L, Marchesini G and Webber B R 1995 preprint archive hep-ph/9512336

[53] Akhoury R and Zakharov V I 1995 *Phys. Lett.* **B357** 646

[54] Feynman R P 1972 *Photon Hadron Interactions* (New York: W A Benjamin)

[55] L3 Collaboration, Adriani O *et al* 1992 *Phys. Lett.* **B292** 472
ALEPH Collaboration, Buskulic D *et al* 1993 *Z. Phys.* **C57** 17
OPAL Collaboration, Acton P D *et al* 1993 *Z. Phys.* **C58** 405
DELPHI Collaboration, Abreu P *et al* 1995 *Z. Phys.* **C69** 1

[56] Seymour M H, 1994 *Z. Phys.* **C64** 445

[57] Cartwright S *et al* *Photon radiaion from quarks* 1992 yellow report CERN 92-04

[58] OPAL Collaboration, Akers R *et al* 1993 *Z. Phys.* **C67** 15
ALEPH Collaboration, Buskulic D *et al* 1996 *Z. Phys.* **C69** 365

[59] OPAL Collaboration, 1996 submission to *ICHEP96 (Warsaw)* PA04-026

[60] Azimov Ya I, Dokshitser Yu L, Khoze V A and Troyan S I 1985 *Phys. Lett.* **B165** 147

[61] Khoze V A and Lönnblad L 1990 *Phys. Lett.* **B241** 123

[62] Dokshitser Yu L, Khoze V A, Troyan S I and Mueller A H 1988 *Rev. Mod. Phys.* **60** 373

[63] Azimov Ya A, Dokshitzer Yu L, Khoze V A and Troyan S I 1985 *Z. Phys.* **C27** 65

[64] 't Hooft G 1974 *Nucl. Phys.* **B72** 461

[65] Andersson B, Gustafson G and Sjögren C 1992 *Nucl. Phys.* **B380** 391

[66] JADE Collaboration, Bartel W *et al* 1981 *Phys. Lett.* **B101** 129 and 1985 *Phys. Lett.* **B157** 340
TASSO Collaboration, Althoff M *et al* 1985 *Z. Phys.* **C29** 29
TPC/2γ Collaboration, Aihara H *et al* 1985 *Z. Phys.* **C28** 945

[67] Andersson B, Gustafson G and Sjöstrand T 1980 *Phys. Lett.* **B94** 211

[68] OPAL Collaboration, Akrawy M Z *et al* 1991 *Phys. Lett.* **B261** 334

[69] L3 Collaboration, Acciarri M *et al* 1995 *Phys. Lett.* **B345** 74

[70] MARK II Collaboration, Sheldon P D *et al* 1986 *Phys. Rev. Lett.* **57** 1398
TPC/2γ Collaboration, Aihara H *et al* 1986 *Phys. Rev. Lett.* **57** 945
JADE Collaboration, Ould Saada F *et al* 1988 *Z. Phys.* **C39** 1

[71] Azimov Ya I, Dokshitser Yu L, Troyan S I and Khoze V A 1986 *Sov. J. Phys.* **43** 95

[72] DELPHI Collaboration, Abreu P *et al* 1996 *Z. Phys.* **C70** 179

[73] OPAL Collaboration, Akers R *et al* 1995 *Z. Phys.* **C68** 531

[74] OPAL Collaboration, Acton P D *et al* 1993 *Z. Phys.* **C58** 207

[75] Dokshitzer Yu L, Marchesini G and Oriani G 1992 *Nucl. Phys.* **B387** 675

[76] Chmeisanni M 1992 *Annual Report* I.F.A.E. Universitat Autònima de Barccelona p 49

[77] L3 Collaboration, Acciarri M *et al* 1995 *Phys. Lett.* **B353** 145

[78] Mueller A H 1981 *Proc. 1981 Int. Symp. on Lepton and Photon Ints. at High Energies*

(Bonn 1981) ed W Pfeil (Bonn: Phys. Inst. U. Bonn) p 689

Dokshitzer, Yu L, Fadin V S and Khoze V A 1982 *Phys. Lett.* **B115** 242

[79] Fong C P and Webber B R 1989 *Phys. Lett.* **B229** 289 and 1991 *Nucl. Phys.* **B355** 210

[80] DELPHI Collaboration, Aarnio D *et al* 1990 *Phys. Lett.* **B240** 271

OPAL Collaboration, Akrawy M Z *et al* 1990 *Phys. Lett.* **B247** 617

[81] L3 Collaboration, Adeva B *et al* 1991 *Phys. Lett.* **B259** 199

[82] MARK-II Collaboration, Abrams G *et al* 1990 *Phys. Rev. Lett.* **64** 1334

[83] ALEPH Collaboration, Buskulic D *et al* 1995 *Phys. Lett.* **B357** 487

[84] DELPHI Collaboration, Abreu P *et al* 1996 preprint CERN-PPE/96-185, submitted to *Phys. Lett.* **B**

[85] Boudinov E R, Chliapnikov P V and Uvarov V A 1993 *Phys. Lett.* **B309** 210

[86] Lafferty G D, Reeves P I and Whalley M R 1995 *J. Phys. G: Nucl. Part. Phys.* **21** A1

[87] Mueller A H 1983 *Nucl. Phys.* **B213** 85 and *erratum* 1984 *Nucl. Phys.* **B241** 141

[88] ZEUS Collaboration, Derrick M *et al* 1995 *Z. Phys.* **C67** 93

H1 Collaboration, Aid S *et al* 1996 *Z. Phys.* **C72** 573

[89] OPAL Collaboration, Acton P D *et al* 1992 *Phys. Lett.* **B287** 401

[90] Fong C P and Webber B R 1991 *Nucl. Phys.* **B355** 54

[91] Webber B R 1993 *Proc. XXVI Int. Conf. on H.E.P.* ed J R Sanford (AIP Conference Proceedings: New York) p 878

[92] Nason P and Webber B R 1994 *Nucl. Phys.* **B421** 473

[93] Malaza E D and Webber B R 1986 *Nucl. Phys.* **B267** 702

[94] Mueller A H 1981 *Phys. Lett.* **B104** 161

Bassetto A, Ciafaloni M, Marchesini M and Mueller A H 1982 *Nucl. Phys.* **B207** 189

[95] Furmanski W, Petronzio R and Pokorski S 1979 *Nucl. Phys.* **B155** 253

[96] Webber B R 1984 *Phys. Lett.* **B143** 501

[97] ALEPH Collaboration, Decamp D *et al* 1991 *Phys. Lett.* **B273** 181

[98] DELPHI Collaboration, Abreu P *et al* 1991 *Z. Phys.* **C52** 271

[99] OPAL Collaboration, Acton P D *et al* 1992 *Z. Phys.* **C53** 539

[100] Knowles I G 1996 *Proc. of Int. Europhysics Conf. on H.E.P. (Brussels 1995)* eds J Lemonne *et al* (World Scientific: Singapore) p 349

[101] Fermi E 1950 *Prog. Theor. Phys.* **5** 550

[102] DELPHI Collaboration, Abreu P *et al* 1991 *Z. Phys.* **C50** 185

[103] Polyakov A M 1971 *Sov. Phys. JETP* **32** 296 and **33** 850

Koba Z, Nielsen, H B and Olesen 1972 *Nucl. Phys.* **B40** 317

Golokhvastov A I 1979 *Sov. J. Nucl. Phys.* **30** 128

[104] Carruthers P and Shih C C 1987 *Int. J. Mod. Phys.* **A2** 1447

[105] Carius S and Ingelman G 1990 *Phys. Lett.* **B252** 647

[106] ALEPH Collaboration, Buskulic D *et al* 1995 *Z. Phys.* **C69** 15

[107] DELPHI Collaboration, Abreu P *et al* 1991 *Z. Phys.* **C52** 511

[108] DELPHI Collaboration, Abreu P *et al* 1995 *Phys. Lett.* **B347** 447

OPAL Collaboration, Akers R *et al* 1995 *Phys. Lett.* **B352** 176

SLD Collaboration, Abe K *et al* 1996 *Phys. Lett.* **B386** 475

[109] Mark II Collaboration, Schumm B A *et al* 1992 *Phys. Rev.* **D46** 453

[110] Dokshitzer Yu L, Khoze V A and Troyan S I 1991 *J. Phys. G: Nucl. Part. Phys.* **17**

1602

[111] Schumm B A, Dokshitzer Yu L, Khoze V A and Koetke D S 1992 *Phys. Rev. Lett.* **69** 3025

Petrov V A and Kiselev 1995 *Z. Phys.* **C 66** 453

Dias de Deus J 1995 *Phys. Lett.* **B355** 539

[112] Chrin J 1995 *Proc. Int. Conf. on H.E.P. (Glasgow 1994)* vol 2 eds P J Bussey and I G Knowles (Bristol: Inst. of Physics) p 893

[113] Ochs W 1995 *Proc. XXIVth Int. Symp. on Multiparticle Dynamics (Vietri sul Mare 1994)* eds A Giovaninni *et al* (Singapore: World Scientific) p 243

[114] Amati D and Veneziano G 1979 *Phys. Lett.* **B83** 87

Bassetto A, Ciafaloni M and Marchesini G 1980 *Nucl. Phys.* **B163** 477

Marchesini G, Trentadue L and Veneziano G 1981 *Nucl. Phys.* **B181** 335

[115] Krzywicki A and Petersson B 1972 *Phys. Rev.* **D6** 924

Finkelstein J and Peccei R D 1972 *Phys. Rev.* **D6** 2606

Niedermayer F 1974 *Nucl. Phys.* **B79** 355

Casher A, Kogut J and Suskind L 1974 *Phys. Rev.* **D10** 732

Hoyer P *et al* 1979 *Nucl. Phys.* **B161** 349

Ali A, Pietarinen E, Kramer G and Willrodt J 1980 *Nucl. Phys.* **B93** 155

[116] Paige F and Protopopescu S 1986 *Super Collider Physics* ed D Soper (Singapore: World Scientific) p 41

[117] Bidulph P and Thompson G 1989 *Comp. Phys. comm* **54** 13

[118] Sjöstrand T 1984 *Z. Phys.* **C26** 93

Bengtsson M, Sjöstrand T and van Zijl M 1986 *Phys. Lett.* **B179** 164

[119] Montevay I 1979 *Phys. Lett.* **B84** 331

[120] Collins P D B 1977 *Regge Theory and High Energy Physics* (Cambridge University Press)

[121] Johnson K and Thorn C B 1976 *Phys. Rev.* **D13** 1934

[122] Wilson K G 1974 *Phys. Rev.* **D10** 2445

[123] Appelquist T, Barnett R M and Lane K 1978 *Ann. Rev. Nucl. Part. Sci.* **28** 387

SESAM Collaboration, Glässner *et al* 1996 *Phys. Lett.* **B383** 98

[124] Nambu Y 1970 Chicago preprint EFI 70-07

[125] Nielsen H B and Olesen P 1973 *Nucl. Phys.* **B61** 45

[126] Artru X 1983 *Phys. Rep.* **97** 147

[127] Andersson B and Gustafson G 1980 *Z. Phys.* **C3** 33

[128] Sjöstrand T 1984 *Nucl. Phys.* **B248** 469

[129] Morris D A 1987 *Nucl. Phys.* **B288** 717

[130] Chodos A and Thorn C B 1974 **B72** 509

Bardeen W A, Bars I, Hanson A J and Peccei R D 1976 *Phys. Rev.* **D13** 2364

[131] Green M B, Schwarz J H and Witten E 1987 *Superstring theory* (Cambridge: Cambridge University Press)

[132] Ferrara S 1996 preprint archive hep-th/9610085

[133] Andersson B, Gustafson and Sjöstrand T 1985 *Physica Scripta* **32** 574

[134] Artru X and Mennessier G 1974 *Nucl. Phys.* **B70** 93

[135] Gottschalk T D and Morris D A 1987 *Nucl. Phys.* **B288** 729

[136] Buchanan C D and Chun S B UCLA-HEP-95-2 and 1993 *Phys. Lett.* **B308** 153

URL: http://www.physics.ucla.edu/~chuns

[137] Gottschalk T D 1984 *Nucl. Phys.* **B239** 325

[138] Andersson B, Gustafson G and Peterson C 1979 *Z. Phys.* **C1** 105

[139] Bowler M G 1981 *Z. Phys.* **C11** 169

[140] Andersson B, Gustafson G and Söderberg B *Z. Phys.* 1983 **C20** 317

[141] Bowler M G 1984 *Z. Phys.* **C22** 155

[142] Bohr H and Nielsen H B 1978 Niels Bohr Institute preprint NBI-HE-78-3
   Andersson B, Gustafson G and Sjöstrand 1980 *Z. Phys.* **C6** 235

[143] Heisenberg W and Euler H 1936 *Z. Phys.* **98** 36
   Schwinger J 1951 *Phys. Rev.* **82** 664
   Brezin E and Itzykson C 1970 *Phys. Rev.* **D2** 1191

[144] Casher A, Neuberger H and Nussinov 1979 *Phys. Rev.* **D20** 179

[145] Andersson B, 1992 *J. Phys. G: Nucl. Part. Phys.* **17** 1507

[146] Andersson B and Gustafson G 1982 Lund University preprint LU TP 82-5

[147] Andersson B, Gustafson G and Samuelsson J 1994 *Z. Phys.* **C64** 653

[148] Buchanan C D and Chun S B 1987 *Phys. Rev. Lett.* **59** 1997

[149] Andersson B, Gustafson G and Ingelman G 1979 *Phys. Lett.* **B85** 417

[150] Andersson B and Hofmann W 1986 *Phys. Lett.* **B169** 364
   Bowler M G 1987 *Phys. Lett.* **B185** 205 and **276** 237
   Bowler M G and Artru X 1992 *Z. Phys.* **C37** 293

[151] Hanbury-Brown R and Twiss R G 1954 *Phil. Mag.* **45** 663 and 1956 *Nature* **177** 27
   Goldhaber G, Goldhaber S, Lee W and Pais A 1960 *Phys. Rev.* **120** 300

[152] Gyulassy M, Kauffman S K and Wilson L W 1979 *Phys. Rev.* **C20** 2267

[153] Bowler M G 1988 *Z. Phys.* **C39** 81

[154] Bowler M G 1990 **C46** 305

[155] Sjöstrand T 1989 *Multiparticle Production* eds R Hwa *et al*   (Singapore: World
   scientific) p 237
   Zajc W A 1987 *Phys. Rev.* **D35** 3396

[156] Lönblad L and Sjöstrand T 1995 *Phys. Lett.* **B351** 293

[157] Anselmino M *et al* 1993 *Rev. Mod. Phys* **65** 1199

[158] Andersson B, Gustafson and Sjöstrand 1982 *Nucl. Phys.* **B197** 45
   Meyer T 1982 *Z. Phys.* **C12** 77

[159] Bowler M G 1981 Oxford preprint OUNP 76/81

[160] Edén P and Gustafson G 1996 preprint archive hep-ph/9606454, to be published in *Z.
   Phys.* **C**
   Edén P 1996 preprint archive hep-ph/9610246

[161] Bowler M G, Burrows P N and Saxon D H 1989 *Phys. Lett.* **B221** 415
   Bowler M G and Artru X 1991 *Phys. Lett.* **B256** 557

[162] DELPHI Collboration, Abreu P *et al* 1997 preprint CERN-PPE/97-027, submitted to
   Phys. Lett. **B**

[163] Gottschalk T D 1984 *Nucl. Phys.* **B239** 349

[164] Hagedorn R 1965 *Nuovo Cimento* **3** 147
   Frautschi S C 1971 *Phys. Rev.* **D3** 2821

[165] Berger E L and Fox G C 1973 *Phys. Lett.* **B47** 162
   Hamer C J and Peierls R F 1973 *Phys. Rev.* **D8** 1358

[166] Wolfram S 1980 *Proc. XVth Recontre de Moriond (Les Arcs 1980)* vol 2 ed J. Tran
   Thanh Van (Gif-sur-Yvette: Editions Frontière) p 549

Field R D and Wolfram S 1983 *Nucl. Phys.* **B213** 65

[167] Bertolini S and Marchesini G 1982 *Phys. Lett.* **B117** 449

Webber B R 1984 *Proc. XVth Int. Symp. on Multiparticle Dynamics (Lund 1984)* eds G Gustafson and C Peterson (Singapore: World scientific) p 627

[168] Okubo S 1963 *Phys. Lett.* **5** 165

Zweig G 1964 CERN reports TH-401,412

Iizuka J, Okada K and Shito O 1966 *Rep. Prog. Phys.* **35** 1061

[169] Kunszt Z *et al* 1996 *Physics at LEP 2* vol 1 yellow report CERN 96-01 p 141

[170] Gustafson G and Hakkinen J 1994 *Z. Phys.* **C64** 659

[171] Lönnblad L 1996 *Z. Phys.* **C70** 107

[172] Sjöstrand T and Khoze V A 1994 *Z. Phys.* **C62** 281

[173] Andersson B, Dahlqvist P and Gustafson G 1989 *Z. Phys.* **C44** 453

[174] Bjorken J D, Brodsky S J and Lu H J 1992 *Phys. Lett.* **B286** 153

Lönnblad L 1996 *J. Phys. G: Nucl. Part. Phys.* **22** 947

Friberg C, Gustafson G and Hakkinen J 1996 preprint archive hep-ph/9604347

SLD Collaboration, Abe K *et al* 1995 *Phys. Rev. Lett.* **76** 4890

[175] ALEPH Collaboration, Buskulic D *et al* 1990 *Nucl. Instrum. Methods* **A294** 121 and 1995 *Nucl. Instrum. Methods* **A360** 481

[176] DELPHI Collaboration, Abreu P *et al* 1996 *Nucl. Instrum. Methods* **A378** 57

[177] L3 Collaboration, Adeva B *et al* 1990 *Nucl. Instrum. Methods* **A289** 35 and Adriani O *et al* 1993 *Phys. Rep.* **236** 1

[178] OPAL Collaboration, Ahmet K *et al* 1990 *Nucl. Instrum. Methods* **A305** 275

Allport P P *et al* 1993 *Nucl. Instrum. Methods* **A324** 34 and 1994 *Nucl. Instrum. Methods* **A346** 476

[179] Junk, T R 1995, PhD Thesis, SLAC-R-96-476

[180] Lafferty G D and Wyatt T R 1995 *Nucl. Instrum. Methods* **A355** 541

[181] Böhrer A 1996 preprint CERN-OPEN/96-021, submitted to *Phys. Rep.*

[182] OPAL Collaboration, Akers R *et al* 1994 *Z. Phys.* **C63** 181

[183] ALEPH Collaboration, Barate R *et al* 1996 preprint CERN-PPE/96-168, submitted to *Z. Phys.* **C**

[184] DELPHI Collaboration, Adam W *et al* 1996 *Z. Phys.* **C69** 561

[185] L3 Collaboration, Acciarri M *et al* 1994 *Phys. Lett.* **B328** 223

[186] L3 Collaboration, Acciarri M *et al* 1996 *Phys. Lett.* **B371** 126

[187] ALEPH Collaboration, Buskulic D *et al* 1995 *Z. Phys.* **C69** 379

[188] DELPHI Collaboration, Abreu P *et al* 1994 *Z. Phys.* **C65** 587

[189] L3 Collaboration, Acciarri M *et al* 1996 preprint CERN-PPE/96-171, to be published in *Phys. Lett.* **B**

[190] DELPHI Collaboration, Abreu P *et al* 1996 preprint CERN-PPE/96-077, submitted to *Z. Phys.* **C**

[191] OPAL Collaboration, Akers R *et al* 1995 *Z. Phys.* **C68** 1

[192] DELPHI Collaboration, Abreu P *et al* 1996 *Phys. Lett.* **B379** 309

[193] DELPHI Collaboration, Abreu P *et al* 1995 *Nucl. Phys.* **B444** 3

[194] ALEPH Collaboration, Buskulic D *et al* 1994 *Z. Phys.* **C64** 361

[195] OPAL Collaboration, Akers R *et al* 1995 *Z. Phys.* **C67** 389

[196] OPAL Collaboration, Acton P *et al* 1993 *Phys. Lett.* **B305** 407

[197] ALEPH Collaboration, Buskulic D *et al* 1994 *Z. Phys.* **C62** 1

[198] DELPHI Collaboration, Abreu *et al* 1993 *Z. Phys.* **C59** 533 *erratum* **C65** 709
[199] OPAL Collaboration, Alexander G *et al* 1996 *Z. Phys.* **C72** 1
[200] DELPHI Collaboration, Abreu P *et al* 1995 *Z. Phys.* **C68** 353
[201] DELPHI Collaboration, Abreu P *et al* 1994 *Phys. Lett.* **B345** 598
[202] ALEPH Collaboration, Buskulic D *et al* 1992 *Phys. Lett.* **B295** 396
[203] DELPHI Collaboration, Abreu P *et al* 1994 *Phys. Lett.* **B341** 109
[204] L3 Collaboration, Adriani O *et al* 1993 *Phys. Lett.* **B317** 467
[205] OPAL Collaboration, Alexander G *et al* 1996 *Z. Phys.* **C70** 197
[206] OPAL Collaboration, Alexander G *et al* 1996 *Phys. Lett.* **B370** 185
[207] DELPHI Collaboration, Abreu P *et al* 1995 *Phys. Lett.* **B361** 207
[208] OPAL Collaboration, Alexander G *et al* 1995 *Phys. Lett.* **B358** 162
[209] DELPHI Collaboration, Abreu P *et al* 1993 *Phys. Lett.* **B318** 249
[210] OPAL Collaboration, Alexander G *et al* 1996 preprint CERN-PPE/96-099, to be published in *Z. Phys.* **C**
[211] OPAL Collaboration, Alexander G *et al* 1996 preprint CERN-PPE/96-100, to be published in *Z. Phys.* **C**
[212] DELPHI Collaboration, Abreu P *et al* 1995 *Z. Phys.* **C67** 543
[213] DELPHI Collaboration, Abreu P *et al* 1996 *Z. Phys.* **C70** 371
[214] Suzuki M 1977 *Phys. Lett.* **B71** 139
     Bjorken J D 1978 *Phys. Rev.* **D17** 171
[215] Close F E *et al* 1993 *Phys. Lett.* **B319** 291
[216] Gribov V N 1991 Lund preprint Lu-TP 91-7
[217] Pomeranchuk I and Smorodinsky Ya 1945 *J. Fiz, USSR* **9** 97
[218] ZEUS Collaboration, Derrick M *et al* 1995 *Z. Phys.* **C68** 29
     H1 Collaboration, Aid S *et al* 1996 DESY-96-122
[219] Lafferty G D 1995 *Phys. Lett.* **B353** 541
[220] SLD collaboration, Abe K *et al* 1997 preprint SLAC-PUB-7395, submitted to *Phys. Rev. Lett.*
[221] ALEPH collaboration, Buskulic D *et al* 1996 *Z. Phys.* **C69** 393
[222] L3 Collaboration, Acciarri M *et al* 1995 *Phys. Lett.* **B345** 589
[223] Becattini F 1996 *Z. Phys.* **C69** 485
[224] Chliapnikov P V and Uvarov V A, 1995 *Phys. Lett.* **B345** 313
[225] Hofmann W, 1987 *Ann. Rev. Nucl. Part. Sci.* **38** 279
[226] Yi-Jin Pei 1996 *Z. Phys.* **C72** 39
[227] OPAL Collaboration, Ackerstaff K *et al* 1997 preprint CERN-PPE/97-035, submitted to *Z. Phys.* **C**
[228] ALEPH Collaboration, McNeil M 1996 submission to *ICHEP96 (Warsaw)* PA05-066
[229] CLEO Collaboration, Balest R *et al* 1995 *Phys. Rev.* **D52** 2661 and submission to *ICHEP96 (Warsaw)* PA05-074
[230] Barger V, Cheung K and Keung W Y 1990 *Phys. Rev.* **D41** 1541
     Braaten E, Cheung K and Yuan T C 1993 *Phys. Rev.* **D48** 4230
[231] Hagiwara K, Martin A D and Stirling W S, 1991 **B267** 527 *Erratum* 1993 **B316** 631
     Braaten E and Yuan T C 1993 *Phys. Rev. Lett.* **71** 1673
[232] DELPHI Collaboration, Abreu P *et al* 1996 *Z. Phys.* **C69** 575
     OPAL Collaboration, Alexander G *et al* 1996 *Phys. Lett.* **B384** 343
[233] Cho P 1996 *Phys. Lett.* **B368** 171

Cheung K, Keung W Y and Yuan T C 1996 *Phys. Rev. Lett.* **76** 877

[234] Kühn J H and Schneider H 1981 *Z. Phys.* **C11** 263

Keung W Y 1981 *Phys. Rev.* **D23** 2072

Abraham K J 1989 *Z. Phys.* **C44** 467

[235] CDF Collaboration, Abe F *et al* 1995 *Phys. Rev. Lett.* **75** 4358 and 1996 preprint FERMILAB-CONF-96-156

[236] Cho P and Leibovich A K 1996 *Phys. Rev.* **D53** 150, 6203

[237] Braaten E and Yuan T C 1994 *Phys. Rev.* **D50** 3176

Braaten E, Fleming S and Yuan T C 1996 *Ann. Rev. Nucl. Part. Sci.* **46** 197

Yuan F, Qiao C-F and Chao K-T 1997 preprint archive hep-ph/9703438

[238] Schuler G A 1997 preprint archive hep-ph/9702230

[239] Bodwin G T, Kim S and Sinclair D K 1996 *Phys. Rev. Lett.* **77** 2376

[240] Cho P and Wise M B 1995 *Phys. Lett.* **B346** 129

Braaten E and Chen Y-Q 1996 *Phys. Rev. Lett.* **76** 730

Beneke M and Rothstein I Z, 1996 *Phys. Lett.* **B372** 157

Baek S, Ko P, Lee J and Song H S 1997 preprint archive hep-ph/9701208

[241] Ernström P and Lönnblad L 1996 preprint archive hep-ph/9606472, to be published in *Z. Phys.* **C**

Ernström P, Lönnblad L and Vanttinen 1996 preprint archive hep-ph/9612408, to be published in *Z. Phys.* **C**

[242] Dokshitzer Yu L, Khoze V A and Troyan S I 1992 *J. Mod. Phys.* **A7** 1875

[243] Brummer N C 1995 *Z. Phys.* **C66** 367

[244] Dokshitzer Yu L, Khoze V A and Troyan S I 1991 *J. Phys. G: Nucl. Part. Phys.* **17** 1481 and 1992 *Z. Phys.* **C55** 107

[245] ALEPH Collaboration, Buskulic D *et al* 1995 *Z. Phys.* **C66** 355

[246] Brodsky S J and Ma B-Q 1997 *Phys. Lett.* **B392** 452

[247] Martin A D, Roberts R G and Stirling W J 1994 *Phys. Rev.* **D50** 6734

CTEQ Collaboration, Lai H L *et al* 1995 *Phys. Rev.* **D51** 4763

[248] Gribov V N and Lipatov L N 1971 *Phys. Lett.* **B37** 78

[249] De Angelis A, Cosmo G and Cossutti 1995 *Int. J. Mod. Phys.* **C6** 585

[250] Bigi I, Dokshitzer Yu, Kühn J and Zerwas P 1986 *Phys. Lett.* **B181** 157

[251] Mele B and Nason P 1991 *Nucl. Phys.* **B361** 626

Dokshitzer Yu L, Khoze V A and Troyan S I 1995 *Phys. Rev.* **D55** 89

[252] Peterson C, Schlatter D, Schmitt I and Zerwas P M 1983 *Phys. Rev.* **D27** 105

[253] Chrin J 1987 *Z. Phys.* **C36** 163 and 1988 *Annals. N.Y. Acad. Sci.* **535** 131

[254] ALEPH Collaboration: Buskulic D *et al* 1995 *Phys. Lett.* **B357** 699

[255] DELPHI Collaboration, Podobrin O and Feindt M 1995 submission to *EPS-HEP 95 (Brussels)* eps0560

[256] L3 Collaboration, Adeva O 1991 *Phys. Lett.* **B261** 177

[257] OPAL Collaboration, Alexander G *et al* 1995 *Phys. Lett.* **B364** 93

[258] Church E 1996 report SLAC-R-0495

[259] Brodsky S J and Ferrar G R 1973 *Phys. Rev. Lett.* **31** 1153

[260] Collins P D B and Spiller T P 1985 *J. Phys. G: Nucl. Part. Phys.* **11** 1289

[261] Kartvelishvili V G, Likehoded A K and Petrov V A 1978 *Phys. Lett.* **B78** 615

Kartvelishvili V G, Likehoded A K and Slabosnitskiĭ 1983 *Sov. J. Nucl. Phys.* **38** 952

[262] Morris D A 1989 *Nucl. Phys.* **B313** 634

[263] Kühn J H *et al* 1989 Z Physics at LEP 1 vol 1 ed G Alterelli *et al* yellow report CERN 89-08 p 269

[264] Podobrin O 1995 *Nucl. Phys.* **B** (*Proc. Supp.*) **C39** 373

[265] OPAL Collaboration, Akers R *et al* 1995 *Z. Phys.* **C66** 19

[266] Gustafson G and Häkkinen J 1993 *Phys. Lett.* **B303** 350

[267] Saleev V A 1997 preprint archive hep-ph/9702370

[268] ALEPH Collaboration, Buskulic D *et al* 1996 *Phys. Lett.* **B365** 437

[269] Bonvicini G and Randall L 1994 *Phys. Rev. Lett.* **73** 392

[270] ALEPH Collaboration, Buskulic D *et al* 1996 *Phys. Lett.* **B374** 319

[271] Bourrely C, Leader E and Soffer J 1980 *Phys. Rep.* **59** 95

[272] Bigi I I Y 1977 *Nuovo Cimento* **A41** 581

[273] Donoghue J F 1979 *Phys. Rev.* **D19** 2806

[274] Augustin J E and Renard F M 1979 *Proc. of the LEP Summer Study* vol 1 yellow report CERN 79-01 p 185

[275] OPAL Collaboration, Ackerstaff K *et al* 1996 preprint CERN-PPE/96-192, to be published in *Z. Phys.* **C**

[276] OPAL Collaboration, Ackerstaff K *et al* 1996 preprint CERN-PPE/97-005, to be published in *Z. Phys.* **C**

[277] HRS Collaboration, Abachi S *et al* 1987 *Phys. Lett.* **B199** 585
CLEO Collaboration, Kubota Y *et al* 1991 *Phys. Rev.* **D44** 593
TPC-2γ Collaboration, Aihara H *et al* 1991 *Phys. Rev.* **D43** 29

[278] Anselmino M, Kroll P and Pire B 1985 *Z. Phys.* **C29** 135
Anselm A, Anselmino M, Murgia F and Ryskin M G 1994 *J. Exp. Th. Phys.* **60** 496

[279] Haywood S 1994 Rutherford Appleton Laboratory preprint RAL-94-074

[280] ALEPH Collaboration, Buskulic D *et al* 1992 *Z. Phys.* **C54** 75

[281] DELPHI Collaboration, Abreu P *et al* 1992 *Phys. Lett.* **B286** 201 and 1994 *Z. Phys.* **C63** 17

[282] OPAL Collaboration, Acton P D *et al* 1991 *Phys. Lett.* **B267** 143

[283] DELPHI Collaboration, Abreu P *et al* 1995 *Phys. Lett.* **B355** 415

[284] DELPHI Collaboration, Abreu P *et al* 1996 *Phys. Lett.* **B379** 330

[285] OPAL Collaboration, Alexander G *et al* 1996 *Z. Phys.* **C72** 389

[286] Lafferty G D 1993 *Z. Phys.* **C60** 659

[287] OPAL Collaboration, Acton P *et al* 1992 *Z. Phys.* **C56** 521

[288] DELPHI Collaboration, Abreu P *et al* 1997 preprint CERN-PPE/97-030, submitted to *Phys. Lett.* **B**

[289] OPAL Collaboration, Alexander G *et al* 1996 *Phys. Lett.* **B384** 377

[290] TPC/2γ Collaboration, Aihara H *et al* 1986 *Phys. Rev. Lett.* **57** 3140

[291] SLD Collaboration, Abe K *et al* 1995 preprint SLAC-PUB-95 6920
Maruyama T 1996 *Proc. Int. Europhysics Conf. on H.E.P. (Brussels 1995)* eds J Lemonne *et al* (world Scientific: Singapore) p 330

[292] OPAL Collaboration, Acton P *et al* 1993 *Phys. Lett.* **B305** 415

[293] Bell K W, Foster B, Hart J C, Proudfoot J, Saxon D H and Woodworth P L 1982 Rutherford Appleton Laboratory preprint RL-82-011

[294] Ekelin S, Fredriksson S, Jändel M and Larsson T I 1984 *Phys. Rev.* **D30** 2310

[295] Das K P and Hwa R C 1977 *Phys. Lett.* **B77** 459

[296] Migneron R, Jones L M and Lassila K E 1982 *Phys. Rev.* **D26** 2235
Eilam G and Zahir M S 1982 *Phys. Rev.* **D26** 2991

[297] de Grand T A and Miettinen H I 1981 *Phys. Rev.* **D23** 1227

[298] MARK II Collaboration, de la Vaissiere C *et al* 1985 *Phys. Rev. Lett.* **54** 2071

[299] TASSO Collaboration, Althoff M *et al* 1984 *Z. Phys.* **C17** 5

[300] JADE Collaboration, Bartel W *et al* 1981 *Phys. Lett.* **B104** 325
ARGUS Collaboration, Albrecht H *et al* 1989 *Z. Phys.* **C43** 45

[301] TPC/2γ Collaboration, Aihara H *et al* 1985 *Phys. Rev. Lett.* **55** 1047

[302] van Hove L 1989 *Modern Physics Letters* **A4** 1867

[303] OPAL Collaboration, Akrawy M Z *et al* 1991 *Phys. Lett.* **B262** 351
ALEPH Collaboration, Decamp D *et al* 1992 *Z. Phys.* **C53** 21

[304] Murray W N, Frey R E and Ogren H O 1993 Oregon (Eugene) preprint OREXP
93-0016

[305] Konishi K, Ukawa A and Veneziano G 1978 *Phys. Lett.* **B78** 243: see also
Brodsky S J and Gunion J 1976 *Phys. Rev. Lett.* **37** 402

[306] Shizuya K and Tye S-H H 1978 *Phys. Rev. Lett.* **41** 787
Einhorn M and Weeks B G 1978 *Nucl. Phys.* **B146** 445

[307] OPAL Collaboration, Alexander G *et al* 1991 *Phys. Lett.* **B265** 462, Acton P D *et al*
1993 *Z. Phys.* **C58** 387 and Akers R *et al* 1995 *Z. Phys.* **C68** 179
ALEPH Collaboration, Buskulic D *et al* 1995 *Phys. Lett.* **B346** 389

[308] SLD Collaboration, quoted by Fuster J and Martiì 1996 *Proc. Int. Europhysics Conf
on HEP* ed J Lemonne *et al* (Singapore: World Scientific) p 319

[309] ALEPH Collaboration, Buskulic D *et al* 1995 *Phys. Lett.* **B384** 353
OPAL Collaboration, Alexander G *et al* 1996 *Z. Phys.* **C69** 543

[310] Gary J W 1994 *Phys. Rev.* **D49** 4503
OPAL Collaboration, Alexander G *et al* 1996 *Phys. Lett.* **B388** 659

[311] ALEPH Collaboration, Barate R *et al* 1997 preprint CERN-PPE/97-003, submitted
to *Z. Phys.* **C**

[312] Gaffney J B and Mueller A H 1985 *Nucl. Phys.* **B250** 109

[313] Dremin I M and Hwa R C 1994 *Phys. Lett.* **B324** 477
Dremin I M and Nechitailo V A 1994 *Mod. Phys. Lett.* **A9** 1471

[314] Peterson C and Walsh T F 1980 *Phys. Lett.* **B91** 455

[315] Chang V and Hwa R C 1981 *Phys. Rev.* **D23** 728

[316] Chang V, Eilam G and Hwa R C 1981 *Phys. Rev.* **D24** 1818

[317] DELPHI Collboration, Abreu P *et al* 1996 preprint CERN-PPE/96-193, submitted
to *Phys. Lett.* **B**

[318] OPAL Collaboration 1996 submissions to *ICHEP96 (Warsaw)* PA02-011, PA02-016

[319] ARGUS Collaboration, Albrecht H *et al* 1990 *Z. Phys.* **C46** 15: see also 1989 *Z. Phys.*
C41 557

[320] Crystal Ball Collaboration, Bieler Ch *et al* 1991 *Z. Phys.* **C49** 225

[321] DASP-II Collaboration, Albrecht H *et al* 1981 *Phys. Lett.* **B102** 291
CLEO Collaboration, Behrends S *et al* 1985 *Phys. Rev.* **D31** 2161
ARGUS Collaboration, Albrecht H *et al* 1988 *Z. Phys.* **C39** 177

[322] JADE Collaboration, Bartel W *et al* 1985 *Z. Phys.* **C28** 343 and 1983 *Phys. Lett.*
B130 545

[323] Field R D 1984 *Phys. Lett.* **B135** 203

[324] Scheck H 1989 *Phys. Lett.* **B224** 343

[325] ARGUS Collaboration, Albrecht H *et al* 1990 *Phys. Lett.* **B236** 102

[326] Gustafson G and Häkkinen J 1994 *Z. Phys.* **C61** 683